AREVA

Response to RAIs on WCAP-17788 Volume 4 - B&W Plants

ANP-3584NP

LICENSING REPORT

Revision 1

December 2017

AREVA Inc.

Nature of Changes

Item	Section(s) or Page(s)	Description and Justification
1	Sect 2.1.2.1	Modified response to be consistent with WEC response.
2	Sect 2.1.2.3	Modified response to be consistent with WEC response.
3	Sect 2.5.2.1	Modified response to RAI 4.5 to be more explicit regarding checks of core power, core peaking, and ECCS flow rate.
4	Sect 2.16.2.2	Modified response to refer to CE plants.
5	Sect 2.16.2.3	Modified response to refer to CE plants.

Contents

List of Tables vi

List of Figures vii

Nomenclature 0-1

1 Summary 1-1

2 REQUESTS FOR ADDITIONAL INFORMATION AND RESPONSES 2-1
2.1 RAI 4.1 . . . 2-1
2.1.1 Statement of RAI 4.1 . . . 2-1
2.1.2 Response to RAI 4.1 . . . 2-2
2.2 RAI 4.2 . . . 2-4
2.2.1 Statement of RAI 4.2 . . . 2-4
2.2.2 Response to RAI 4.2 . . . 2-6
2.3 RAI 4.3 . . . 2-7
2.3.1 Statement of RAI 4.3 . . . 2-7
2.3.2 Response to RAI 4.3 . . . 2-8
2.4 RAI 4.4 . . . 2-9
2.4.1 Statement of RAI 4.4 . . . 2-9
2.4.2 Response to RAI 4.4 . . . 2-10
2.5 RAI 4.5 . . . 2-20
2.5.1 Statement of RAI 4.5 . . . 2-20
2.5.2 Response to RAI 4.5 . . . 2-21
2.6 RAI 4.6 . . . 2-32
2.6.1 Statement of RAI 4.6 . . . 2-32
2.6.2 Response to RAI 4.6 . . . 2-33
2.7 RAI 4.7 . . . 2-35
2.7.1 Statement of RAI 4.7 . . . 2-35
2.7.2 Response to RAI 4.7 . . . 2-35
2.8 RAI 4.8 . . . 2-40
2.8.1 Statement of RAI 4.8 . . . 2-40

2.8.2 Response to RAI 4.8 2-41
2.9 RAI 4.9 2-45
2.9.1 Statement of RAI 4.9 2-45
2.9.2 Response to RAI 4.9 2-46
2.10 RAI 4.10 2-59
2.10.1 Statement of RAI 4.10 2-59
2.10.2 Response to RAI 4.10 2-59
2.11 RAI 4.11 2-61
2.11.1 Statement of RAI 4.11 2-61
2.11.2 Response to RAI 4.11 2-61
2.12 RAI 4.12 2-62
2.12.1 Statement of RAI 4.12 2-62
2.12.2 Response to RAI 4.12 2-62
2.13 RAI 4.13 2-63
2.13.1 Statement of RAI 4.13 2-63
2.13.2 Response to RAI 4.13 2-63
2.14 RAI 4.14 2-64
2.14.1 Statement of RAI 4.14 2-64
2.14.2 Response to RAI 4.14 2-64
2.15 RAI 4.15 2-65
2.15.1 Statement of RAI 4.15 2-65
2.15.2 Response to RAI 4.15 2-65
2.16 RAI 4.16 2-66
2.16.1 Statement of RAI 4.16 2-66
2.16.2 Response to RAI 4.16 2-67
2.17 RAI 4.17 2-75
2.17.1 Statement of RAI 4.17 2-75
2.17.2 Response to RAI 4.17 2-76
2.18 RAI 4.18 2-87
2.18.1 Statement of RAI 4.18 2-87
2.18.2 Response to RAI 4.18 2-87
2.19 RAI 4.19 2-88
2.19.1 Statement of RAI 4.19 2-88

2.19.2 Response to RAI 4.19 2-89
2.20 RAI 4.20 2-90
2.20.1 Statement of RAI 4.20 2-90
2.20.2 Response to RAI 4.20 2-91
2.21 RAI 4.21 2-93
2.21.1 Statement of RAI 4.21 2-93
2.21.2 Response to RAI 4.21 2-94
2.22 RAI 4.22 2-95
2.22.1 Statement of RAI 4.22 2-95
2.22.2 Response to RAI 4.22 2-95
2.23 RAI 4.23 2-106
2.23.1 Statement of RAI 4.23 2-106
2.23.2 Response to RAI 4.23 2-110
2.24 RAI 4.24 2-123
2.24.1 Statement of RAI 4.24 2-123
2.24.2 Response to RAI 4.24 2-124
2.25 RAI 4.25 2-128
2.25.1 Statement of RAI 4.25 2-128
2.25.2 Response to RAI 4.25 2-129
2.26 RAI 4.26 2-131
2.26.1 Statement of RAI 4.26 2-131
2.26.2 Response to RAI 4.26 2-131
2.27 RAI 4.27 2-132
2.27.1 Statement of RAI 4.27 2-132
2.27.2 Response to RAI 4.27 2-133
2.28 RAI 4.28 2-141
2.28.1 Statement of RAI 4.28 2-141
2.28.2 Response to RAI 4.28 2-141
2.29 RAI 4.29 2-142
2.29.1 Statement of RAI 4.29 2-142
2.29.2 Response to RAI 4.29 2-142
2.30 RAI 4.30 2-145
2.30.1 Statement of RAI 4.30 2-145

2.30.2 Response to RAI 4.30 2-145

List of Tables

RAI-4.4-1 Loss Coefficient for Baffle Region 2-14
RAI-4.4-2 Baffle Region Drawings for B&W Plants 2-15
RAI-4.9-1 RAI 4.9(b) – Requested Data for B&W Plants at Peak Power Location in Hot Channel 2-47
RAI-4.9-2 RAI 4.9(c) – Requested Data for B&W Plants - Instantaneous Void Fraction in Hot Channel 2-54
RAI-4.16-1 ECCS Flow and Temperature Sensitivity Cases 2-69
RAI-4.22-1 Sequence of Events and Results of the DEG HLB LBLOCA vs. SBLOCA Method 2-102
RAI-4.27-1 Core Crossflow Resistance and Mass Flow Rates for B&W Plant Analysis at 1290 s 2-138

List of Figures

RAI-4.4-1 B&W Baffle/Barrel Design 2-16
RAI-4.4-2 Lower Grid Rib to Upper Grid Rib Hydraulic Configuration 2-17
RAI-4.4-3 Baffle/Former Plate Configuration 2-18
RAI-4.4-4 Fuel Pin & Baffle Hole/Slot Arrangement 2-19
RAI-4.5-1 B&W LPI Flow Rates before SSO 2-25
RAI-4.5-2 B&W HPI Flow Rates before SSO 2-26
RAI-4.5-3 Elevation vs. Axial Power Profiles in Hot Pin/Channel for B&W Analyses 2-27
RAI-4.5-4 Elevation vs. Axial Power Profiles in Average Channel for B&W Analyses 2-28
RAI-4.8-1 RBHT Summary RELAP5/MOD2-B&W: Calculated vs. Measured Void Fraction for Seven RBHT Tests 2-43
RAI-4.9-1 Vapor Mass Flow Rates 2-48
RAI-4.9-2 Vapor Mass Fluxes 2-49
RAI-4.9-3 Liquid Mass Flow Rates 2-50
RAI-4.9-4 Liquid Mass Flux Rates 2-51
RAI-4.9-5 Vapor Velocities 2-52
RAI-4.9-6 Liquid Velocities 2-53
RAI-4.9-7 Vapor Void Fraction in Hot Channel at Peak Power Location 2-56
RAI-4.10-1 Normalized Decay Heat for B&W Analyses 2-60
RAI-4.16-1 Total Liquid Volume Available for ECCS Sensitivity Cases 2-70
RAI-4.16-2 Reactor Vessel Downcomer Collapsed Level for ECCS Sensitivity Cases 2-71
RAI-4.16-3 Average Channel Collapsed Level for ECCS Sensitivity Cases . . . 2-72
RAI-4.16-4 Reactor Vessel Upper Plenum Void Fraction for ECCS Sensitivity Cases 2-73
RAI-4.17-1 Break Mass Flow Rates for B&W Analyses 2-77
RAI-4.17-2 ECCS Liquid Mass Flow Rates for B&W Analyses 2-78
RAI-4.17-3 Liquid Mass Flow Rates Entering RV through CLs for B&W Analyses 2-79
RAI-4.17-4 Mass Flow Rates Entering RV through Intact HL for B&W Analyses 2-80
RAI-4.17-5 Steam Flow Quality (RV Side of Break) for B&W Analyses 2-81

RAI-4.17-6 Integrated Break Mass Flow Rates for B&W Analyses 2-83
RAI-4.17-7 Integrated ECCS Liquid Mass Flow Rates for B&W Analyses . . . 2-84
RAI-4.17-8 Integrated Liquid Mass Flow Rates Entering RV through CLs for B&W Analyses 2-85
RAI-4.17-9 Integrated Mass Flow Rates Entering RV through Intact HL for B&W Analyses 2-86
RAI-4.22-1 DEG HLB Comparison of RV Liquid Volumes with the Large and Small LOCA Models 2-103
RAI-4.22-2 DEG HLB Comparison of RV DC Collapsed Liquid Levels with the Large and Small LOCA Models. 2-104
RAI-4.23-1 B&W 177 FA Reactor Vessel and Internals Arrangement 2-114
RAI-4.23-2 B&W 177 FA Reactor Vessel and Internals Arrangement with Representative LTCC Levels 2-115
RAI-4.23-3 B&W 177 FA Reactor Vessel Flow Patterns after Complete Core Inlet Blockage 2-116
RAI-4.23-4 B&W DC to Core Elevation Head Difference to Overcome AFP Resistance 2-117
RAI-4.23-5 DEG HL Break Core Mixture Level versus Time 2-120
RAI-4.23-6 DEG HL Break Upper Plenum to Containment Pressure Difference versus Time 2-121
RAI-4.24-1 ECCS Mass Flow Rates per RCS Loop for Small Break LOCA . . . 2-127
RAI-4.27-1 Core Crossflow below the LOCA Holes 2-139

Nomenclature

Acronym	Definition
AC	Average Channel
AFP	Alternate Flow Path
ANS	American Nuclear Society
AOR	Analysis of Record
B&W	Babcock & Wilcox
BAP	Boric Acid Precipitation
BB	Barrel/Baffle
BOC	Beginning of Cycle
BOL	Beginning of Life
BU	Burn-up
BWNT	Babcock & Wilcox Nuclear Technologies
BWST	Borated Water Storage Tank
CE	Combustion Engineering
CFT	Core Flood Tank
CHF	Critical Heat Flux
CLDP	Cold Leg Pump Discharge
CSS	Containment Spray System
DC	Downcomer
DEG	Double-Ended Guillotine
DH	Decay Heat
DHHE	Decay Heat Heat-Exchanger
DNB	Departure from Nuclate Boiling
ECCS	Emergency Core Cooling System
EM	Evaluation Model
EOC	End of Cycle
GDC	General Design Criteria
GSI	Generic Safety Issue
HC	Hot Channel

Acronym	Definition
HL	Hot Leg
HLB	Hot Leg Break
HPI	High Pressure Injection
LBLOCA	Large Break Loss of Coolant Accident
LHR	Linear Heat Rate
LOCA	Loss of Coolant Accident
LPI	Low Pressure Injection
LTCC	Long Term Core Cooling
NPSH	Net Positive Suction Head
NRC	Nuclear Regulatory Commission
ONS	Oconee Nuclear Station
PCT	Peak Cladding Temperature
PWR	Pressurized Water Reactor
PWROG	Pressurized Water Reactor Owner's Group
RAI	Request for Additional Information
RBHT	Rod Bundle Heat Transfer
RCP	Reactor Coolant Pump
RCS	Reactor Coolant System
RV	Reactor Vessel
RVVV	Reactor Vessel Vent Valve
SBLOCA	Small Break Loss of Coolant Accident
SG	Steam Generator
SI	Safety Injection
SIRB	Safety Issues Resolution Branch
SSO	Sump Switch Over
STCC	Short Term Core Cooling
TCD	Thermal Conductivity Degradation
TH	Thermal Hydraulic
TIL	Time in Life

Acronym	Definition
TR	Topical Report
UH	Upper Head
UP	Upper Plenum
V&V	Verification and Validation
VAFT	Volume Average Fuel Temperature
WEC	Westinghouse Electric Company

1.0 Summary

In July of 2015, the Pressurized Water Reactor Owner's Group (PWROG) submitted licensing Topical Report (TR) WCAP-17788 "Comprehensive Analysis and Test Program for GSI-191 Closure" intended for Generic Safety Issue (GSI)-191 closure (Reference 1). The TR is an approach to define an in-vessel fibrous debris limit and provides a means for increasing the approved fibrous debris limit used by licensees to resolve GSI-191.

By letter dated August 18, 2016, the Safety Issues Resolution Branch (SIRB) of the Nuclear Regulatory Commission (NRC) provided Requests for Additional Information (RAIs) on Volume 4 of WCAP-17788 in order to complete their review (Reference 2). This report is intended to capture the response to these RAIs that fall within AREVA's scope of the project for the B&W plants.

The results of the original thermal-hydraulic analyses are presented in WCAP-17788-P, Volume 4, Section 11. These analyses were based on a 0.5 ft^2 break. In RAI 4.22, the NRC requested a justification that this break is appropriate for use in representing a full Double-Ended Guillotine (DEG) break of the Hot Leg (HL) piping. In response to that RAI, a new "base" case was developed. The new DEG Loss of Coolant Accident (LOCA) break case described in the response to RAI 4.22 is used as a basis for all of the other RAI responses, as appropriate. As a consequence of this and other RAI responses, WCAP-17788-P, Volume 4 was extensively revised. The markups from the original submittal are provided separately.

References

1 PWROG letter dated July 17, 2015, Stringfellow, N.J. (PWR Owners Group) to Rowley, J.G. (U.S. NRC), Submittal of WCAP-17788, "Comprehensive Analysis and Test Program for GSI-191 Closure (PA-SEE-1090)," (ML15210A668).

2 NRC letter dated August 18, 2016, Rowley, J.G. (U.S. NRC) to Nowinowski, W.A. (PWR Owners Group), Request for Additional Information Re: Pressurized Water Reactor Owners Group Topical Report WCAP-17788, Comprehensive Analysis and Test Program for GSI-191 Closure (TAC No. MF6536), (ML16195A362).

2.0 REQUESTS FOR ADDITIONAL INFORMATION AND RESPONSES

2.1 RAI 4.1

2.1.1 Statement of RAI 4.1

General Design Criteria (GDC) 35, "Emergency Core Cooling," in Appendix A, "General Design Criteria for Nuclear Power Plants," to Title 10 of the Code of Federal Regulations (10 CFR) Part 50, requires that a single failure be assumed when analyzing safety system performance. Sections 8.2, 9.2, 10.2, and 11.2 present safety system performance analysis results for four different plant categories.

(a) Describe the single failure assumptions implemented in the analyses of the safety system performance for the four analyzed plant categories. Identify the single failure assumption(s) applied in the modeling of the reactor coolant system (RCS) response including the performance of the emergency core cooling system (ECCS). Justify the assumptions by describing pertinent conditions, supporting considerations, and applicable analyses.

(b) The analyses for the Combustion Engineering (CE) plant category were performed with the containment backpressure computed by a coupled containment code. Demonstrate how the single failure assumptions implemented in the RCS response analysis for this plant category, as well as any additional and related assumptions, were considered for the purposes of calculating the containment backpressure response. Verify that treatment is consistent with Assumption No. 6 in Section 4.1, "Major Assumptions," and Input No. 6 in Section 4.2, "Critical Inputs".

(c) Provide information that demonstrates whether plant-specific considerations are necessary to address GDC 35 when considering safety system performance on a plant-specific basis. Explain how the single failure assumptions implemented in the T-H analyses in Sections 8.2, 9.2, 10.2, and 11.2, as considered in the response to Items a and b above, remain valid for each plant category. Describe how it was determined whether additional single failure assumptions and applicable supporting considerations were required for plant specific T-H analyses. If necessary, identify the types of plant specific information related to systems, conditions, parameters, and other relevant items that will need to be considered for adequate implementation of the topical report (TR) with respect to GDC 35 on a plant specific basis.

2.1.2 Response to RAI 4.1

2.1.2.1 Part a

The analyses consider the effect of the limiting single failure on Emergency Core Cooling System (ECCS) performance. The minimum Safety Injection (SI) flow rate and maximum SI delay times are used based on plant technical specification limits from the base plant models selected for each plant category. The base plant models are identified and described in RAI 4.29. The ECCS inputs (which consider a single failure) are described in detail in RAI 4.5a.

The limiting single failure also takes into account the effect on containment pressure. Failure of an entire safety train would result in the loss of one or several containment spray and fan cooling units, reducing containment cooling, and increasing containment pressure, which will reduce cladding temperatures during a debris-induced secondary heatup. As such, the inputs to the containment pressure are skewed in order to obtain a conservative (low) pressure transient such that cladding temperatures during any calculated debris-induced secondary heatup are maximized.

The single failure assumptions applied during the recirculation phase of the accident are disconnected from those applied during the injection phase of the accident transient. In the simulations, an early sump switchover time is applied that is representative of two trains of safety injection during the injection phase. An early sump switchover time is more limiting for Generic Safety Issue (GSI) -191 scenarios since the decay heat is higher and Reactor Coolant System (RCS) liquid inventory is lower. Sensitivity studies performed by Westinghouse Electric Company (WEC) demonstrate that an earlier arrival of debris results in a higher calculated cladding temperature during the debris-induced secondary heatup (see WEC response to RAI 4.19, Item b). As described in the response to RAI-4.1 Item c., utilities implementing the WCAP-17788 in-vessel debris methodology will need to verify that they fall within the range of conditions considered by the analyses. More details regarding how this check is performed are provided in the response to RAI-4.5 Item a.

2.1.2.2 Part b

This RAI pertains to the Combustion Engineering (CE) plant categories and therefore requires no response for the B&W plant category.

2.1.2.3 Part c

Plant-specific considerations are necessary to address GDC 35. This will be completed by each utility when implanting the WCAP-17788 methodology. Each plant will have to justify applicability of the methodology as part of their plant-specific submittal. Each plant will need to determine their limiting GSI-191 scenario relative to debris accumulation in the reactor vessel, considering appropriate single-failure assumptions. Once the limiting GSI-191 in-vessel debris accumulation scenario is defined, a plant will need to demonstrate that it falls within the bounds of the WCAP-17788 methodology. The response to RAI 4.5 provides details regarding the confirmation checks that each utility must complete to justify applicability of the WCAP-17788 methodology.

2.2 RAI 4.2

2.2.1 Statement of RAI 4.2

Section 6.1 states that "a method was developed to calculate appropriate BB (Barrel/Baffle) flow resistances for use in this analysis" so that all Westinghouse upflow plants in operation in the U.S. are represented. The section further clarifies that "the method and supporting calculations are contained in Reference 6-2, which confirms that the BB flow resistances shown in Table 6-1 bound all Westinghouse upflow plants". With regard to the Westinghouse downflow plant design category, Section 6.2 explains that "a method was developed to calculate appropriate UHSN (Upper Head Spray Nozzle) flow resistances for use in this analysis" and that "the method and supporting calculations are contained in Reference 6-2, which confirms that the UHSN flow resistances shown in Table 6-2 bound all Westinghouse downflow plants". Reference 6-2 is identified in Section 6.5, as follows.

Reference 6-2: [

]

(a) Provide a copy of Reference 6-2.

(b) Include a description of the assumptions used in the maximum and minimum BB flow resistance calculations given in Table 6-1.

(c) Include a description of the assumptions used in the maximum and minimum UHSN calculations provided in Table 6-2.

(d) For Items a and b, describe whether the flow passages between the downcomer and upper plenum regions via the hot leg nozzle gaps were modeled and provide a justification for the modeling approach.

(e) For each Westinghouse unit considered in determining the BB and UHSN resistances in Tables 6-1 and 6-2, provide the following information in a table format, separately for both Westinghouse upflow and downflow plant category. In individual columns, include a description for each of the following items:

   (i) Name and rated power

   (ii) Identification numbers of design drawings, including the name of the unit for which they were produced, containing the geometric data to calculate the resistance associated with the

      i. lower core plate to baffle region gap

ii. former holes including the number of former plates with holes
iii. upper core plate to baffle region gap
iv. UHSNs

(iii) For each category of flow passage, identify all types and sizes of openings that are credited in the resistance calculation. As a minimum, include

i. the number of holes or gaps
ii. hole diameter or gap width and perimeter length
iii. individual hole or gap flow area for each type of holes/gaps
iv. total resulting flow area

(iv) Loss coefficients associated with each category of passage along with the reference flow area

(v) Total unadjusted and adjusted BB/UHSN resistances along with the units

(vi) Assumptions related to the way geometric data in the drawings was treated for the purpose of calculating resistances and assumptions related to the consideration of any other existing flow passages such as pressure relief holes in the baffle plates.

(f) For each table in Item e, include a figure that illustrates the BB region and UHSN region geometries for each Westinghouse plant category and a separate figure showing an example of a BB former region top view for one-quarter of the core region. (Appropriate examples of such figures appear as Figures 1 and 2 in a March 26, 2001, letter by Exelon Generation Company, LLC, ADAMS Accession No. ML010890050.)

(g) During the NRC staff audit of supporting Westinghouse documents and drawings on February 2-4, 2016, it was observed, for the upflow BB plant category, former plate holes of Type 1 were assigned a loss coefficient of [ ] and those of Type 2 were assigned a loss coefficient of [ ]. The staff could not determine the basis for those values. Provide the calculations and supporting documentation for each of these loss coefficients, as well as for other loss coefficients identified in the response to Item e.iv above.

(h) During the NRC staff audit of supporting Westinghouse documents and drawings on February 2-4, 2016, the average loss coefficient for the upflow plant category, K_{AVG}, from former plate holes of Type 1 and Type 2 was computed from the individual loss coefficients, K_i, [

]. Explain the rationale for using an averaging equation to obtain an equivalent loss coefficient value and demonstrate whether physical parameters are preserved by using this method

(e.g., flow or pressure loss). Examine the effects of the averaging method on the resulting resistances for both maximum and minimum resistance cases. If the averaging method is found inconsistent, implement an appropriate approach and update the BB resistance results for the Westinghouse upflow and downflow plant categories.

2.2.2 Response to RAI 4.2

This RAI pertains to the Westinghouse Electric Company (WEC) plant categories and therefore requires no response for the Babcock & Wilcox (B&W) plant category.

2.3 RAI 4.3

2.3.1 Statement of RAI 4.3

Section 6.3, "Combustion Engineering Plant Model," states that a method and supporting calculations for calculating appropriate BB flow resistances that represent all CE plants in operation in the U.S. are contained in Reference 6-3 and Reference 6-4. These two references are identified in Section 6.5 and updated in Letter OG-16-42 dated February 12, 2016, as follows.

Reference 6-3: [

].

Reference 6-4: [

].

(a) Provide copies of References 6-3 and 6-4 listed above.

(b) Provide a description of the assumptions used in the maximum and minimum BB flow resistance calculations provided in Table 6-3.

(c) Identify the physical units for the BB flow resistances in Table 6-3.

(d) Describe whether or not the flow passages between the downcomer and upper plenum regions via the hot leg nozzle gaps were modeled. If they were not, provide a justification for the omission.

(e) Provide the information requested in Items e, f, g, and h in RAI 4.2 as it applies to the CE plant category. As both AREVA and Westinghouse performed BB flow resistance calculation for CE plant units, all requested information from each vendor for the analyzed plant units should be provided.

(f) During the NRC audit of supporting AREVA documents and drawings on March 1-4, 2016, it was found in document [

] that two different values for the maximum BB flow resistance case, [ ], were reported for [ ]. During the audit, it was explained that the values resulted from the calculations performed by AREVA and Westinghouse. This significant difference in resistances is a concern regarding the limiting representative resistances determined for the CE plant category. Provide an explanation for the difference in the BB resistance results for [ ]. Since both results

may be incorrect, examine the methods used by AREVA and Westinghouse. Identify whether deficiencies in the calculational methodologies or differences in geometrical plant data related to the BB region were involved in both analyses. If deficiencies are discovered, provide a description and results of any changes to the methods for the corrected BB resistance calculation(s). Provide full calculations and final results for [ ] using both methods with applicable modifications. Provide the input derived from geometrical plant data related to the BB region for this unit as used in both analyses.

(g) Verify that the issues associated with Item f above do not affect the other plant categories.

2.3.2 Response to RAI 4.3

This RAI pertains to the Combustion Engineering (CE) plant categories and therefore requires no response for the B&W plant category.

2.4 RAI 4.4

2.4.1 Statement of RAI 4.4

Section 6.4, "Babcock and Wilcox (B&W) Plant Model," states that "the BB design for all B&W plants is the same" and explains that the BB flow resistance shown in Table 6-4 is representative of all B&W plants. It is also explained that the method and supporting calculations confirming the provided BB flow resistance value are contained in Reference 6-3, which is identified in Section 6.5 and updated with Letter OG-16-42 dated February 12, 2016, as follows.

Reference 6-3: [

]

(a) The above identified document appears to be related to the CE plant category. Confirm whether this is the proper reference for B&W plants. If a reference other than Reference 6-3 was used for B&W plants, provide a copy of the document.

(b) Include a description of the assumptions used in the calculation of the BB total flow resistance value provided in Table 6-4.

(c) Identify the physical units for the BB flow resistance shown in Table 6-4.

(d) State whether any other flow passages between the downcomer and upper head/plenum regions were modeled in the analyses. If they were, provide a description of these additional passages and how they are evaluated.

(e) Provide the information requested in Items e, f, g, and h in RAI 4.2 as it applies to the B&W plant design category.

(f) During the NRC staff audit of AREVA documents and drawings on March 1-4, 2016, the NRC staff encountered difficulty in interpreting, following, and confirming calculations and results pertaining to the BB resistance calculations for the B&W plant design category. Therefore, ensure that the information provided in response to Items a through e above include all necessary clarifying and supporting information to support an independent review of the BB resistance calculation methodology and the results documented for the B&W plant category.

2.4.2 Response to RAI 4.4

2.4.2.1 Part a

The document cited is the correct reference for the B&W plants and provides the B&W baffle resistance under the heading B&W Plant Input just before the list of references. However, the document cited does not provide the details of the baffle resistance or calculation. This information is provided as part of this RAI response.

2.4.2.2 Part b

The assumptions relevant to the calculation of the Barrel/Baffle (BB) total flow resistance value for the B&W plants are included as part of the discussion for part "f" of this RAI.

2.4.2.3 Part c

The physical units for the BB flow resistance are ft^{-4}.

2.4.2.4 Part d

No flow paths that can pass debris from the Downcomer (DC) to the Upper Head (UH)/Upper Plenum (UP) region were modeled in the B&W analyses. While certain flow passages may exist (e.g. hot leg nozzle gaps), they cannot be confirmed to be open so they were excluded. Neglecting these flow patterns maximizes the quantity of debris reaching the core inlet by limiting the quantity that bypasses the core inlet. It should further be noted that the response to RAI 4.20 indicates that the fiber limit for the B&W plants will be [ ]. Any debris that bypasses the core inlet will progress to the heated core and contribute to this limit. Therefore, even if flow paths between the DC and UH/UP region were considered, the debris limit would not change. The B&W plant designs also include Reactor Vessel Vent Valves (RVVVs) that allow flow and pressure equalization between the UH and upper DC. However, these are one-way valves and do not let flow (or debris) travel from the DC to the UH.

2.4.2.5 Part e

This information requested for the B&W plants is included as part of the discussion for part "f" of this RAI.

2.4.2.6 Part f

The baffle region for the B&W plants is shown in Figure RAI-4.4-1. As shown in Figure RAI-4.4-2, steady-state flow in this region consists of flow from the lower plenum into the baffle region through the lower grid rib (which is similar to the lower core support plate for Westinghouse Electric Company (WEC) plant designs), flow through eight former plates, and flow out of the baffle region into the upper plenum through the upper grid rib (which is similar to the upper core plate for WEC plant designs). The former plates are shown in Figure RAI-4.4-3. Flow can also divert from the baffle region into the core periphery through holes in the baffle plates and slots at the corners of the baffle plates as shown in Figure RAI-4.4-4.The form-loss coefficients through these paths are described as follows.

Loss Coefficient from Lower Plenum to Baffle through Lower Grid Rib

The loss-factor for this path is computed with the flow distribution in lower core support region such that the area directly below the hole area passes through the lower grid rib. The loss-factor for each path is based on [

]. The holes in the rib then expand into the baffle area. The loss-factor is computed using standard industry practices. The dimensions are from drawing [

]. Table RAI-4.4-2 identifies the relevant drawings for the other B&W plants.

Coefficient through All Baffle Former Plates Except Fourth Former Plate

The loss-factor for each path is based on [

]. The loss-factor is computed based on a contraction and expansion using standard industry practices and conservatively includes friction through the holes computed for flow at full power conditions. The dimensions are from drawing [

] Table RAI-4.4-2 identifies the relevant drawings for the other B&W plants.

Loss Coefficient Through Fourth Baffle Former Plate

The fourth baffle former plate is at the midplane level, and has a different physical arrangement. The loss-factor for this path is based on [

]. The loss-factor is computed

based on a contraction and expansion using standard industry practices and conservatively includes friction through the holes computed for flow at full power conditions. The dimensions are from drawing [

]

Table RAI-4.4-2 identifies the relevant drawings for the other B&W plants.

Loss Coefficient from Baffle to Upper Plenum through Upper Core Support Plate

The loss-factor for this path is based on [

]. The loss-factor is computed based on a contraction and expansion using standard industry practices and conservatively includes friction through the holes computed for flow at full power conditions. Specifically, a beveled edge contraction is used to account for the gradual contraction before the abrupt contraction. The dimensions are from drawing [ ].
Table RAI-4.4-2 identifies the relevant drawings for the other B&W plants.

Loss Coefficients for LOCA Holes and Baffle Slots

There are five rows of holes in the baffle plates (so-called "LOCA" holes) that allow flow from the baffle to the peripheral fuel assemblies in the core. Each hole is [ ] in diameter. Three of the axial core levels have [ ] holes and two axial core levels have [ ] holes. Between 56.75" and 99.5", there are [

]. The dimensions are from drawings

[

]. Table RAI-4.4-2 identifies the relevant drawings for the other B&W plants.

In the RELAP5 model, the [

]. Each row of LOCA holes is located at the centerline elevation of the row of holes in the plant. The form-loss coefficient from the baffle to the core through these holes could involve a turn, contraction into the hole, and expansion out of the hole. A similar path would be seen in the reverse direction (from the core to the baffle). At the conditions following a LOCA, the velocities are low such that the turning losses are negligible. To that end, [ ] is applied to all rows of LOCA holes and slots.

[1]The ONS-1 model is slightly different. Three of the axial levels have [ ] holes and two axial levels have [ ] holes. However, the ONS-1 model is treated the same as the other B&W plants in terms of modeling. The additional [ ] holes will have little to no effect on the Loss of Coolant Accident (LOCA) transient results.

Loss Coefficients for Baffle Region

The loss-factors for the baffle region are summarized in Table RAI-4.4-1. Also shown in Table RAI-4.4-1 are the centerline elevations of the former plates, the computed k/A^2 for the full baffle area, and the summation of the k/A^2 for the baffle region through the eighth baffle former plate. Table RAI-4.4-2 provides a list of the plant-specific drawings for the baffle region.

Table RAI-4.4-1: Loss Coefficient for Baffle Region

[

]

[2]Elevations are relative to the top of the core support pad.

[3]The values used in the analysis were slightly different, resulting in a K/A^2 value of [ ]. At the flow rates analyzed, the difference in dP due to the difference in K/A^2 is less than 0.01 psid and will have a negligible effect on the transient results.

[4]The area stated here is slightly different from that calculated in the source documentation (A=[ ]). However, the variation in final K/A^2 will have a negligible effect on the results.

[5]The loss factor from the baffle to upper plenum is not modeled in the analysis. However, there will be no affect on the analysis results relative to GSI-191, because this flow path is not involved in providing flow to the core for DH removal.

Table RAI-4.4-2: Baffle Region Drawings for B&W Plants

[

]

[6]The drawings are maintained by the plant; therefore, the specific revision level must be obtained from the plant.

Figure RAI-4.4-1: B&W Baffle/Barrel Design

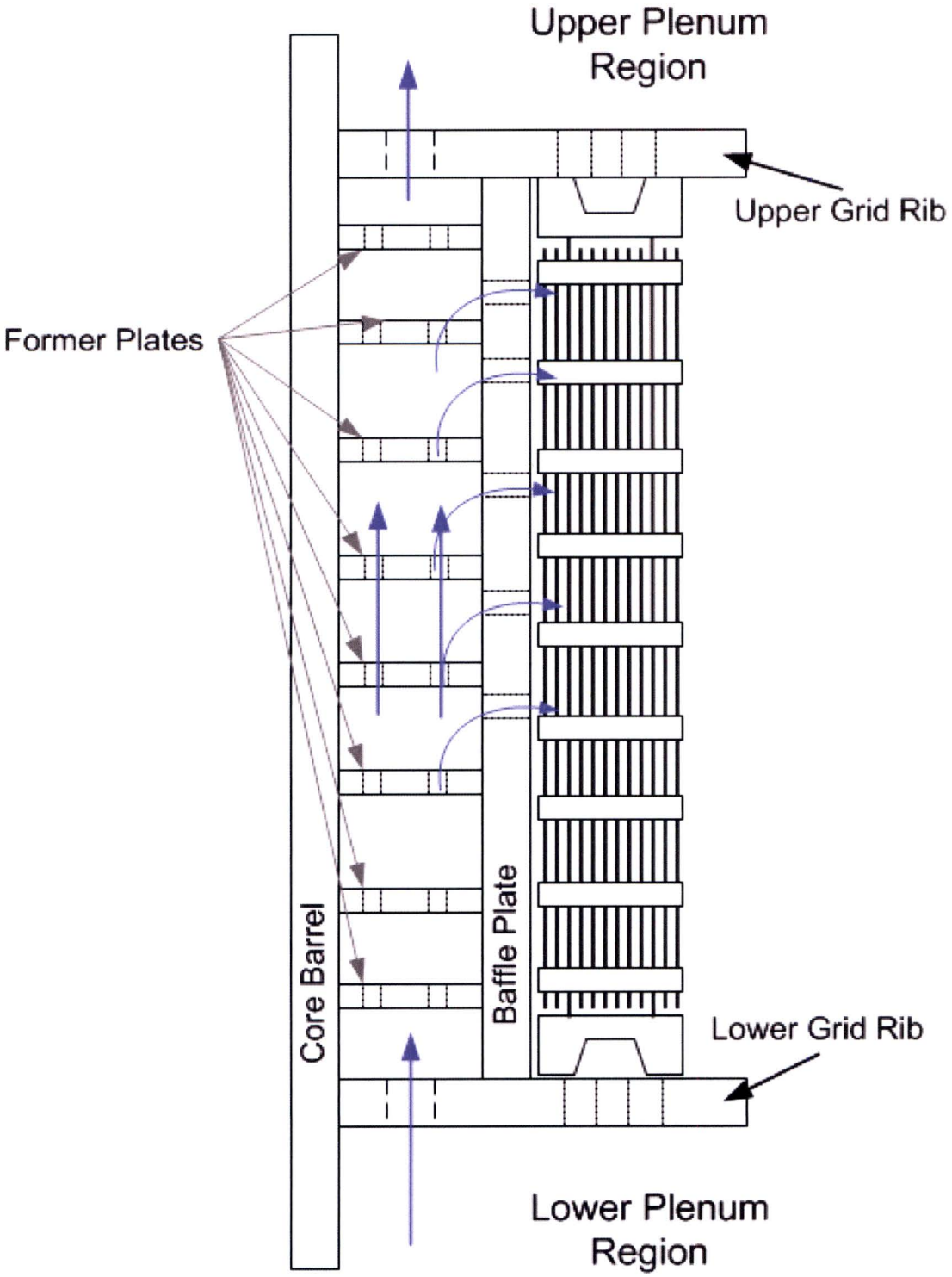

Figure RAI-4.4-2: Lower Grid Rib to Upper Grid Rib Hydraulic Configuration

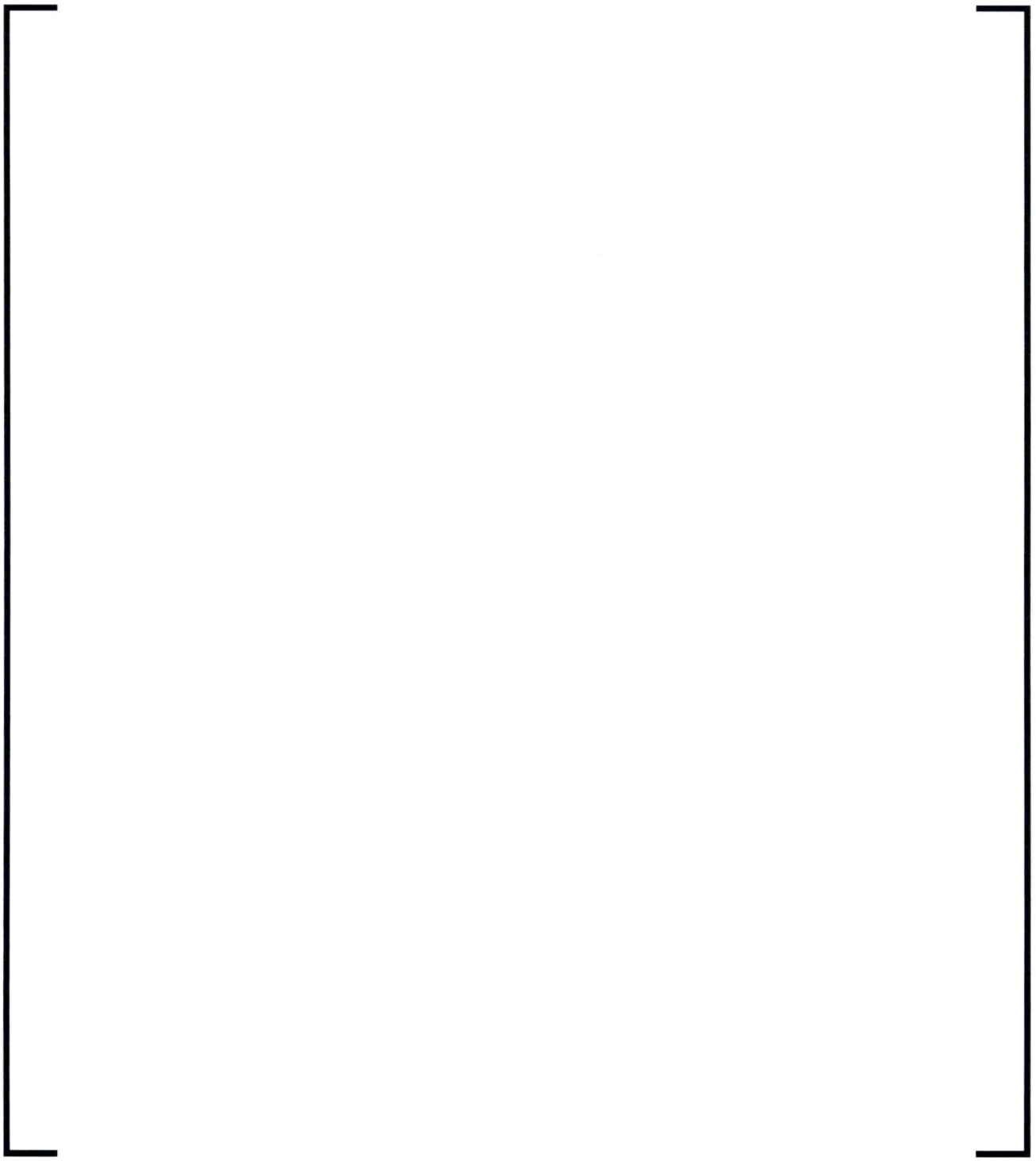

Figure RAI-4.4-3: Baffle/Former Plate Configuration

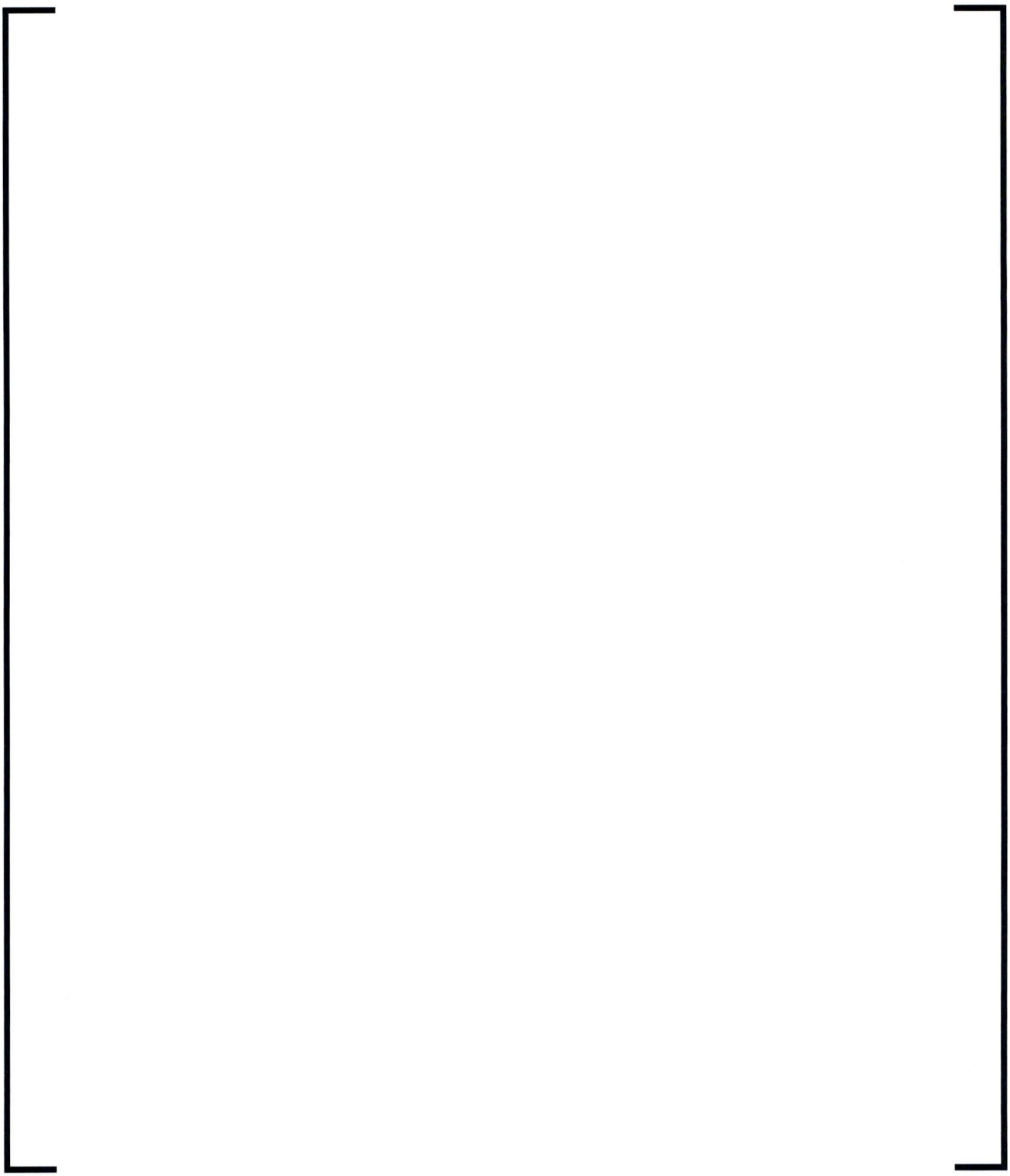

Figure RAI-4.4-4: Fuel Pin & Baffle Hole/Slot Arrangement

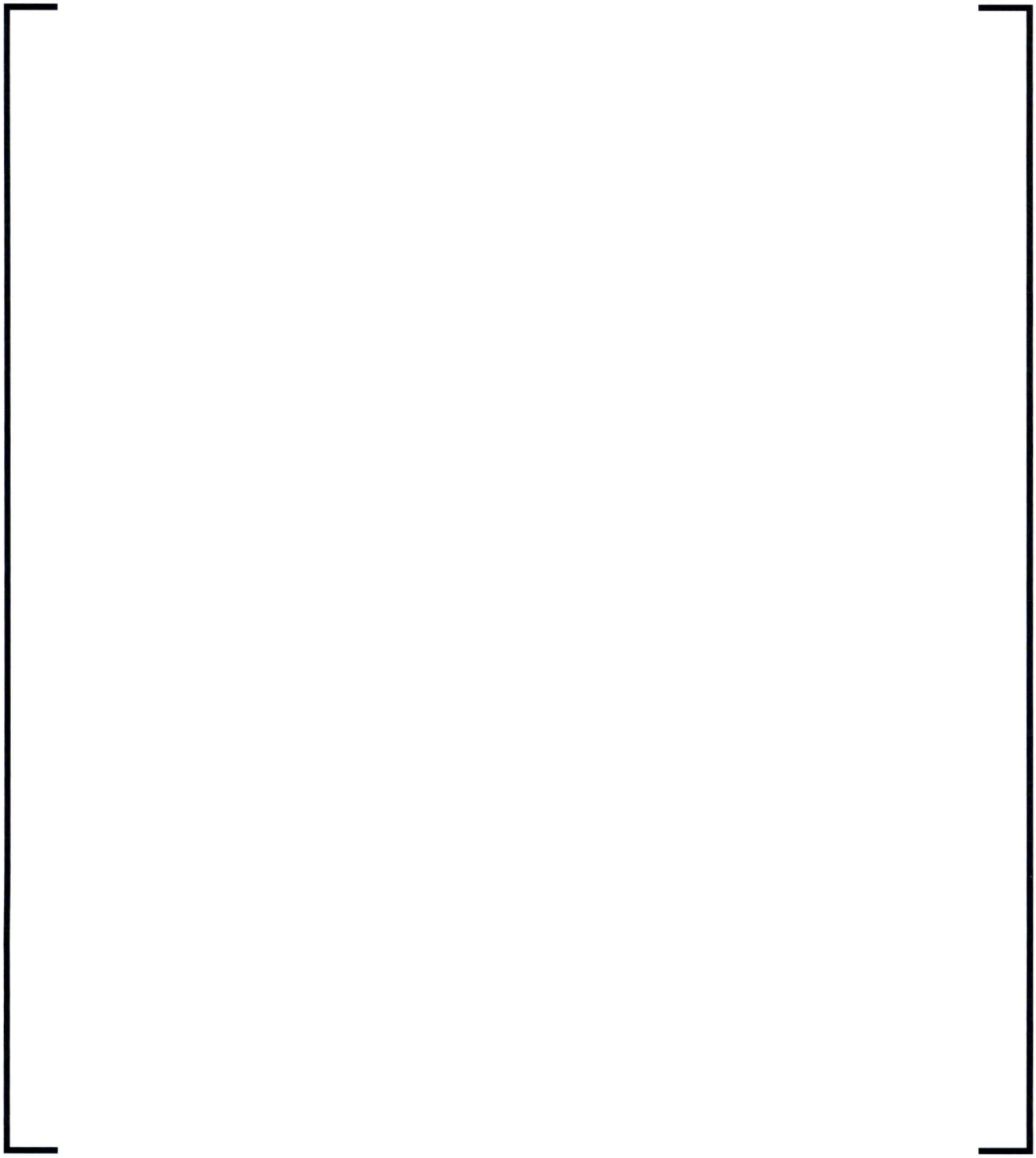

2.5 RAI 4.5

2.5.1 Statement of RAI 4.5

Tables 6-1 through 6-4 provide a summary of key inputs for each plant category. Provide the following information related to the key inputs for the HLB methodology:

(a) Justify that the values for the parameters listed in Tables 6-1 through 6-4 are bounding or demonstrate that these values can be considered appropriate and applicable for all of the plant units covered by the TR. If certain key input values have not been validated as bounding, state how the use of the TR methodology will ensure that the applicable acceptance criteria are met for the specific plant application. Include enough information for each key parameter so that the NRC staff can verify that they are bounding for the plants intended to use the TR. Ensure that the information includes, as necessary, plant specific characteristics, operating conditions, licensing basis assumptions (including single failure), regulatory limits, operating procedures, technical specifications limits, uncertainties, and full ranges of the inputs and variables that could affect the evaluation. If it is determined that these parameters are valid for plants using the methodology, how will the plants ensure the variables that can affect these parameters are maintained at acceptable values?

(b) Provide graphs of the physical axial power profiles implemented in the plant design analyses in Sections 8 through 11. Provide each physical axial power profile on a separate plot and for each profile show its nodal approximation based on the core axial nodalization.

    (i) Specify the elevation of the axial peak power location associated with the profile described in Table 6-3 for the CE plant design analysis.

(c) Clarify the approach to determining the axial power shapes simulated in the LOCA analyses. Explain if any bounding, or otherwise considered appropriate, assumptions were introduced to define the shapes requested in Item a. Explain if any physical axial power shapes, representative of individual units for each of the NSSS plant design categories included in Table 3-1 were considered in analyzing and determining the applicability of the simulated axial power profiles. Describe and justify the basis on which a single axial power profile, applied in the analyses for each plant category, can be considered valid and applicable to reactor core conditions across various units represented by each NSSS design category. An axial power profile applied for the purpose of a small-break LOCA analysis using a model based on 10 CFR Part 50, Appendix K, would represent an acceptable axial power profile on a plant specific basis.

2.5.2 Response to RAI 4.5

2.5.2.1 Part a

Each of the parameters on Table 6-3 is discussed in the order they are presented.

Core Power:

A core power level of 2827.4 MWt was analyzed in the new B&W analyses presented in response to RAI 4.22. This power level includes instrument uncertainty and bounds all operating B&W plants. (Note that this power level is lower than the 3026 MWt identified in Volume 4, Table 6-4. That power level corresponded to a power uprate level at the CR-3 plant, which has recently shut down. The revised analyses for the B&W plants presented in Request for Additional Information (RAI) 4.22 were analyzed at 2827.4 MWt.) For these analyses, a high power level is conservative. However, as discussed in the RAIs for the Westinghouse Electric Company (WEC) and Combustion Engineering (CE) plant categories, core power alone is not a sufficient metric to ensure that all plants in a given category are bounded. Instead, the combination core power level and barrel/baffle resistance is used. Once a blockage is applied at the core inlet, the flow required through the baffle must at least match the core boiloff flow rate. The core boiloff rate is defined by the core power level and decay heat model selected. The flow through the baffle is defined by the baffle resistance. Therefore, the core power level and baffle resistance must be considered together. As demonstrated in the response to RAI 4.4, the barrel/baffle resistance is the same for all operating B&W plants. Therefore, the core power level used in the B&W plant analyses bounds all operating B&W plants. Provided the plant power level is not above 2827.4 MWt (including instrument uncertainty), no additonal work is required.

Number of Fuel Assemblies:

All operating B&W plants have 177 fuel assemblies. This configuration is considered in the analysis plant model. Therefore, plant-specific confirmation of the number of fuel assemblies requires no further validation.

Barrel/Baffle Total K/A^2:

The barrel/baffle design for all of the operating B&W plants is identical. The response to RAI 4.4 provides the methodology for calculating the K/A^2 for this region for all B&W plants. The resulting K/A^2 values are used in the analysis plant model. Therefore, plant-specific confirmation of the barrel/baffle resistance requires no further validation.

Core Peaking:

The allowable Loss of Coolant Accident (LOCA) Linear Heat Rate (LHR) is produced from a reasonable combination of radial and axial peaking factors in the hot channel. A nominal axial peak of [ ] for all elevations is selected based on Reference 4.5-1. The hot channel radial peaking factor (RPF_{HC}) contribution is then used as a multiplicative factor to push the total normalized peak, F_q, where $F_q = RPF_{HC} * APF$, to the hot channel LOCA LHR limit (LHR_{HC}), where $LHR_{HC} = F_q * LHR_{core-ave}$.

As shown in part "b" and described in part "c" to this RAI, a core exit axial peaking profile was selected for the analysis. This profile is peaked to [ ] (as required by the Evaluation Model (EM) and peaked near the core exit ([ ] elevation of the heated core). This is the same profile used by the Small Break Loss of Coolant Accident (SBLOCA) EM.

The peak LHR limit was set to 17.3 kW/ft. This value bounds all operating B&W plants for a core exit peak.

Consistent with WEC nomenclature, the above limits equate to:

- Total peaking: [ ]
- Radial peaking: [ ]

The core reload methodology for the B&W plants (described in Reference 4.5-2) identifies the method that is used to verify the above parameters for cycle-specific application (i.e. each core reload). Since the above parameters are dependent on the core design, these parameters will need to be reconfirmed for each reload core to demonstrate the continued applicability of the analyses for GSI-191 application. That is, so long as the peak LHR limit for a core-exit peak is not above 17.3 kW/ft, no additional work is required.

ECCS Recirculation Flow Rate:

The ECCS injection rate during the transient has a direct effect on the core mixture level and cladding temperature response should core uncovering occur. Higher flow rates will provide significant excess flow above core boiloff. Lower flow rates may be closer to the core boiloff rate such that when blockage is imposed, decay heat removal may be challenged while the flow through the core is reconfigured to go through the barrel/baffle region instead of the core inlet. Studies presented in WCAP-17788-P, Volume 4 confirmed that lower flow rates are more conservative for the TH analyses. Therefore, a minimum flow rate for the B&W plants was targeted.

ECCS flow for the B&W plants consists of flow from the Core Flood Tanks (CFTs), Low Pressure Injection (LPI) system, and High Pressure Injection (HPI) system. Initiation of flow from the CFT is passive and occurs early in the event. The CFTs are typically empty

before 50 seconds for a Large Break Loss of Coolant Accident (LBLOCA). Since CFTs are passive, they are not subject to single failure assumptions. Since they empty early in the event (well before a blockage is imposed), they have no effect on the GSI-191 TH analyses. Therefore, no plant-specific validation is required for the CFTs.

The LPI flow rates were selected to bound the operating fleet of B&W plants. The minimum assured LPI flow before Sump Switch Over (SSO) is taken from the LOCA LHR limit analyses and is shown in Figure RAI-4.5-1. Before SSO, the values for Oconee Nuclear Station (ONS) were used. The minimum assured flow incorporates the limiting single failure assumption as described in RAI 4.1.

The HPI flow rates were also selected to bound the operating fleet of B&W plants. The minimum assured HPI flow before SSO is taken from the LOCA LHR limit analyses and is shown in Figure RAI-4.5-2. Before SSO, a composite curve that bounds all of the plants was used (shown as "Analyzed" in the figure). The minimum assured flow incorporates the limiting single failure assumption as described in RAI 4.1.

After SSO, the operators have the flexibility to throttle Emergency Core Cooling System (ECCS) flow depending on the Reactor Coolant System (RCS) conditions to manage pump Net Positive Suction Head (NPSH) or long term pump operation. When the core exit is not adequately subcooled the operators will try to maximize the ECCS flow, but may also throttle the flow for the reasons indicated with a reasonable minimum flow targeted flow of 2000 gpm to the RCS. In order to bound the possible flow rates after SSO and to account for the limiting single failure, the analysis reduced the total ECCS flow rate (LPI plus HPI) to 1500 gpm to the RCS.

Since the minimum assured ECCS flow rates are modeled in the analyses, plant-specific confirmation of the ECCS flow rate requires no further validation. Possible changes to the minimum flow rate in the future are covered by the plant design change process, which should include validation that the GSI-191 thermal hydraulic analyses remain applicable. Provided the ECCS flow rates is not below the flow rates analyzed, no additional work is required.

Containment Pressure During Recirculation:

As described in WCAP-17788, Volume 4, Section 4.2 (under break flow), the containment pressure is set to 14.7 psia to maximize the break flow rate. For shorter duration events, the pressure will likely be higher up to the point of SSO, but will decrease over time. For this analysis, it was modeled at a reasonable lower bound on containment pressure following a LOCA for the operating B&W plants. Therefore, this parameter requires no further validation.

ECCS Temperature After Sump Switchover:

The B&W plants include Decay Heat Heat-Exchanger (DHHE) to cool the sump fluid

before it is injected to the RCS as ECCS. The temperature exiting the DHHE is not readily available for each operating B&W plant. However, examination of an analysis for a B&W plant at power uprate conditions (3026 MWt) can provide a reasonable value for the sump temperature at the exit of the DHHE. (Note that a power level of 3026 MWt is significantly higher than the current power levels for the currently operating B&W plants as described above. A lower power level will add less energy to the fluid exiting the break in the long term such that the containment liquid temperature would decrease with power level. Consequently, the DHHE exit temperature would decrease with power level as well.) At the uprated power under post-LOCA conditions, the sump liquid temperature will peak at approximately [ ] one hundred seconds after a large Hot Leg Break (HLB); at 1200 seconds, the temperature will be approximately [ ]. At these sump conditions, the temperature leaving the DHHE will be less than [ ] and will decrease with time. It should be noted that these temperatures are achieved for containment pressures that are higher than the 14.7 psia identified above. The use of the different conditions assures a conservative solution for the TH analyses.

Based on this bounding analysis, a DHHE exit temperature used for the analysis was set to 200 °F. A sensitivity study on ECCS temperature during the recirculation phase of the event presented in RAI 4.16 demonstrated that lower ECCS temperatures during recirculation had no significant effect on the results. Therefore, use of 200 °F for the ECCS temperature during sump recirculation reasonably bounds the B&W fleet such that this parameter requires no further validation.

Sump Switchover Time:

For the TH analyses, a SSO time of 20 minutes was modeled. The plant switchover time is defined by the Borated Water Storage Tank (BWST) level at the start of the event and the ECCS and Containment Spray System (CSS) flow rates during the BWST drain period. In order to define the earliest switchover time, the minimum BWST level and maximum ECCS flow and CSS rates are assumed. Under these conditions, the earliest time of sump switchover was calculated for the operating B&W plants to be greater than 28 minutes. Therefore, the use of 20 minutes for the SSO time bounds the B&W fleet such that this parameter requires no further validation.

Figure RAI-4.5-1: B&W LPI Flow Rates before SSO

Figure RAI-4.5-2: B&W HPI Flow Rates before SSO

2.5.2.2 Part b

The axial power profiles used for the B&W analyses are provided in Figures RAI-4.5-3 and RAI-4.5-4.

Figure RAI-4.5-3: Elevation vs. Axial Power Profiles in Hot Pin/Channel for B&W Analyses

Figure RAI-4.5-4: Elevation vs. Axial Power Profiles in Average Channel for B&W Analyses

2.5.2.3 Part c

The axial power shapes for the B&W plants are defined by the EM described in Reference 4.5-1, Rev 00. For a typical cold leg break evaluation (which has been shown to be the limiting break location for Peak Cladding Temperature (PCT) considerations), calculations are performed at five locations within the core. The location of the peak power is analyzed at the mid-point between the spacer grid locations from approximately 2 feet to 10 feet above the bottom of the core (Reference 4.5-1, Volume 1, Section 4.3.2.2). For each axial power profile the peak local heating is iteratively increased in a

series of runs until the maximum local heating rate that meets the targeted range and will not exceed the acceptance criteria has been determined. The allowable LOCA LHR is produced from a reasonable combination of radial and axial peaking factors in the hot channel. The choice of these factors is set by choosing a nominal axial peak of [ ] for all elevations and using the hot channel radial peaking factor (RPF_{HC}) contribution as a multiplicative factor that pushes the total normalized peak, F_q, where $F_q = RPF_{HC} * APF$, to the hot channel LOCA LHR limit (LHR_{HC}), where $LHR_{HC} = F_q * LHR_{core-ave}$.

A radial versus axial peaking factor study justified the use of a constant axial peak of [ ] that adjusts the radial peaking factor to give the maximum allowable linear heat rate limit (Reference 4.5-1, Volume 1, Section A.5). The maneuvering analyses confirm the radial and axial peaks achieved in the core power distribution analyses are in a range that will not increase the PCT vs the radial and axial peaks that were analyzed. If they do not fall within the necessary range, the allowed LHR limit is reduced to protect the calculated PCT.

The axial power shape originally used for SBLOCA analyses with the Babcock & Wilcox Nuclear Technologies (BWNT) LOCA EM (Reference 4.5-1) used a [ ]. This is consistent with the uppermost axial peak from the LBLOCA LOCA limits axial power shape. The EM selected this peak to create a conservative SBLOCA PCT by reducing the power and the boiling rate below the mixture level and maximizing the heating rates in the uncovered region of the core. Comparisons of typical limiting full power Beginning of Life (BOL) axial peaks at the time the EM was being developed were used to show that an axial peak of [ ] was reasonable to bounding and it was fixed for use in the large LOCA applications and this shape was also applied to the SBLOCA applications.

At the time the EM demonstration cases were developed (1993-94), there was little to no core uncovering predicted by the SBLOCA analyses. Through the years since the approval of the EM, fuel cycle lengths have increased, fuel designs have changed, core designs have evolved (e.g., peaking, gadolinia fuel, axial blankets, etc.), and Steam Generator (SG) tube plugging has increased with the analyses applying bounding high levels of tube plugging. In addition, ECCS flows have changed due to HPI system modifications, pump degradation, uncertainty treatment, and power uprates. With these changes, the severity of some SBLOCA transients have increased with more significant core uncovering and increases to the length of time during which the core is uncovered. With these changes, the adequacy of the axial power shape used for SBLOCA was questioned.

Comparisons between the Beginning of Cycle (BOC) axial power shapes and the [ ] core elevation showed the latter was still bounding. For fresh

fuel, there are no burnup differences over the rod and axial peaking remains relatively flat. While it is possible to skew the peak below the core's mid-plane, it is difficult to force the peak to be high in the core due to the regulating rods being partially inserted throughout most of an operating cycle. However, because the regulating rods are partially inserted for most of the cycle, the Burn-up (BU) near the top of the core remains lower than that of the remainder of the core. Later in cycle, withdrawal of the regulating rods can cause the peaking to move up in the core. This exacerbates the peaking problem as the cycle progresses.

Comparisons of the [ ] against End of Cycle (EOC) axial power shapes were not as favorable because some of the axial shapes peaked in the [ ] range at this fuel time in cycle. Near EOC, the planned withdrawal of the regulating rods allows the flux profile to be skewed higher in the core where the burnup is lower. Thus, the SBLOCA axial peak location at the top of the core may not be sufficiently high enough to bound some of the flux peaks from the maneuvering analyses that reach approximately [ ]. The [ ] axial peaking factor remains reasonable to bounding, but the location of the peak was no longer supportable. Since a higher elevation axial peak would likely increase the PCT for cases that did predict core uncovering, a new SBLOCA axial peak location that bounded the [ ] elevation along the active fuel length (Reference 4.5-3). The EM stipulates the axial peaking factor to be [ ] and it will remain the same herein. Therefore, the [ ] axial peak power shape provided in RAI 4.5b is bounding for use in SBLOCA analyses and for GSI-191. The NRC found the general approach to be acceptable for demonstrating the LOCA limits methodology (Reference 4.5-1, p. LA-160). However, as future fuel or core designs evolve, the basic approaches that were used to establish these conclusions may change. Therefore, the NRC required that AREVA (FTI at the time) must re-validate the acceptability of the evaluation model peaking methods if: (1) significant changes are found in the core elevation at which the minimum core LOCA margin is predicted or (2) the core maneuvering analyses radial and axial peaks that approach the LOCA LHR limits differ appreciably from those used to demonstrate Appendix K compliance. These restrictions on the Short Term Core Cooling (STCC) LOCA applications are monitored for each subsequent fuel reload on a cycle-by-cycle basis.

The core inlet blockage from GSI-191 is applied during the Long Term Core Cooling (LTCC) phase of the LOCA. The highly skewed core exit peaks that can be achieved when the core is operating at power via the core maneuvering analyses that use of partial control rod insertion for roughly 8 hours until peak xenon builds in the bottom of the core. At the time of peak xenon, the control rods are fully withdrawn rapidly to achieve the highest core elevation axial peaks. The fission product isotopic concentrations in the fuel at the highest axial peaking location do not have sufficient time

to achieve values that approach infinite operation for the skewed xenon peaking condition. Therefore, the use of infinite operation decay heat conditions for a limiting top skewed power peak is very conservative for STCC LOCA applications. It is even more conservative for a LTCC LOCA application as the short-lived isotopes decay prior to the LTCC phase and the long-lived isotopes never achieve an equilibrium state at the highest peaking. Therefore, use of the skewed axial peak from the STCC LOCA applications is very conservative for the GSI-191 LTCC applications relative to core mixture level swell and PCT in the event the top of the core uncovers.

References - RAI 4.5

4.5-1 AREVA Document BAW-10192PA, Revision 0, *BWNT LOCA - BWNT Loss-of-Coolant Accident Evaluation Model for Once-Through Steam Generator Plants.*

4.5-2 AREVA Document BAW-10179PA, Revision 8, *Safety Criteria and Methodology for Acceptable Cycle Reload Analyses.*

4.5-3 *Response to Request for Additional Information (RAI) Regarding Topical Report BAW- 10192P, Revision 2, "BWNT LOCA- BWNT Loss of Coolant Accident Evaluation Model for Once-Through Steam Generator Plants (ML102100201).*

2.6 RAI 4.6

2.6.1 Statement of RAI 4.6

The evaluation models (EMs) used for the LOCA T-H computational analyses are described in Section 5. The plant models used to perform the analyses for each plant category presented in Sections 8 through 11 are described in Section 6. Table 1 below summarizes the computer codes and models used in these analyses.

Table 1: Identification of Computer Codes and Plant Models Used in the Thermal-Hydraulic Computational Analyses

Code and Plant Model Used	**Plant Category**			
	Westinghouse Upflow BB Plant Category	**Westinghouse Downflow BB Plant Category**	**CE Plant Design**	**B&W Plant Category**
System Code	WCOBRA/TRAC MOD7A	WCOBRA/TRAC MOD7A	S-RELAP5	RELAP5/MOD2-B&W
Code Version	Not provided	Not provided	Provided	Provided
EM Topical Report	WCAP-14747 (CQD), WCAP-16009-NP-A (ASTRUM)	WCAP-14747 (CQD), WCAP-16009-NP-A (ASTRUM)	[ ]	[ ]
Code Modified for WCAP-17788 Methodology	Yes (see Section 5.1)	Yes (see Section 5.1)	Yes	No
Base Plant Model	Westinghouse four-loop BE plant model	Westinghouse three-loop BE plant model	CE high-power BE plant model	B&W high-power Appendix K plant model (SBLOCA)

Provide the following information:

(a) Identify the code version of WCOBRA/TRAC MOD7A used in the analyses in Sections 8 and 9.

(b) Clarify if NRC staff approval of subsequent TRs related to WCOBRA/TRAC, S-RELAP5, and RELAP5/MOD2-B&W can have an impact on the EMs applicability or validity of the T-H analysis results presented in WCAP-17788-P.

(c) As seen in Table 1 above, code modifications were made to both WCOBRA/TRAC and S RELAP5 for the analyses presented in Volume 4 of WCAP-17788-P. Section 5.1 explains that "in order to simulate transient resistance at the core inlet due to the build-up of debris, it was necessary to modify the baseline WCOBRA/TRAC version". Letter OG-16-42 dated February 12, 2016, described a modification of the

baseline S-RELAP5 code version to produce "a development version of S-RELAP5" that was used to obtain the updated analyses submitted with OG-16-42 to replace the original results in Section 10 of Volume 4. Describe briefly the code changes and provide the validation and verification results for the "single-application" WCOBRA/TRAC code version and the S-RELAP5 "development version". Confirm that the code modifications were performed in conformance with applicable quality assurance procedures and provide references to related documents for both code modifications.

2.6.2 Response to RAI 4.6

2.6.2.1 Part a

This RAI pertains to the Westinghouse Electric Company (WEC) plant categories and therefore requires no response for the B&W plant category.

2.6.2.2 Part b

The EM for the B&W plants is given in BAW-10192P-A Revision 0 (Reference 4.6-1) plus any changes that were adopted under 10 CFR 50.46. This deterministic Evaluation Model (EM) method was used for the analyses provided in WCAP-17788-P and any Request for Additional Information (RAI) responses applicable to the B&W plant design. The blowdown system code used for the deterministic EM analyses is RELAP5/MOD2-B&W (BAW-10164P-A Revision 6, Reference 4.6-2). This code is used for the blowdown phase of the Double-Ended Guillotine (DEG) Hot Leg Break (HLB) Short Term Core Cooling (STCC) analyses. The BEACH (BAW-10166P-A Revision 5, Reference 4.6-0) topical report describes the code used for core refill and reflood phases for a DEG hot leg break. The Large Break Loss of Coolant Accident (LBLOCA) methods used for the STCC were compared to those from the Small Break Loss of Coolant Accident (SBLOCA) methods in the response to RAI 4.22 wherein the RELAP5/MOD2-B&W system code with SBLOCA methods was validated for extension of the results into the Long Term Core Cooling (LTCC) phase of the Loss of Coolant Accident (LOCA).

Since the start of work to support WCAP-17788-P, a supplement to BAW-10192P-A (Reference 4.6-3) has been prepared and submitted to the Nuclear Regulatory Commission (NRC) for review and approval. This supplement addresses Thermal Conductivity Degradation (TCD) with fuel burnup and how it is addressed in the EM. The changes incorporated in the new supplement were primarily to increase the Volume Average Fuel Temperature (VAFT) and the change in the fuel properties for higher

burnup rods at elevated Time in Life (TIL). The thermal-hydraulic analyses that were performed for WCAP-17788 used Beginning of Life (BOL) fuel pin initial conditions as BOL has the highest peaking or Linear Heat Rate (LHR) for all TIL. Some of the fuel pin initialization adjustments that were developed for TIL analyses will also be used for future STCC BOL initialization techniques, however these changes do not change the approach or conclusions of the WCAP-17788-P LTCC analyses, which show that the core remains covered with a two-phase mixture for the entirety of LTCC, even when a complete core inlet blockage is imposed at 20 minutes during a DEG HLB transient. The core decay heat is removed constantly by the nucleate boiling in the core region and this continuous heat removal during a boiling pot phase of the event is unaltered by the TCD modifications. Therefore, the subsequent topical report review will not alter the applicability or validity of the thermal-hydraulic analyses contained in WCAP-17788-P, Volume 4 and the RAI responses.

In the future, other items may be discovered that require code or EM changes. Once the GSI-191 analyses are approved, then they become part of the Analysis of Record (AOR) for LTCC and would need to be reassessed when a new issue or error is discovered. Changes to the GSI-191 analyses will be evaluated and addressed appropriately based on the AREVA procedures governing errors in codes or results of approved methodologies if some future deviations in the analysis approach is deemed necessary.

2.6.2.3 Part c

This RAI pertains to the WEC and Combustion Engineering (CE) plant categories and therefore requires no response for the B&W plant category.

References - RAI 4.6

4.6-1 AREVA Document BAW-10192PA, Revision 0, *BWNT LOCA - BWNT Loss-of-Coolant Accident Evaluation Model for Once-Through Steam Generator Plants.*

4.6-2 AREVA Document BAW-10164PA, Revision 6, *RELAP5/MOD2-B&W - An Advanced Computer Program for Light Water Reactor LOCA and NON-LOCA Transient Analysis.*

4.6-3 AREVA Document BAW-10192PA, Revision 0, Supplement 1P, Revision 0, *BWNT LOCA - BWNT Loss-of-Coolant Accident Evaluation Model for Once-Through Steam Generator Plants.*

2.7 RAI 4.7

2.7.1 Statement of RAI 4.7

Section 4 states "it was determined that all computer codes and methods utilized have the ability to accurately predict the RCS response to simulated core inlet blockage during the sump recirculation phase of the post-LOCA transient". Describe the technical basis for this determination for each code methodology used in the analyses. Include identification and description of key governing processes and explain how the code capabilities were evaluated in terms of adequacy for the modeling of such processes. Explain how the code capabilities and accuracy in predicting the system and core response, including important parameters associated with the consequences of core inlet blockage, were evaluated. Include comparisons and assessments using experimental data as applicable.

2.7.2 Response to RAI 4.7

The RELAP5/MOD2-B&W blowdown system code (Reference 4.7-1) has had extensive Verification and Validation (V&V) and NRC review for use in Loss of Coolant Accident (LOCA) and non-LOCA licensing applications for the B&W-designed Pressurized Water Reactor Systems. The same code with the two-dimensional core heat structure rezoning activated is used to calculate the core refill and reflooding phase of the event using the models described in the BEACH (Reference 4.7-0) topical report. The V&V process for the code includes benchmarks to a wide range of separate effects tests (e.g. THTF, FLECHT, CCTF, SCTF, G2, REBEKA and ARC 19 tube OTSG) and integral system experimental facilities (e.g. ROSA, MIST, OTIS, LOFT, SEMISCALE, UPTF and SCTF) as well as, plant transients (e.g. ONS NC Event, TMI-2 LOFW, Rancho-Seco Loss of ICS Power, and TMI-1 NC tests) used to validate the B&W non-LOCA safety analysis topical report (Reference 4.7-2). The accuracy and quality of the predictions to the data is provided by the benchmark comparisons given in the topical reports (References 4.7-1 and 4.7-0).

The benchmarks selected cover critical aspects of the Small Break Loss of Coolant Accident (SBLOCA), Large Break Loss of Coolant Accident (LBLOCA), and non-LOCA events and related thermal-hydraulic phenomena. Most of the benchmarks that were performed cover phenomena and processes that are important to and control the evolution of the (Short Term Core Cooling (STCC)) transient phase of a LOCA. Boric Acid Precipitation (BAP) mitigation during the Long Term Core Cooling (LTCC) phase following a Cold Leg Pump Discharge (CLDP) LOCAs is also evaluated using a simple extension of STCC methods to determine the mass inventory in the Reactor Vessel (RV)

when the plant is in an extended boiling pot phase that exists following core quench. In addition, benchmarks of various Rod Bundle Heat Transfer (RBHT) tests were recently performed to confirm the applicability of the code to calculate the core void distribution during low pressure, low decay heat conditions encountered during LTCC GSI-191 scenarios (see response to RAI 4.8). While there are some subtle differences in the liquid inventories due to the CLDP LOCA versus the post-quench Hot Leg Break (HLB) LOCA scenario seen in the WCAP-17788-P application, the important physical processes (like the core void distribution) and key boundary conditions (like the decay heat contributions) are similar.

In the WCAP-17788-P analyses following the short-term LOCA phase (after core quench), the RV refills until the mixture level reaches the break location. Once at this elevation, the core Decay Heat (DH) is removed via single pass heat exchanger type configuration where the Emergency Core Cooling System (ECCS) is injected into the cold legs or upper Downcomer (DC) and flows into the lower plenum and core based on the manometric balance between the DC and core collapsed liquid levels. The DH is removed by the ECCS by first heating the fluid to saturation and then boiling in the core if there is insufficient subcooling of the ECCS fluid. The saturated nucleate boiling at low pressures creates substantial core and upper plenum mixture level swell that rises to the elevation of the HLB. Once the mixture level rises to the break elevation, the steam produced in the core along with any excess ECCS liquid not boiled off, simply spills out of the break. The core and upper plenum collapsed level is supported by the water level in the DC. The DC level must also include an elevation head to push the ECCS and any condensate into the core, up and out the break.

This simple boiling pot configuration is not nearly as complicated or complex as the blowdown and reflooding phases of the event. The ECCS flow is injected into a steam space, in either the upper DC for the low pressure injection or into the cold leg for the high pressure injection. The injection into a steam space allows efficient condensation of steam. The ECCS that is heated by the condensation process, plus the condensate, fall downward into the DC pool. This flow pattern supports and perpetuates the manometer that forces flow into the core.

While there is a direct throughput in the RV, the core region has additional internal circulation paths that occur due to variations in the core power densities within the fuel. This internal flow pattern is in an upward direction in the higher power regions in the core while it is in the downward direction in the low power periphery regions or in the core baffle region. The conditions present in the WCAP-17788-P analyses for this phase are quasi-steady, until the blockage of the core is applied. This phase (after the short-term LOCA phase) is representative of a boiling pot, where the phenomena is not complex and is easily within the code predictive capabilities.

Once the blockage of the core inlet is postulated, the net throughput flow pattern is perturbed as is the internal circulation within the core. The net throughput that is

controlled by the quiescent collapsed levels, change in response to the altered core inlet resistances and flow rates. The initial loss of core flow causes a momentary small reduction in the core collapsed level from the continuous boil-off that had existed to remove the core DH. The increased resistance at the core inlet causes the DC level leg of the manometer to rise due to the momentary loss of core inlet flows. Within a minute, the reduced core levels and increased DC levels achieve a new manometric forcing function sufficient to reverse the direction of flow in the lower baffle region. The flow from the lower plenum enters the baffle and flows through the large openings in the lower grid rib and former plates until it reaches the lower most row of pressure relief holes (otherwise known as LOCA holes shown in Figure RAI-4.23-1) in the baffle plates (see response to RAI 4.4 for baffle details). Once this flow pattern is established (see Figure RAI-4.23-3), it restores the single pass core cooling (equivalent to the ECCS injection flow rate) that existed prior to establishment of a total core inlet blockage. This Alternate Flow Path (AFP) with flow up through the baffle region maintains the mixture in the upper plenum via the core collapsed levels that are supported by the DC collapsed level.

The low resistance of the AFP in the B&W plants only slightly perturbs the core and DC levels that were established prior to the core inlet blockage when the ECCS flows remain similar. Changes in ECCS flow before and after sump switchover can change the manometric balance between the DC and the core. At the time of sump switchover the DH determines the core mixture level and requires a specific collapsed level to support this mixture level. The DC level is higher than the core collapsed level based on the aggregate resistance between the DC and the core. Prior to core inlet blockage the resistance is small, but following inlet blockage the resistance to flow increases as the ECCS flow has to enter the core through the AFP. The DC level must increase to overcome this slightly higher resistance through the AFP. However, the ECCS flows after sump switchover are less than those when taking suction from the Borated Water Storage Tank (BWST). Therefore, the amount of DC level increase needed is limited.

With the establishment of the core inlet blockage and AFP, the internal core flow patterns change slightly. The ECCS flow and condensate now enters the core from the baffle region through the periphery LOCA holes in the baffle plates. The flow from the AFP will combine with the downward internal circulation flow and travel down to the bottom of the core. These mixed fluids, flow across to the inner fuel assemblies and upward in the higher power core regions. While there are some small changes in how and where the flows enter the core, the power differences that established the internal core circulation prior to blockage are still present and still drive the internal circulation within the core region after the blockage is imposed. As such, the good mixing from the internal core circulation continues after the blockage and the code can predict such a scenario. The flow split between the AFP and the core inlet is a simple flow network calculation, which a system code like RELAP5/MOD2-B&W can easily predict.

The main phenomena that control the WCAP-17788-P analyses in the B&W-designed

plants are as follows:

- **Void distribution/mixture level swell** - Capturing the void distribution in the core and upper plenum regions, as well as the resulting mixture level swell, is an important phenomenon for this event. The amount of mixture level swell during the transient progression supports continuous core coverage due to the low resistance of the AFP in the B&W-designed plants. Benchmarks were performed with RELAP5/MOD2-B&W to show the predictive capabilities relating to the core boiling pot void distribution and mixture level swell at pressures near atmospheric pressure. These results are provided in response to RAI 4.8.

- **Decay heat modeling** - The amount of decay heat controls the steam production rate and the core mixture level swell. If the core becomes uncovered, the DH will also influence the rate of cladding heat-up. The RELAP5/MOD2-B&W code has several of the American Nuclear Society (ANS) standards for decay heat built in to the code and has the ability to include a multiplier on the decay heat. For the WCAP-17788-P analysis, the 1973 ANS Decay Heat Standard (Reference 4.7-3) was used with a 1.2 multiplier on the fission product decay with an infinite operation assumption. All fissions come from U-235 with a fission energy of 200 MeV/fission. In addition, the default actinide capture decay power is computed from the 1979 ANS Decay Heat Standard equations (Reference 4.7-4) and is included.

- **Liquid carryover from Upper Plenum to Hot Leg** - There is a continuous flow of liquid that is carried to the hot leg due to the quiescent mixture level in the upper plenum that is sufficient to continuously flow liquid out of the break. This is important both from a RV inventory (potential Peak Cladding Temperature (PCT) impact only if the core uncovered) and a BAP control point of view. A detailed discussion of the liquid carryover from the upper plenum is provided in the response to RAI 4.23.

- **Core inlet resistance due to debris accumulation** - The value of the resistance applied at the core inlet due to debris, as well as how the resistance is increased, is an important factor for the WCAP-17788-P analysis.

  The amount of resistance sets the effective blockage of the core and the amount of makeup flow that can enter from the bottom. Perhaps even more important is the rate at which the core blockage is applied. If the buildup of debris is slow, the system levels have time to response and the core levels remain quasi-steady such that the core does not uncover as the AFP flow rapidly increases to effectively the same as the ECCS flow. The AFP flow is in excess of the boil-off rate due to decay heat before the core can uncover. An instantaneous increase in the blockage is the most restrictive as it abruptly restricts flow through the core inlet. The flow then has to quickly divert through the AFP, which has a higher resistance than an unblocked

core. In order for sufficient flow to get through the AFP, the core and DC levels need to change. The rate at which the DC level can change depends on the amount of (ECCS) flow available with the lower flow rates being more limiting than higher flow rates. Therefore, the most limiting scenario is an instantaneous blockage with a minimum ECCS flow as was modeled in the WCAP-17788-P analysis.

The RELAP5/MOD2-B&W code will directly use the resistance values and ramp rate entered. These single-phase flow pressure drops at high resistance and low flow conditions can be properly predicted by the code.

- **AFP ΔP form losses** - The ΔP form losses of the AFP is important as it determines how much the DC level has to build before sufficient flow is available once core blockage occurs.

  The RELAP5/MOD2-B&W code will directly use the form losses provided by the analyst (as described in the response to RAI 4.4). The corresponding single-phase flow pressure drops are modeled by the code based on the well understood theory of single-phase flow.

- **Single-phase flow split between core and Barrel/Baffle** - Related to core inlet blockage and AFP ΔP form losses, the code must be able to partition the flow coming from the DC and lower plenum between the inlet of the core and the AFP. The flow is single-phase liquid. The partitioning of the flow is a basic flow network with the various resistances modeled and can be easily modeled with a system code like RELAP5/MOD2-B&W without any difficulties.

References - RAI 4.7

4.7-1 AREVA Document BAW-10164PA, Revision 6, *RELAP5/MOD2-B&W - An Advanced Computer Program for Light Water Reactor LOCA and NON-LOCA Transient Analysis*.

4.7-2 AREVA Document BAW-10193P-A, Revision 0, *RELAP5/MOD2-B&Wfor Safety Analysis of B&W-Designed Pressurized Water Reactors*.

4.7-3 American Nuclear Society Proposed Standard, ANS 5.1, Decay Energy Release Rate Following Shutdown of Uranium-Fueled Thermal Reactors, October 1971, Revised October 1973.

4.7-4 American Nuclear Society ANSI/ANS-5.1-1979, *American National Standard for Decay Heat Power in Light Water Reactors*.

2.8 RAI 4.8

2.8.1 Statement of RAI 4.8

Adequate prediction of the two-phase mixture level swell under core pool boiling conditions at atmospheric or close to atmospheric pressures during the long term core cooling (LTCC) phase of a PWR LOCA is of primary importance for demonstrating adequate core cooling in association with core inlet blockage. Sections 6.1 and 6.2 state "it is known that the version of WCOBRA/TRAC utilized tends to over predict two-phase mixture level swell in the core under low pressure pool boiling conditions (Reference 6-1). To account for this, a multiplier on the core axial interfacial drag is applied consistent with the approach taken in Reference 6-1". Reference 6-1 is listed in Section 6.5 as follows.

Reference 6-1: WCAP-15644-P, Rev. 2 (Proprietary) and WCAP-15644-NP, Rev. 2 (Non Proprietary), "AP1000 Code Applicability Report," March 2004.

Revised Section 7.1.1, "Debris Collection at the Core Inlet," of WCAP-17788-P Vol. 1, provided with Letter CAW-15-4339 dated November 24, 2015, further clarifies that an "interfacial drag multiplier of 0.8 x nominal" was used to analyze a double-ended cold leg break in a three-loop Westinghouse plant "consistent with Westinghouse NSSS analyses in WCAP-17788, Volume 4". Sections 8 through 11 of Vol. 4 provide no information relative to the capabilities of the other codes used for the analyses to predict two-phase mixture level swell in the core under low pressure pool boiling conditions. Also, Reference 6-1 has not been approved by the NRC.

(a) Provide assessment results that demonstrate the codes used for the analyses documented in Sections 8 through 11 adequately predict two-phase mixture level swell under core pool boiling conditions at pressures close to atmospheric. These results should be based on level swell test data relevant to the analyzed plant conditions. Provide figures comparing code predictions to low pressure test data. Include tables identifying the test facilities, test runs, test flow conditions, measured void fractions, and predicted void fractions for the code assessments performed.

(b) Clarify whether the "interfacial drag multiplier of 0.8 x nominal" identified in revised Section 7.1.1 was used in the HLB LOCA analyses in WCAP-17788-P Vol. 4 performed with WCOBRA/TRAC. If the multiplier was used in the analyses presented in Vol. 4:

  (i) Describe the basis for determining the multiplier value.

  (ii) Provide data assessments and the established range for this multiplier.

  (iii) Demonstrate the applicability of the multiplier value to near-atmospheric pressure conditions.

(iv) Explain whether the multiplier has a significant impact on t_{block}, K_{max}, K_{split}, and m_{split}. Use results of sensitivity studies, if necessary, to demonstrate the acceptability of the results in Section 8 and 9 in this regard.

(c) Explain how interfacial drag was treated in the codes used for the CE and B&W analyses in Sections 10 and 11, respectively. Provide the information requested in Item b above as it applies to the EMs used for the analyses of the CE and B&W design categories.

2.8.2 Response to RAI 4.8

2.8.2.1 Part a

The prediction of the mixture level, the void distribution below the mixture level, and the cladding thermal response above the mixture level in the core during the core uncovering following a Loss of Coolant Accident (LOCA) are of paramount importance under low flow conditions. During the post core quench, the superficial liquid velocities in the core are small. Consequently, the acceleration and viscous forces will be negligible compared to the buoyancy force in predicting the two-phase flow distribution in the core. As a result, a simplified approach can be used to extend the bundle boil-off benchmark results to different decay heat power levels.

RELAP5/MOD2-B&W (References 4.8-2 and 4.8-0) has been extensively benchmarked against a wide range of test facilities. These benchmarks demonstrate that the code can predict the thermal-hydraulic response within the core region during core uncovering following a Small Break Loss of Coolant Accident (SBLOCA), or during the reflooding phase of a Large Break Loss of Coolant Accident (LBLOCA), for a B&W or a Westinghouse 3- and 4-loop Pressurized Water Reactor (PWR) with cold leg Emergency Core Cooling System (ECCS) injection. The LOCA benchmarks simulated using RELAP5/MOD2-B&W also demonstrate that the code can predict the core thermal response during the Long Term Core Cooling (LTCC) phase of the event. For LBLOCAs that have a lower plenum refill phase, the RELAP5/MOD2-B&W code with the two-dimensional heat structures activated during the reflooding phase of the event is used. In this mode, the code is referred to as BEACH. The reflooding phase core benchmarks performed for BEACH were in the 14.7 to 73 psia range.

For the GSI-191 thermal-hydraulic analysis, the code is used to predict results at low pressures. To add confidence to these RELAP5/MOD2-B&W predictions, additional low power, low pressure benchmarks were performed. Seven Rod Bundle Heat Transfer (RBHT) (References 4.8-3 and 4.8-4) bundle boil-off tests were simulated using RELAP5/MOD2-B&W. These tests used low bundle inlet flow rates, an upper plenum

pressure of approximately 20 psia, and power levels equivalent to the decay heat at 2000 to 4000 seconds after reactor shut down.

Upper plenum pressure (psia)	19.4 – 29.4
Bundle power (kW)	54 – 77
Inlet mass flow rate (lbm/s)	0.039 – 0.164
Inlet fluid temperature (F)	131 – 205

Figure RAI-4.8-1 shows the calculated versus measured void fraction for the seven tests. A twenty second running average is used in obtaining the calculated void fraction. The plot shows reasonable to excellent agreement, with most of the points within a ± 20 percent relative error band.

Bundle uncovering was noted in the four RBHT tests benchmarked using RELAP5/MOD2-B&W. In these cases, the code predicted rod surface temperatures in all four tests were [ ] the test data. From the RBHT tests benchmarks, it is also concluded that RELAP5/MOD2-B&W will calculate higher cladding thermal response in the event of core uncovering.

From a review of the available literature, it was found that very few bundle boil-off tests are available to benchmark the codes at 20,000 to 30,000 second decay heat levels. Therefore, a simple phenomenological approach was developed to extend these benchmark results to lower decay heat levels (20,000 to 30,000 seconds after reactor shut down). Several pool void fraction correlations were reviewed. It was found that for a given plant case with constant containment pressure, the functional relationship between the void fraction and the superficial steam velocity given by

$$\alpha_g = f(j_g), \qquad \text{(RAI-4.8-1)}$$

can be used to extend the benchmark results to different decay heat power levels. This approach was verified by sensitivity studies using an RBHT test benchmark case and by the evaluation of a Combustion Engineering (CE) plant case. Wilson (Reference 4.8-5) and Cunningham-Yeh (Reference 4.8-6) correlations were also used in the evaluation.

It should be noted that the majority of the correlations used in calculating the flow regimes and the interphase drag correlations were developed by the well-known researchers like Taitel, Wallis, Wilson, and Ishii using primarily air-water test data. Therefore, these correlations are appropriate in the calculation of the void fractions in the core and in the Upper Plenum (UP) during the long-term core cooling following a LOCA. In addition, since α_g is primarily a function of j_g, the majority of the parameters used in various sensitivity studies conducted in responding to several RAIs will have only secondary effects in the core and in the UP thermal-hydraulic behavior.

From the RBHT test benchmarks, and the approach developed to extend the benchmark results to lower power levels, it is concluded that RELAP5/MOD2-B&W will correctly

predict the void distribution in the core during post core quench following a Double-Ended Guillotine (DEG) cold or hot leg break in a B&W- or Westinghouse-designed plant.

Figure RAI-4.8-1: RBHT Summary RELAP5/MOD2-B&W: Calculated vs. Measured Void Fraction for Seven RBHT Tests

2.8.2.2 Part b

This RAI pertains to the Westinghouse Electric Company (WEC) plant categories and therefore requires no response for the B&W plant category.

2.8.2.3 Part c

The small break LOCA model used for the Babcock & Wilcox (B&W) analyses included an interfacial drag multiplier of [ ] (Reference 4.8-1). The benchmarks provided in part 'a' above confirm application of this multiplier to the B&W plants. As described above in part 'a' above, the comparison of the code for near-atmospheric conditions to

the RELAP5/MOD2-B&W benchmarks were acceptable to excellent. Further, the ECCS flow rate for the B&W plants is well in excess of what is needed to replace that which is boiled off in the core. The ECCS flow rate in combination with the very low resistance through the baffle region ensures that the core remains covered and liquid continues out the break even in the event of a complete blockage of the core inlet. Therefore, the calculation of t_{block} and K_{max} using RELAP5/MOD2-B&W for the B&W plants are appropriately calculated and reasonable variations in the drag multiplier (i.e., $\pm 20\%$) will have no effect on the results for the B&W plants. Note that this conclusion would also apply to calculations of K_{split} and m_{split}; however, the analyses to calculate these parameters are no longer needed as described in the response to RAI 4.20.

References - RAI 4.8

4.8-1 AREVA Document BAW-10192PA, Revision 0, *BWNT LOCA - BWNT Loss-of-Coolant Accident Evaluation Model for Once-Through Steam Generator Plants*.

4.8-2 AREVA Document BAW-10164PA, Revision 6, *RELAP5/MOD2-B&W - An Advanced Computer Program for Light Water Reactor LOCA and NON-LOCA Transient Analysis*.

4.8-3 Hochreiter, L. E., et al., Rod Bundle Heat Transfer Facility Two-Phase Mixture Level Swell and Uncovery Test Experiments Data, NUREG/CR-7218, Volume 1, September 2016.

4.8-4 Hochreiter, L. E., et al., Rod Bundle Heat Transfer Facility Two-Phase Mixture Level Swell and Uncovery Test Experiments Data, NUREG/CR-7218, Volume 2, September 2016.

4.8-5 R.J. Grenda J.F. Wilson and J.F. Patterson ANS Transactions, Vol 5, *The Velocity of Rising Steam in a Bubbling Two-Phase Mixture*.

4.8-6 Cunningham, J. P., and Yeh, H. C., Experiments and Void Correlations for PWR Small-Break LOCA Conditions, Trans. Amer. Nucl. Soc., Vol 17, pp. 370-371, 1973.

2.9 RAI 4.9

2.9.1 Statement of RAI 4.9

Sections 8 through 11 provide LOCA T-H analysis results for determining the earliest transient point in time, t_{block}. T_{block} is defined so that the acceptance criteria for maintaining LTCC would be satisfied should complete core inlet blockage occur at or after this point in time following a HLB LOCA. Figures 8-16 (Case 1B), 9-15 (Case 1A), 10-13 (Case 1), and 11-9 (Case 1) show the core peak cladding temperature (PCT) responses following the application of complete core inlet blockage with temperature excursions being observed in Figures 8-16 and 9-15. Provide the following information in a table format (where applicable) for the limiting analyses. For example, Case 1B in Section 8 and Case 1A in Section 9 for each plant category. Include the axial void fraction profile results (Item c) in separate tables. If a parameter exhibits an oscillatory behavior within the vicinity of the time point of interest, include the parameter's variation range along with the observed predicted value itself.

(a) Provide the following prediction results relative to the PCT excursions:

  (i) Time of PCT (relative to break opening)
  (ii) PCT
  (iii) The core channel and axial elevation associated with the PCT location

(b) Provide the following results relative to the axial elevation in the channel where the PCT was observed and the timing of PCT:

  (i) Fuel rod local linear heat generation rate
  (ii) Predicted two-phase flow regime
  (iii) Vapor/liquid mass flow rates and mass fluxes for predicted continuous/dispersed flow fields (axial and cross-flow)
  (iv) Vapor/liquid phase velocities for predicted continuous/ dispersed flow fields (axial and cross-flow)
  (v) Wall heat transfer mode
  (vi) Fuel rod heat transfer fluxes to continuous/dispersed flow fields (clarify if any radiation heat transfer of significance was predicted)
  (vii) Heat transfer coefficients to continuous/dispersed flow fields.

(c) Provide the axial void fraction distribution in the channel where the PCT was observed at the time when the PCT occurred and corresponding predicted two-phase mixture level in the channel.

(d) Identify the closure heat transfer correlations associated with the heat transfer regimes identified as controlling with regard to the PCT values in Figures 8-16 and 9-15. Provide the ranges of applicability of these correlations and compare them against the predicted core limiting T-H parameters.

(e) Identify the constitutive correlations for computing void fraction and any predicted entrained droplets/liquid film fields, as applicable, associated with the two-phase flow regime predicted at the PCT location and time of its occurrence. Provide their ranges of applicability and compare them against the predicted core limiting T-H parameters.

2.9.2 Response to RAI 4.9

(a) Once the core is quenched and Long Term Core Cooling (LTCC) has begun, the Babcock & Wilcox (B&W) plants do not uncover the core. Consequently, there is no cladding heatup after the blockage is imposed at 1200 seconds in the B&W analysis. Therefore, the requested data are not pertinent with respect to Peak Cladding Temperature (PCT) after core blockage.

(b) As noted above in the response to RAI 4.9(a), the requested data are not pertinent with respect to PCT after core blockage. Instead, the data are provided at 1290 seconds, a convenient edit in the output file 1.5 minutes after imposing a complete core blockage at 1200 seconds. The requested data at the peak power location in the hot channel are provided in Table RAI-4.9-1.

Table RAI-4.9-1: RAI 4.9(b) – Requested Data for B&W Plants at Peak Power Location in Hot Channel

Parameter	Value
Fuel rod local linear heat generation rate	0.44 kW/ft
Predicted two-phase flow regime	annular-mist
Vapor mass flow rates and mass fluxes for predicted continuous/dispersed flow fields (axial and cross-flow)	flow: Figure RAI-4.9-1 flux: Figure RAI-4.9-2
Liquid mass flow rates and mass fluxes for predicted continuous/dispersed flow fields (axial and cross-flow)	flow: Figure RAI-4.9-3 flux: Figure RAI-4.9-4
Vapor phase velocities for predicted continuous/ dispersed flow fields (axial and cross-flow)	Figure RAI-4.9-5
Liquid phase velocities for predicted continuous/ dispersed flow fields (axial and cross-flow)	Figure RAI-4.9-6
Wall heat transfer mode	Saturated Nucleate Boiling
Fuel rod heat transfer fluxes to continuous/dispersed flow fields (clarify if any radiation heat transfer of significance was predicted)	3.63 Btu/s-ft^2 Note 1 (no radiation)
Heat transfer coefficients to continuous/dispersed flow fields	0.44 Btu/s-ft^2-F

Note 1. Since the liquid at this location is saturated, all of the energy is available for vapor generation.

Figure RAI-4.9-1: Vapor Mass Flow Rates

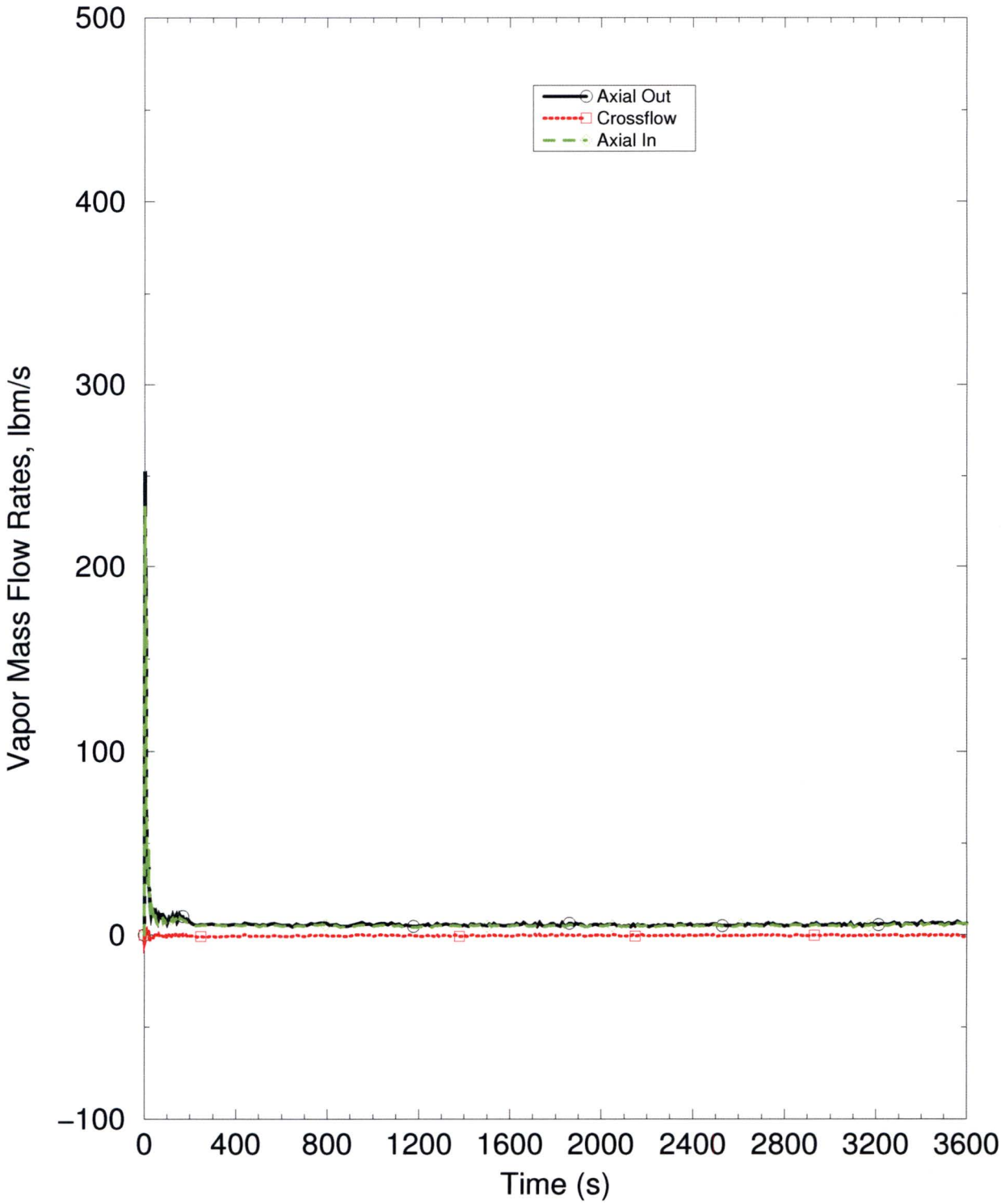

Figure RAI-4.9-2: Vapor Mass Fluxes

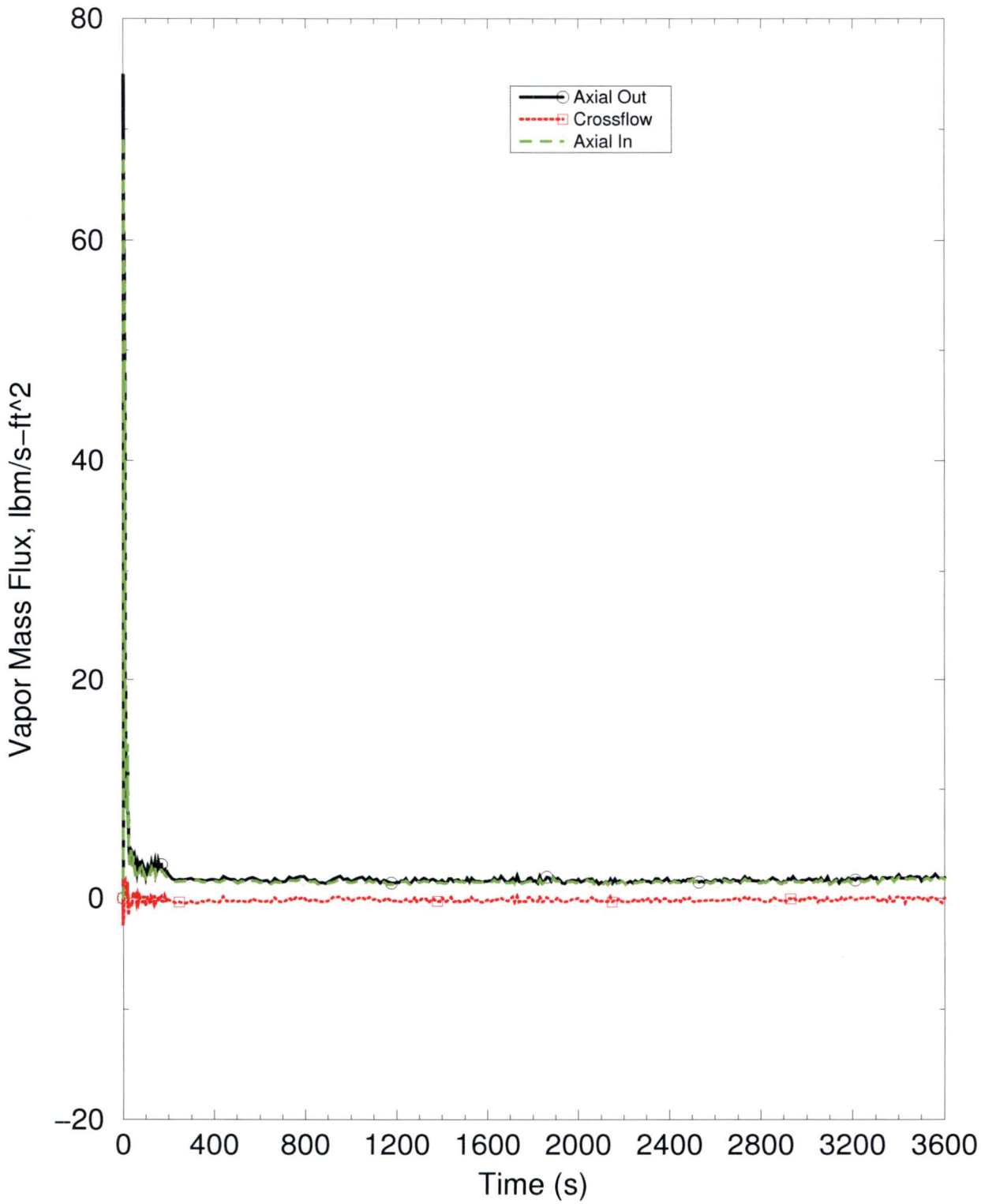

Figure RAI-4.9-3: Liquid Mass Flow Rates

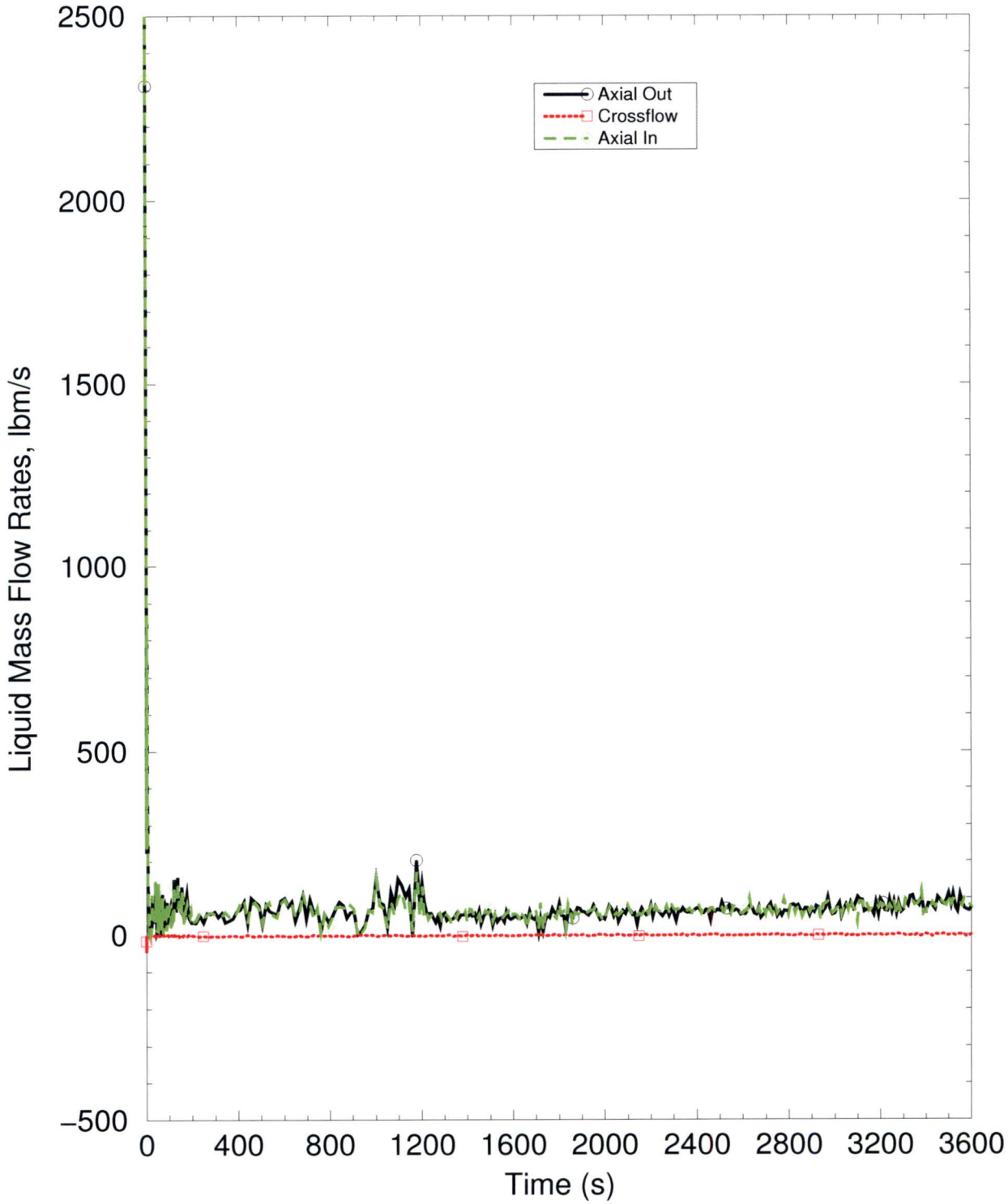

Figure RAI-4.9-4: Liquid Mass Flux Rates

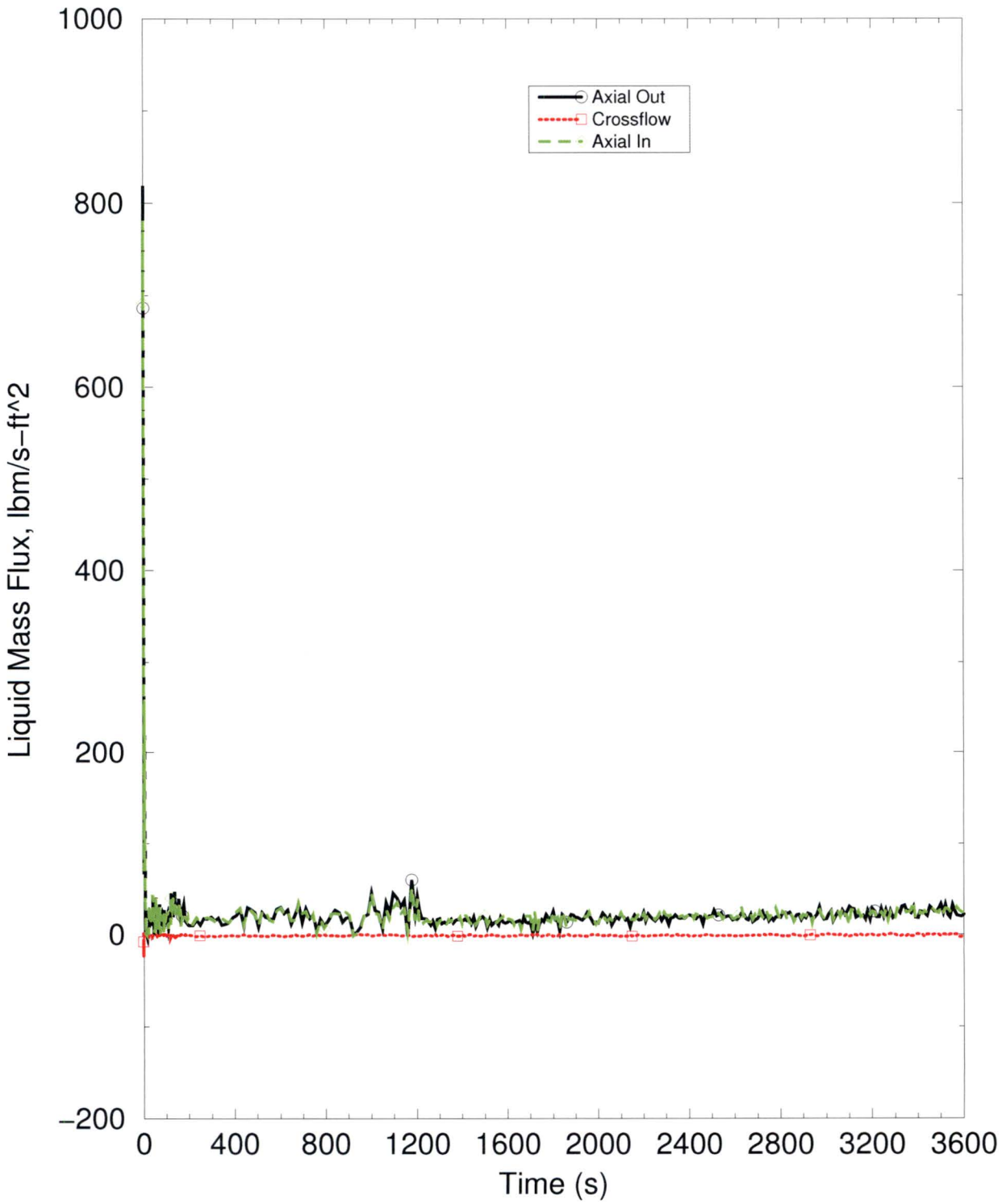

Figure RAI-4.9-5: Vapor Velocities

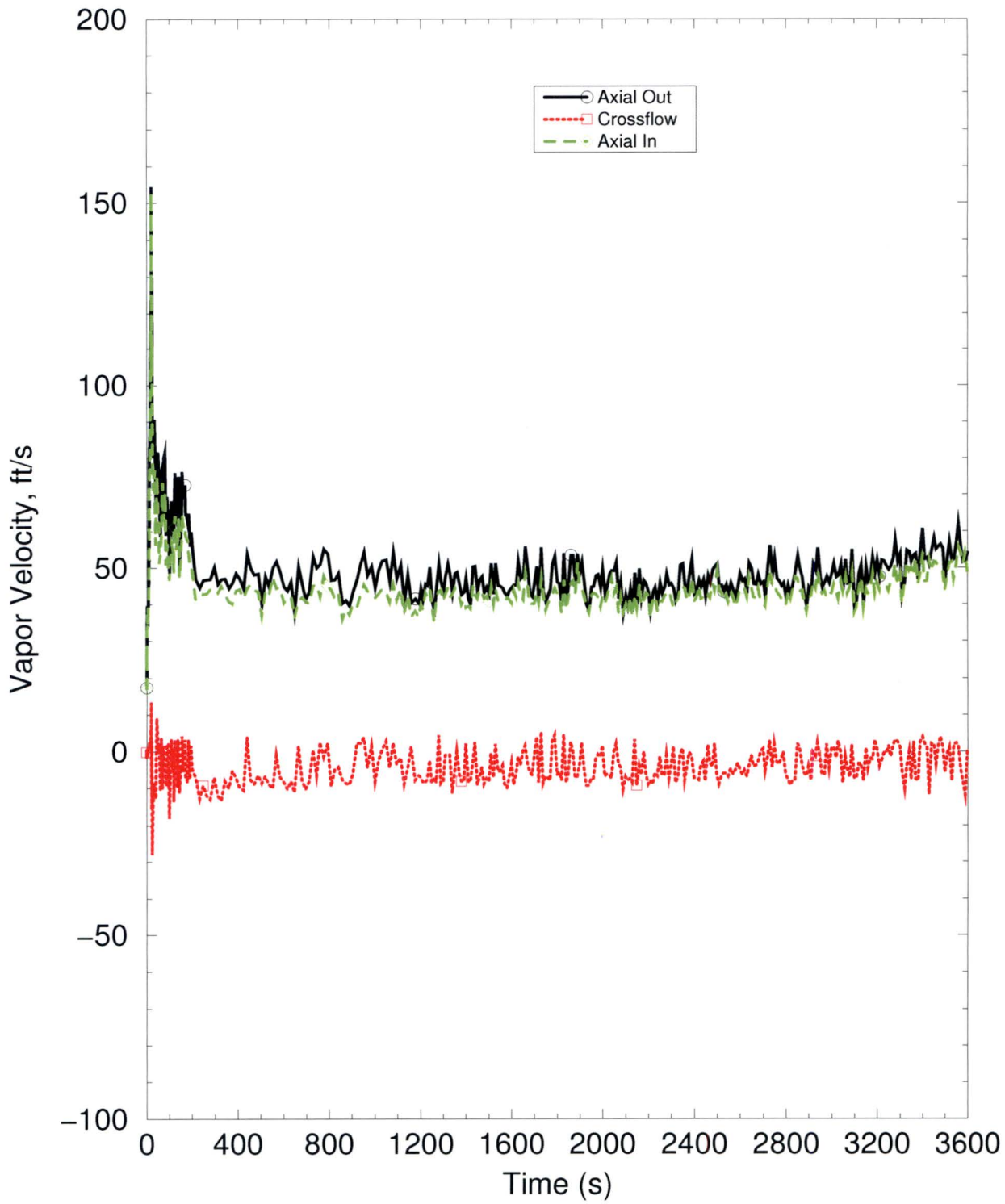

Figure RAI-4.9-6: Liquid Velocities

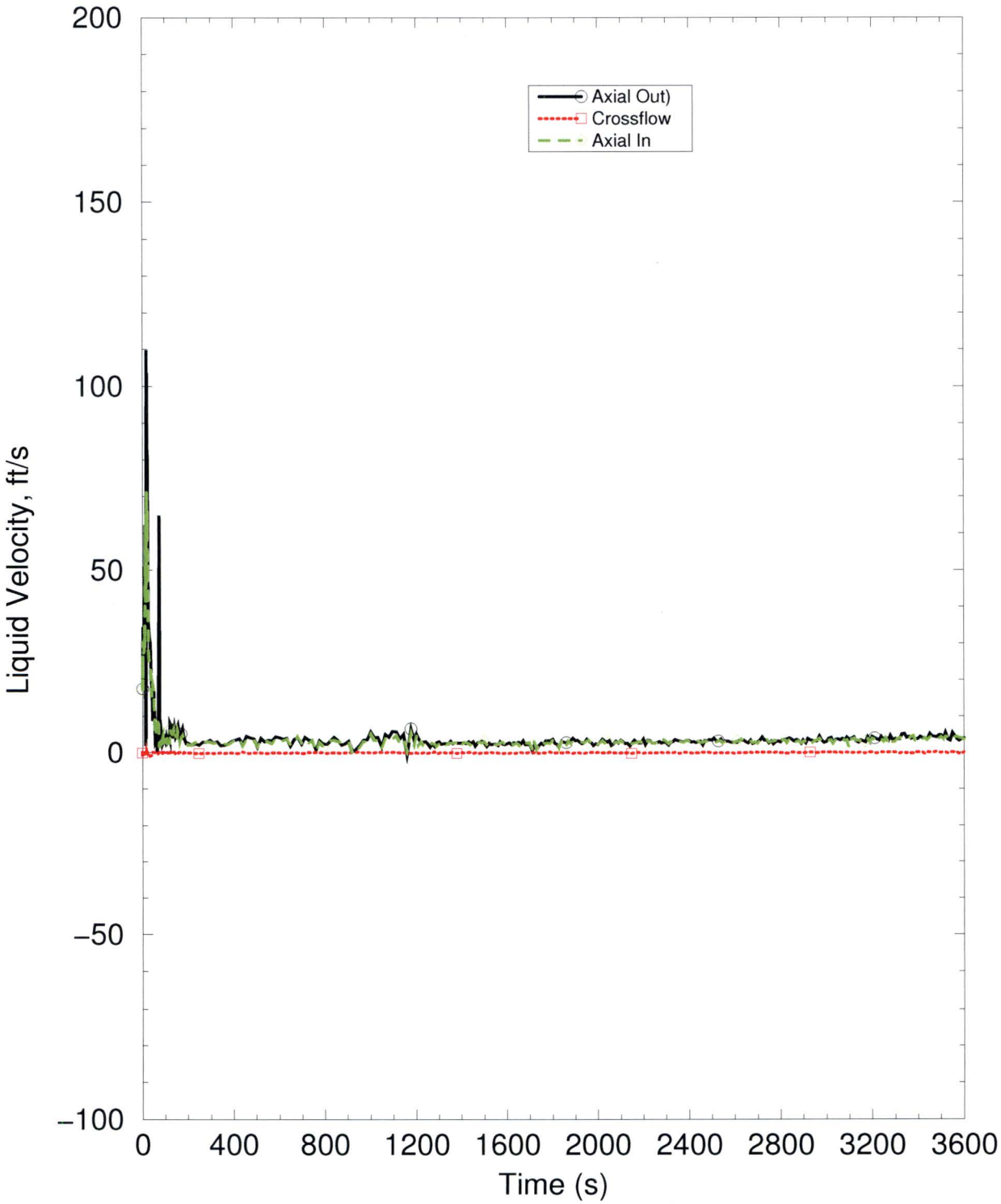

(c) Since the core does not uncover for the B&W plants, requested data cannot be provided. Instead, the instantaneous axial void fraction distribution in the Hot Channel (HC) is provided at 1290 seconds, a convenient edit in the output file following complete core blockage at 1200 seconds. The requested data are provided in Table RAI-4.9-2. The void fraction at the peak power location in the hot channel is provided with time in Figure RAI-4.9-7

Table RAI-4.9-2: RAI 4.9(c) – Requested Data for B&W Plants - Instantaneous Void Fraction in Hot Channel

Core Component	Axial Void Fraction
Lower Unheated Node	0.00000
HC-SEG2	0.20926
HC-SEG3	0.32804
HC-SEG4	0.41603
HC-SEG5	0.49071
HC-SEG6	0.54468
HC-SEG7	0.59334
HC-SEG8	0.65931
HC-SEG9	0.73212
HC-SEG10	0.76743
HC-SEG11	0.78264
HC-SEG12	0.81341
HC-SEG13	0.85934
HC-SEG14	0.88366
HC-SEG15	0.88954
HC-SEG16	0.89383
HC-SEG17	0.89684
HC-SEG18	0.90096
HC-SEG19	0.89867
HC-SEG20	0.89741
HC-SEG21	0.90085

(d) Since the B&W plants do not uncover the core during LTCC, the core remains in saturated nucleate boiling heat transfer regime following the core inlet blockage at 1200 seconds. Core heat transfer models are described in Section 2.3.3 of BAW-10164P-06 (Reference 4.9-1). Based on the correlation selection logic given by Equation 2.3.3-3, RELAP5/MOD2-B&W will use the Chen correlation to calculate the nucleate boiling heat transfer at this time. The correlation will essentially transfer all the decay heat to the fluid.

Figure RAI-4.9-7: Vapor Void Fraction in Hot Channel at Peak Power Location

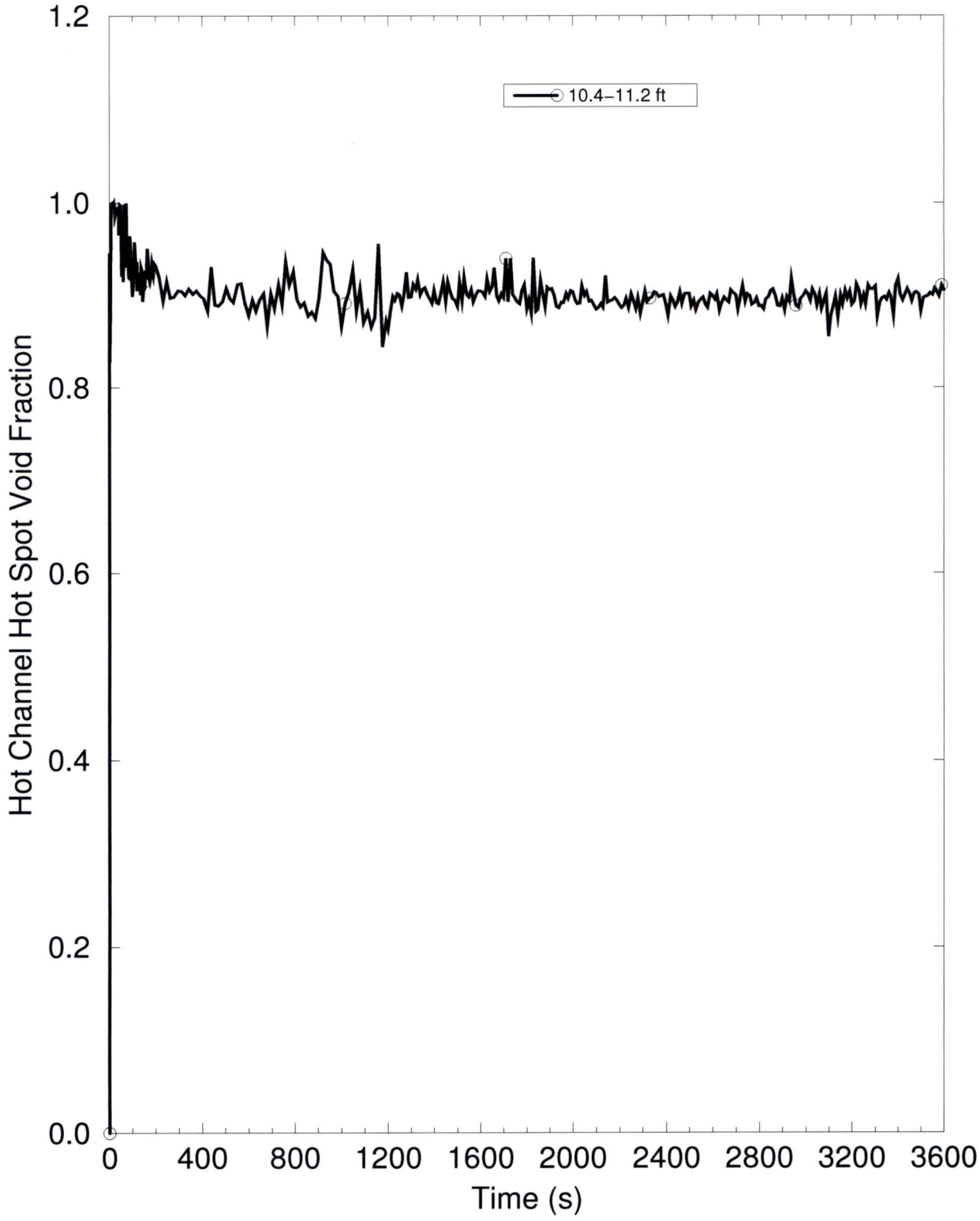

(e) The vertical flow regime map used in RELAP5/MOD2-B&W is described in BAW-10164P-06, Section 2.1.3.1 (Reference 4.9-1). This map is essentially unchanged from the RELAP5/MOD2 code as described in NUREG/CR-5194, Section 3.2 (Reference 4.9-2). From Table RAI-4.9-4, it can be seen that the void fraction at the peak power location is about 90 percent. Since the surface heat transfer is by nucleate boiling, the expected flow regime at this high void fraction is either in the upper end of the slug flow regime or in the lower end of the annular-mist regime as discussed in Section 3.2.2.2 of the NUREG/CR-5194. As noted in the response to part 'b' of this RAI, the predicted two-phase flow regime at 1290 seconds at the peak power location is annular-mist. Since the steam velocity at this time is not large enough for substantial droplet entrainment, the flow regime will be essentially annular form. The transition from slug to annular mist was defined by Taitel and Dukler (Reference 4.9-3) based on the critical vapor velocity required to suspend a liquid droplet. The resulting transition void fraction from slug to annular mist is set to the minimum of 0.75 or that based on the critical velocity and is given by Equation 2.1.3-10 in BAW-10164P-06.

$$\alpha_{S-A} = max\left[0.75, \frac{1.4(\sigma g(\rho_f - \rho_g))^{1/4}}{v_g \rho_g^{1/2}}\right] \qquad \text{(RAI-4.9-1)}$$

It should be noted that the constant 1.4 in the above equation is the value reported by Wallis (Reference 4.9-4) which is somewhat lower than the Dukler constant of 3.1. The reasons for this change is discussed in Section 2.1.3.1 of BAW-10164P-06 and in Section 3.2.2.2 of NUREG/CR-5194.

The calculation of the interphase drag in the annular-mist flow regime is described in BAW-10164P-06, Section 2.1.3.2 (without the BWNT-option) and is essentially same as that is in RELAP5/MOD2 (NUREG/CR-5194, Section 6.1.3.3).

Since the code uses well-established correlations and RELAP5/MOD2-B&W as well as RELAP5/MOD2 have been extensively benchmarked, it is expected that RELAP5/MOD2-B&W will calculate the appropriate interphase drag in the annular flow during the long term core cooling period following a LOCA. In addition, this formulation has been shown to match applicable conditions for LTCC (GSI-191) via code benchmarks to test data as described in the response to RAI 4.8.

References - RAI 4.9

4.9-1 AREVA Document BAW-10164PA, Revision 6, *RELAP5/MOD2-B&W - An Advanced Computer Program for Light Water Reactor LOCA and NON-LOCA Transient Analysis.*

4.9-2 R. A. Dimenna, et al., RELAP5/MOD2 Models and Correlations, NUREG/CR-5194, August 1988.

4.9-3 Y. Taitel, D. Bornea, and A. E. Dukler, "Modeling Flow Pattern Transitions for Steady Upward Gas-Liquid Flow in Vertical Tubes," AIChE Journal, Vol. 26, pp. 345-354, 1980.

4.9-4 G. B. Wallis, One-Dimensional Two-Phase Flow, McGraw-Hill Book Company, New York, 1969.

2.10 RAI 4.10

2.10.1 Statement of RAI 4.10

Provide plots showing the heat generation rates from the decay heat models that were used in the LOCA T-H analyses documented in Sections 8 through 11. Show the decay heat rates as a function of transient time with time zero corresponding to the break opening. Display the decay heat rate in relative dimensionless units using a linear scale with a range from null to 1.2. Plot the time axis in a logarithmic scale in units of seconds. Use a common time range that starts at one second after break opening and ends when the longest analyzed LOCA transient case ends.

2.10.2 Response to RAI 4.10

The normalized decay heat curve used for the Small Break Loss of Coolant Accident (SBLOCA) evaluation is provided in Figure RAI-4.10-1.

Figure RAI-4.10-1: Normalized Decay Heat for B&W Analyses

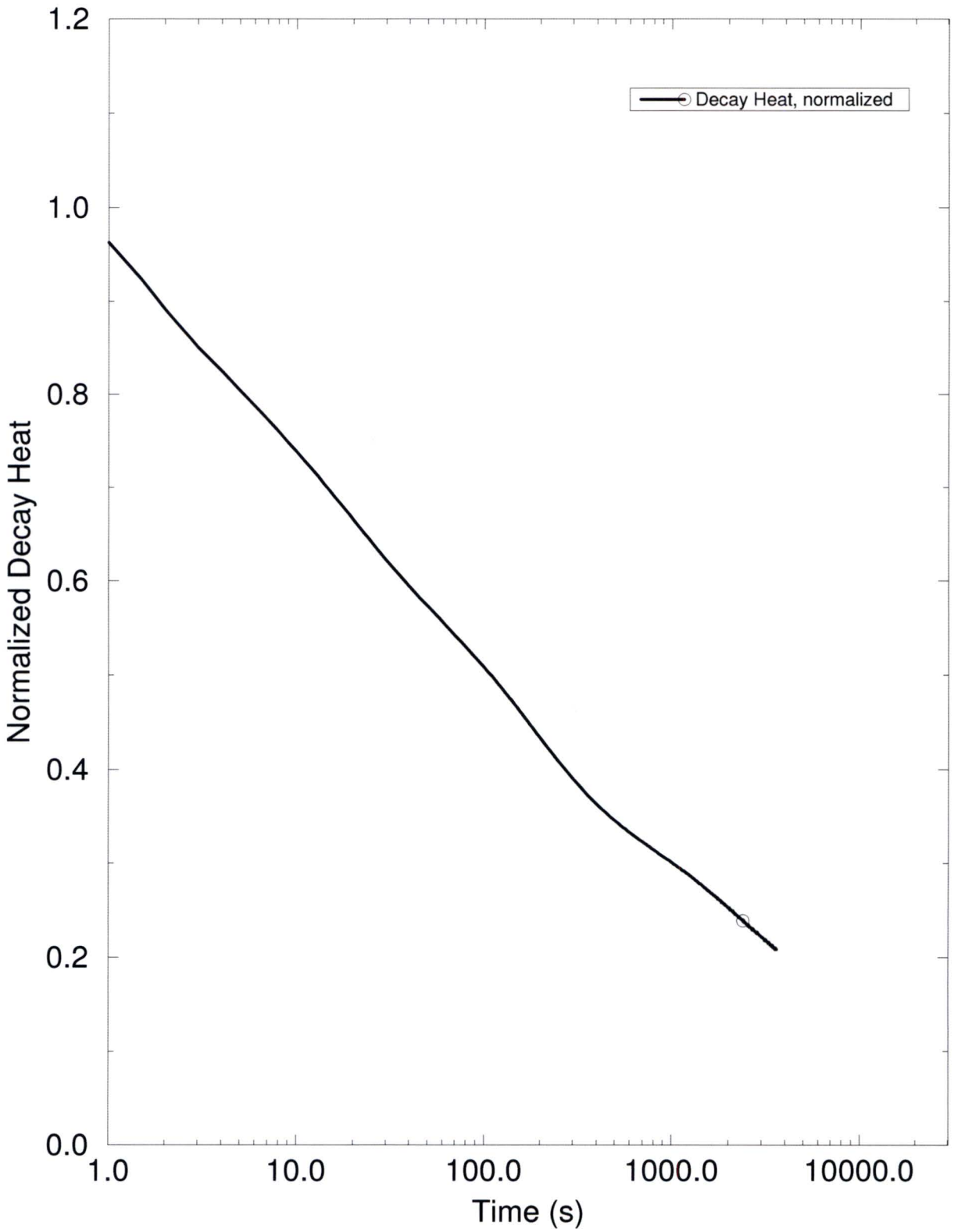

2.11 RAI 4.11

2.11.1 Statement of RAI 4.11

Section 5.4 states that "the analysis completed by AREVA using S-RELAP5 produced results that compared reasonably well to those predicted by WCOBRA/TRAC, which are described in Section 9". The section also explains that "the plant and transient condition analyzed was identical to that used by Westinghouse;" however, "the plant models used for each analysis were developed independently following different methods and techniques". Section 5.4 concludes that "irrespective of the computer codes and methods used, the resulting code predictions are expected to be consistent".

(a) Define the simulated LOCA transient and provide a summary description of the analyses. Provide a table that documents and compares key inputs and modeling features for both studies and explain how this information relates to key inputs provided in Table 6-2 for the Westinghouse downflow plant design analysis.

(b) Provide comparisons of key results from the analyses. Explain any significant discrepancies between the results from the studies and provide an assessment of the degree of conservatism reflected in each of the analyses. Discuss how differences in the prediction results relative to t_{block}, K_{max}, K_{split}, and/or m_{split} could be caused or explained by differences in the applied methodologies, plant model features (such as core nodalization), assumed key inputs, and other relevant conditions.

(c) Provide references for the technical documents containing the calculation notebooks documenting the analyses in Items a and b and confirm that the analyses were quality assured.

2.11.2 Response to RAI 4.11

This RAI pertains to the Westinghouse Electric Company (WEC) and Combustion Engineering (CE) plant categories and therefore requires no response for the B&W plant category.

2.12 RAI 4.12

2.12.1 Statement of RAI 4.12

The UPI plants were not considered as part of the analysis due to their ECCS configurations. Provide justification that plants with the UPI configurations do not require T-H analyses to demonstrate that the acceptance criteria defined in WCAP-17788 are satisfied and that the TR is applicable to their specific plant designs including applicable ECCS features.

2.12.2 Response to RAI 4.12

This RAI pertains to the Westinghouse Electric Company (WEC) plant categories and therefore requires no response for the B&W plant category.

2.13 RAI 4.13

2.13.1 Statement of RAI 4.13

Figure 8-13 shows the mid-core velocity in the BB channel going from negative, interpreted as downward, to about zero very rapidly before switchover time. The plotted BB inlet velocity remains stable at near zero or around a slightly negative value throughout the exhibited part of the transient while the BB exit velocity remains stable at a low negative value. In addition, the BB exit velocity is large in magnitude compared to the BB inlet velocity. Provide an explanation for this behavior.

2.13.2 Response to RAI 4.13

This RAI pertains to the Westinghouse Electric Company (WEC) plant categories and therefore requires no response for the B&W plant category.

2.14 RAI 4.14

2.14.1 Statement of RAI 4.14

Figures 8-16 and 8-25 show a spike in PCT occurring while the downcomer fills. Once the flow begins exiting the BB region, the core begins to cool again and PCT decreases. Were the potential range of flow rates for downcomer fill considered in the analyses? Explain how the analysis accounts for potential uncertainties or variability in the downcomer fill time. If the analysis does not account for such uncertainty/variability, explain how the behavior (PCT spike) would be affected by different downcomer fill times.

2.14.2 Response to RAI 4.14

This RAI pertains to the Westinghouse Electric Company (WEC) plant categories and therefore requires no response for the B&W plant category.

2.15 RAI 4.15

2.15.1 Statement of RAI 4.15

Provide the results of Figures 9-9 and 9-10 on the same graph. Normalize the integrated mass flow on an average channel basis so that a meaningful comparison can be made.

2.15.2 Response to RAI 4.15

This RAI pertains to the Westinghouse Electric Company (WEC) plant categories and therefore requires no response for the B&W plant category.

2.16 RAI 4.16

2.16.1 Statement of RAI 4.16

Assumption 6 in Section 4.1 states that "ECCS temperature during sump recirculation will be set at or near saturation temperature at containment pressure" and explains that "neglecting the presence of subcooling is conservative because it maximizes the steaming rate in the core and minimizes the cooldown rate of the reactor vessel (RV) and steam generators (SGs)". Tables 6-1 through 6-4 include the parameter "ECCS temperature during recirculation phase" as a key input. The CE plant category stands apart in the sense that this input is set at a temperature of 212 °F with the "containment pressure during recirculation phase" specified as "dynamically calculated" according to Table 6-3. During the NRC audit of the AREVA T-H analyses for the CE plant category, it was clarified that S-RELAP5 was used in a coupled mode with the ICECON containment code to calculate the containment backpressure.

(a) Identify contributing physical processes that are dependent on the degree of ECCS fluid temperature subcooling and explain the effects associated with these processes with regard to core cooling. In addition to core steaming, explain whether processes such as condensation, downcomer boiling, liquid entrainment, and boiling in SG tube bundles (if engaged) were considered among such processes. State whether these effects are considered conservative or non-conservative and provide justifications for the conclusions.

(b) Identify the coupled S-RELAP5/ICECON methodology by providing a reference to the technical document that describes it. Explain whether the methodology was validated and assessed for applications similar to the LOCA analyses documented in Vol. 4 for the CE plant category. Clarify whether the coupled code methodology and/or application analyses obtained with this methodology have been reviewed and/or approved by NRC. Provide the key inputs and assumptions relative to the containment model. Explain which of these input parameters were modeled in a bounding manner along with the ranges considered in determining the input values for the parameters.

(c) In order to assess the effect from the major assumption regarding the ECCS temperature subcooling, the NRC staff recommends performing two re-analyses for Cases 1 and 2 documented in Section 10 using S-RELAP5 in a stand-alone mode. For the purpose of these re-analyses it is suggested that an "ECCS temperature during recirculation phase" of 212 °F along with a "containment pressure during recirculation phase" of 14.7 psia consistent with the key inputs applied for the Westinghouse upflow and downflow plant categories is used. Verify that there is

little impact on the K_{max} and t_{block} results compared to the results documented in Section 10.

(d) Tables 6-1 through 6-4 do not provide information regarding the ECCS temperatures prior to sump switch over (SSO). Section 9.3 states that "during transfer to sump recirculation, the ECCS coolant temperature is set to 212 °F". Explain how the ECCS temperatures prior to SSO were defined for the purposes of the analyses and provide the values used for the analyses in Sections 8, 10, and 11. Clarify whether the ECCS temperature prior to SSO should also be considered a contributing factor for the purposes of the T-H analyses in Vol. 4 and justify the response. Describe the effects that the ECCS temperature assumption prior to sump switchover can have on other processes (i.e., voiding, swelling, etc.) if it is found to have a significant impact on the results.

2.16.2 Response to RAI 4.16

2.16.2.1 Part a

The important physical processes applicable to the B&W-designed plants were identified in the response to Request for Additional Information (RAI) 4.7. As identified above, condensation, downcomer boiling, liquid entrainment, and boiling in the Steam Generator (SG) tube bundles (if engaged) were identified as contributing physical processes that can be affected by the degree of Emergency Core Cooling System (ECCS) subcooling. The results of the analysis presented in the response to RAI 4.22 is used to help understand the effect of these processes for the B&W plant design.

In the long-term following a hot leg break, the ECCS flow rate exceeds what is needed to replace that which is boiled off due to decay heat such that the core remains covered. To that end, the Reactor Coolant System (RCS) system response will be controlled by the core decay heat. That is, the boiloff defines the core void fractions and liquid volume, the Downcomer (DC) level will be balanced with the core level, and the excess ECCS flow will exit the break.

After the core has recovered and the system transitioned to the Long Term Core Cooling (LTCC) phase of the event, the heat removal from the Reactor Vessel (RV) wall has become conduction limited. While some amount of boiling may occur in the DC, the consequences are insignificant because the DC level quickly adjusts to the additional voiding (boiling) to balance the core liquid level. Since the ECCS flow rate exceeds that needed to match the core boiloff, DC boiling (if present) will have no effect on the core response.

As shown in the B&W plant analysis, the SG tube bundles are not engaged for LTCC.

Therefore, this process has no effect on the system response for the B&W plants.

The B&W plant analysis demonstrates that the core mixture level remains near the bottom of the hot leg such that liquid is continually passed to the break. Therefore, liquid entrainment has no effect on the system response for the B&W plants.

The magnitude of the condensation effects in a B&W plant response is limited due to the presence of the Reactor Vessel Vent Valves (RVVVs). Condensation in the cold legs or upper DC can reduce the DC over pressure resulting in water hold up in the DC. However, if the condensation is great enough, the pressure in the upper DC will drop below that of the upper plenum such that the RVVVs will open. Steam flowing through the RVVVs interacts with the cold ECCS injection to offset the pressure decrease associated with the additional condensation. Consequently, the RVVVs limit the condensation hold up such that the core or DC levels are not adversely affected. This effect is demonstrated via a number of sensitivity studies on the ECCS fluid temperature and flow rate. Table RAI-4.16-1 lists the sensitivity cases evaluated.

The first comparison considers Case 1 and Case 3. As indicated above, these cases have identical ECCS conditions except for the ECCS temperature after Sump Switch Over (SSO). As expected, there are no discernible differences for the response of the collapsed level in the average channel (Figure RAI-4.16-3). With respect to the DC level (Figure RAI-4.16-2) and total liquid volume available (Figure RAI-4.16-1), the colder fluid results in slightly more condensation, which lowers the upper DC pressure such that a slightly higher DC level is needed to push the flow from the LP into the core. A hand calculation shows that the DC level must increase by at least 0.2 ft, which is consistent with Figure RAI-4.16-2. The void fraction in the upper plenum (Figure RAI-4.16-4) is slightly lower while showing the same trend. The pressure difference across the RVVVs for Case 1 was insufficient to open the valves after the core was blocked, while the RVVVs for Case 3 remained open after the core was blocked.

The second comparison considers Case 1 and Case 4. These cases have identical ECCS conditions except for the ECCS temperature prior to SSO. Prior to SSO the DC level (Figure RAI-4.16-2); the total liquid volume available (Figure RAI-4.16-1); and, the collapsed level in the average channel (Figure RAI-4.16-3) indicate the colder fluid results in slightly higher values while showing the same general trend. With respect to the void fraction in the upper plenum (Figure RAI-4.16-4) prior to SSO, there are no discernible differences in the responses. After SSO, there are no discernible differences for the response of the collapsed level in the average channel (Figure RAI-4.16-3). The additional condensation in the DC resulted in a higher DC level (Figure RAI-4.16-2) and greater total liquid volume available (Figure RAI-4.16-1) at the time of core blockage. The void fraction in the upper plenum (Figure RAI-4.16-4) is slightly lower. Although the pressure difference across the RVVVs for Case 1 was insufficient to open the valves after the core was blocked, the higher DC level allows the RVVVs for Case 4 to remain open after the core was blocked. The RVVV pressure differential in Case 4 was gradually

descending closer to the Case 1 results at one hour.

The final comparison considers Case 1 and Case 2. These cases have identical ECCS conditions before SSO, but different flow rates and temperatures after SSO. The effect of the higher flow rate is immediately apparent as the system realigns to establish new levels in the DC (Figure RAI-4.16-2) and core (Figure RAI-4.16-3). The total liquid volume available (Figure RAI-4.16-1) also increases sharply with the higher flow rate. The higher flow rate is sufficient to maintain the decreasing trend of the void fraction in the upper plenum (Figure RAI-4.16-4). By doubling the flow rate, the pressure drop needed to push the flow from the lower plenum into the core is quadrupled ($dP \propto flow^2$). Consequently, the level in the DC must increase to compensate. A hand calculation shows that the DC level must increase by at least 4.5 above the lower flow rate case, which is consistent with Figure RAI-4.16-2. The additional condensation potential associated with the higher flow rate allows the RVVVs for Case 3 to remain open after the core was blocked.

The cases analyzed had different condensation potentials associated with ECCS at a lower temperature and/or a higher flow rate. In all cases, the DC level rose to the height needed to push all the ECCS plus condensate into the core region. The condensation does not detrimentally alter the system response because all the ECCS flow reaches the core providing abundant core cooling following complete core blockage. Thus, these results affirm that the use of minimum ECCS flow conditions at 200 °F after core blockage produces the lowest RV inventory for the B&W-designed plants that maximizes the potential for core uncovering. Since the core does not uncover with these lower bound minimum flows and maximum injection temperatures, the core will not uncover for any higher ECCS flow, lower injection temperature, or combination thereof.

Table RAI-4.16-1: ECCS Flow and Temperature Sensitivity Cases

Case Number	ECCS Flow Before SSO	ECCS Flow After SSO	ECCS Temp Before SSO	ECCS Temp After SSO
1 (Base Case, RAI 4.22)	Min	1500 gpm	120 °F	200 °F
2	Min	3000 gpm	120 °F	150 °F
3	Min	1500 gpm	120 °F	150 °F
4	Min	1500 gpm	70 °F	200 °F

Figure RAI-4.16-1: Total Liquid Volume Available for ECCS Sensitivity Cases

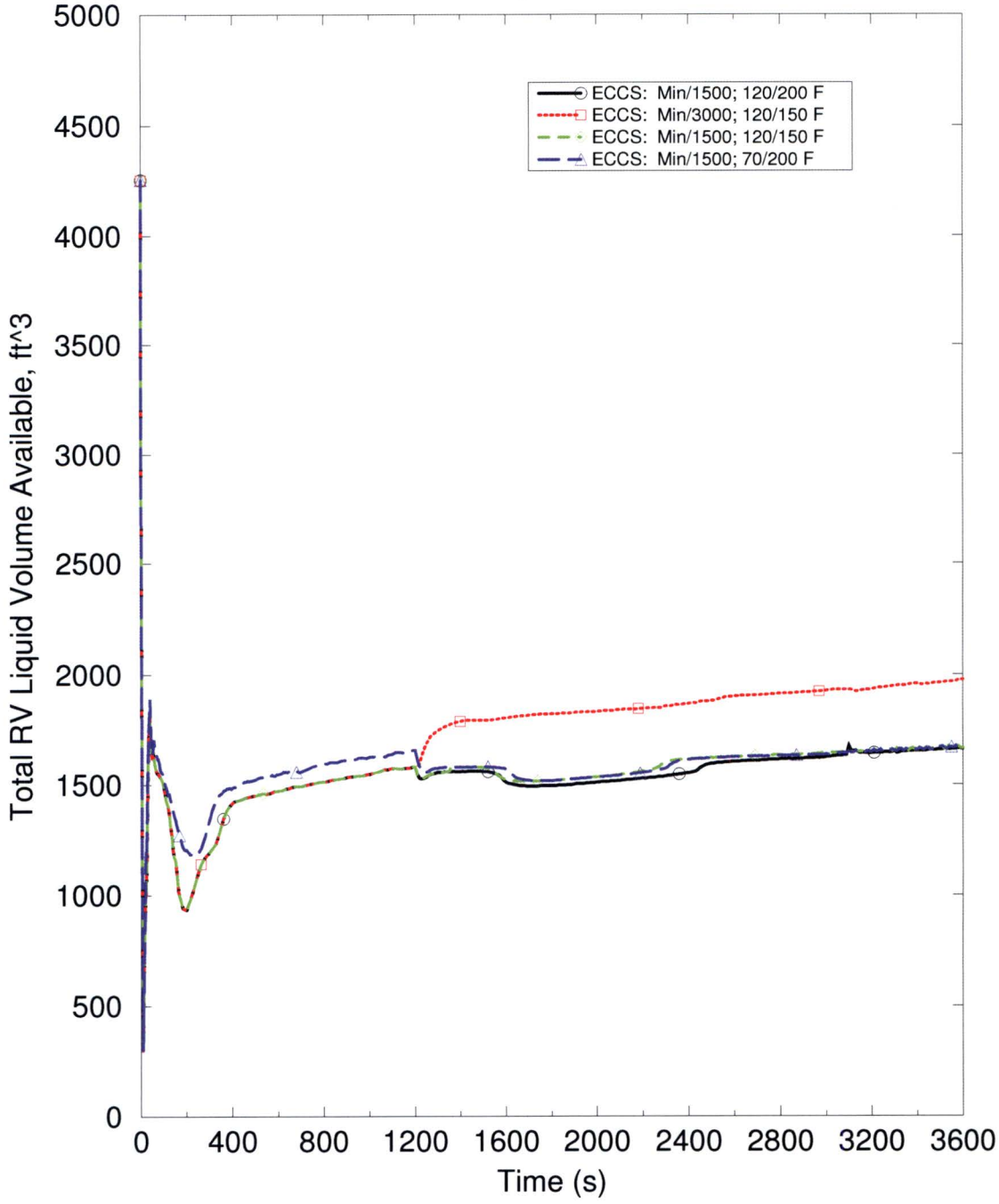

Figure RAI-4.16-2: Reactor Vessel Downcomer Collapsed Level for ECCS Sensitivity Cases

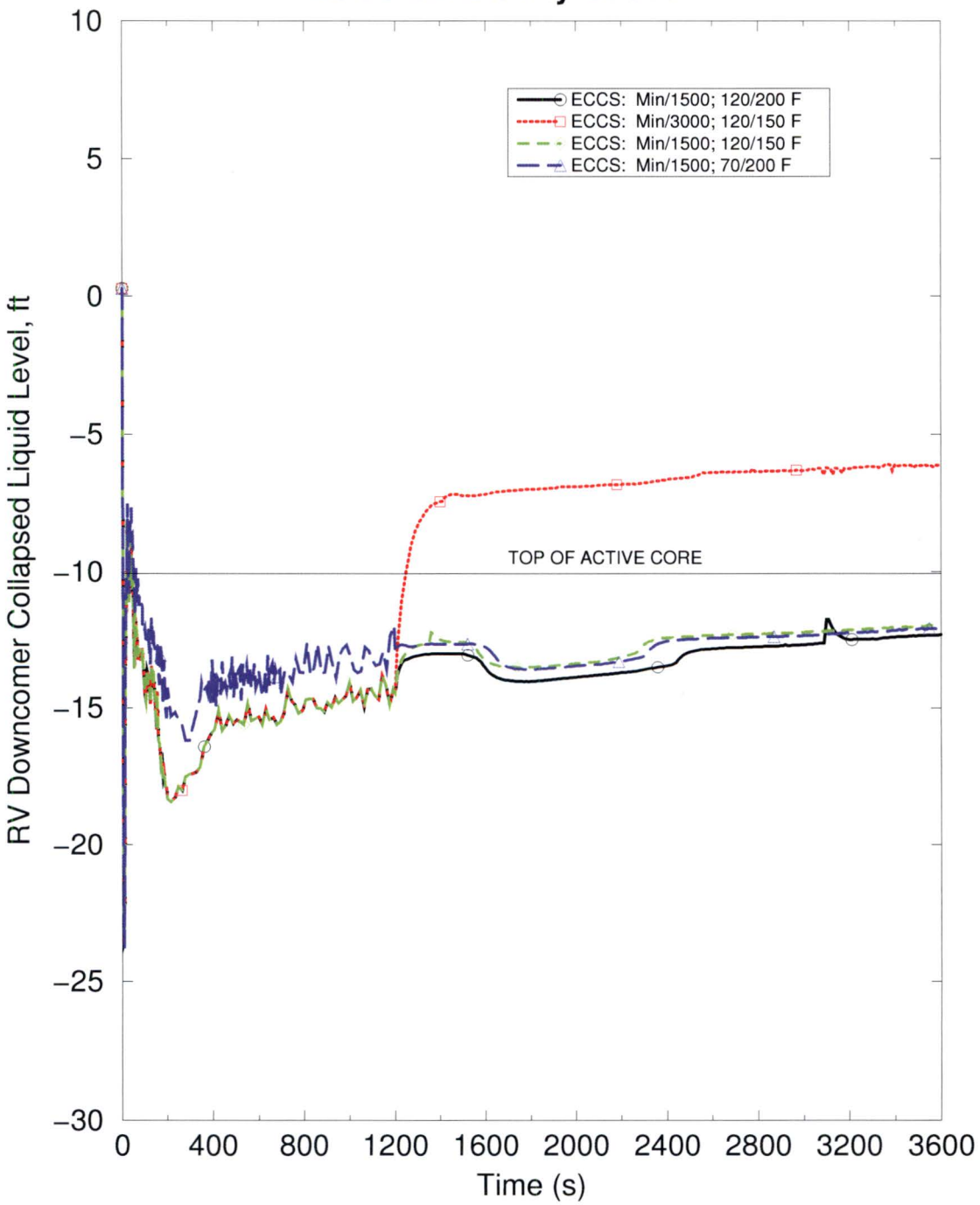

Figure RAI-4.16-3: Average Channel Collapsed Level for ECCS Sensitivity Cases

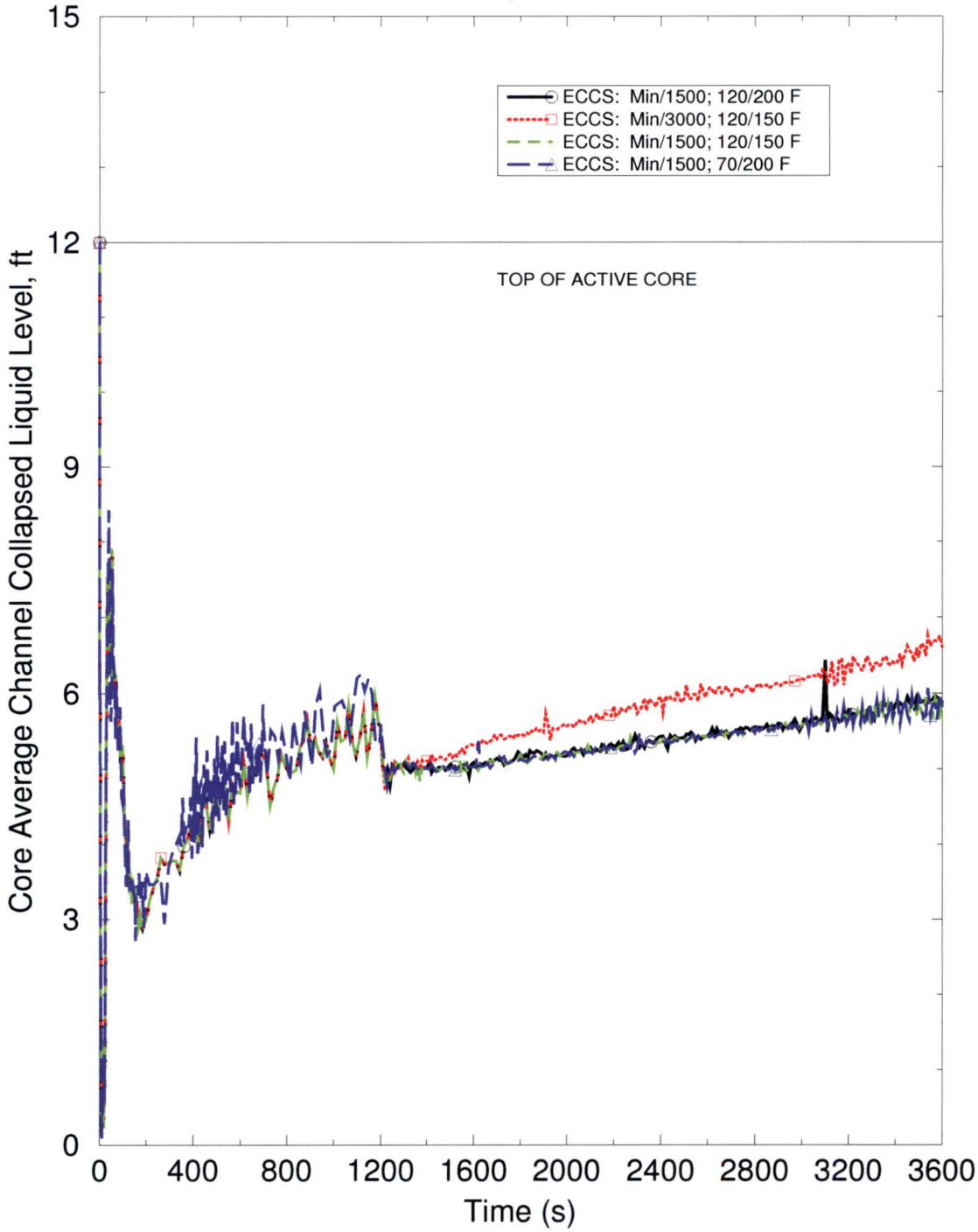

Figure RAI-4.16-4: Reactor Vessel Upper Plenum Void Fraction for ECCS Sensitivity Cases

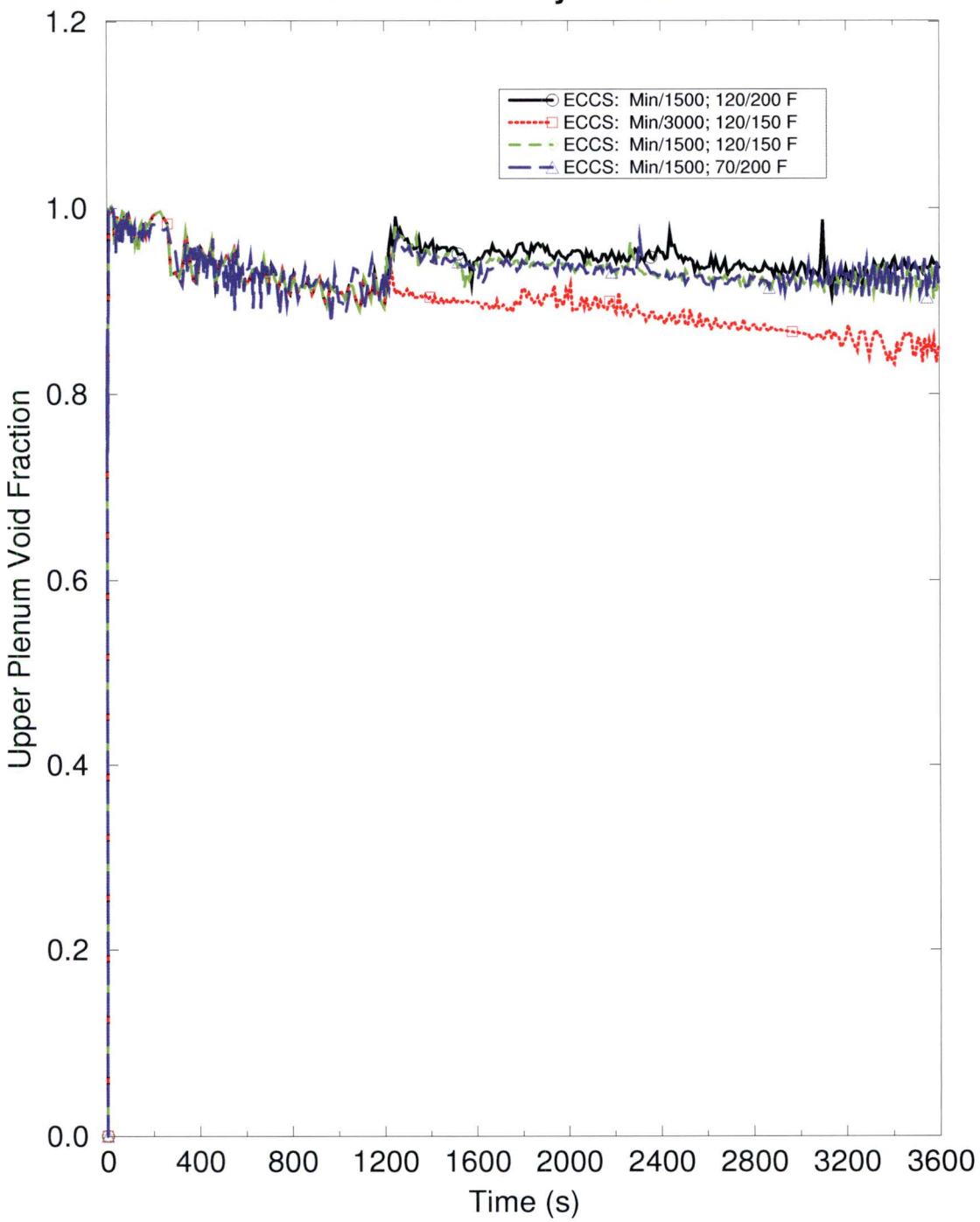

2.16.2.2 Part b

This RAI pertains to the Combustion Engineering (CE) plant categories and therefore requires no response for the B&W plant category.

2.16.2.3 Part c

This RAI pertains to the CE plant categories and therefore requires no response for the B&W plant category.

2.16.2.4 Part d

For the operating B&W plants, the highest allowed Technical Specification Borated Water Storage Tank (BWST) temperature is 120 °F. This is the value used in the B&W analyses described in the response to RAI 4.22.

High ECCS temperatures will provide the biggest challenge to core cooling. To verify this assertion, a study was performed that set the ECCS temperature to 70 °F prior to SSO. The results of this study are described in part "a" above (Case 1 to Case 4 comparison) and demonstrate that the use of the maximum ECCS temperature prior to SSO is conservative for GSI-191 applications.

2.17 RAI 4.17

2.17.1 Statement of RAI 4.17

Section 8.2.2 presents T-H results for Case 1B. Case 1B is presented because it represents the limiting time of complete core blockage, t_{block}, for the Westinghouse upflow plant category. In discussing the quantity identified as "reactor vessel fluid mass," shown in Figure 8-17, it is stated that "when complete core inlet blockage is applied, the RV inventory increases quickly, which can be credited to filling of the downcomer". The explanation for the inventory increase following the simulated core inlet blockage appears implausible if the result in Figure 8-17 represents the fluid mass within the entire RV volume. Since a stable ECCS liquid injection rate is expected during the period discussed in the above citation, the increase in accumulated fluid mass in the RV should be attributed to a reduction in the mass rate at which fluid exits the RV though the break, as suggested by the "break exit quality" shown in Figure 8-24, rather than by accumulation of mass in any sub-region within the entire RV control volume. The same observation applies to a similar statement in Section 8.2.3 that "when partial core inlet blockage is applied, the RV inventory increases quickly, which can be credited to filling of the downcomer". This explanation was provided with regard to the predicted "reactor vessel fluid mass" shown in Figure 8-26 for Case 2B, which was used to determine K_{max}. For Case 2B, the corresponding "break exit quality" response appears in Figure 8-34. To understand the role of entrainment and driving processes in the results:

(a) Explain what causes the increase in the RV inventories shown in Figures 8-17 and 8-26. Provide updates to the explanations provided in the text of Sections 8.2.2 and 8.2.3, as appropriate.

(b) Define the parameter "break exit quality" shown in Figures 8-24 and 8-34. Explain whether the same definition applies to any T-H quantity labeled as "quality" throughout Vol. 4. Otherwise, provide definitions and clarifications.

(c) Provide plots showing the following sets of parameters for Cases 1B and 2B in Section 8.

  (i) Mass flow rates of liquid, steam, and total (liquid and steam) fluid discharges through each opening of the double-ended guillotine (DEG) break

  (ii) ECCS liquid mass flow rates injected into each cold leg and the total ECCS liquid mass flow rate injection into the reactor coolant system

  (iii) Liquid mass flow rates entering the RV through each cold leg nozzle and the total liquid flow for all cold leg nozzles

(iv) Mass flow rates of liquid and steam entering the RV through each intact hot leg nozzle and the total (liquid and steam) flow rate for all intact hot leg nozzles

(v) Steam flow quality defined as a ratio of the steam mass flow rate to the total (liquid and steam) mass flow rate for the RV-side opening of the DEG break

(d) Present plots that show integrals for the identified mass flow rates requested in Item c above (liquid, steam, and/or total liquid and steam, as relevant).

2.17.2 Response to RAI 4.17

2.17.2.1 Part a

This RAI pertains to the Westinghouse Electric Company (WEC) plant categories and therefore requires no response for the B&W plant category.

2.17.2.2 Part b

The break exit quality is defined as the mass quality, which is the ratio of the steam mass flow rate to the total mass flow rate. This usage, which is consistent with the standard definition of the term mass quality, is consistent throughout Volume 4.

2.17.2.3 Part c

The requested information for the Babcock & Wilcox (B&W) t_{block}/K_{max} evaluation is provided in the following figures. These results are from the updated analyses described in RAI 4.22. The break mass flow rates are provided in Figure RAI-4.17-1. The Emergency Core Cooling System (ECCS) liquid mass flow rates into the cold legs; the ECCS liquid mass flow rates into the Reactor Vessel (RV) via the Core Flood Tank (CFT) nozzles; and, the total ECCS liquid mass flow rates into the reactor coolant system are provided in Figure RAI-4.17-2. The liquid mass flow rates into RV from the cold legs are provided in Figure RAI-4.17-3. The mass flow rates into RV from the intact Hot Leg (HL)hot leg are provided in Figure RAI-4.17-4. The steam flow quality for the RV side of the break is provided in Figure RAI-4.17-5.

Figure RAI-4.17-1: Break Mass Flow Rates for B&W Analyses

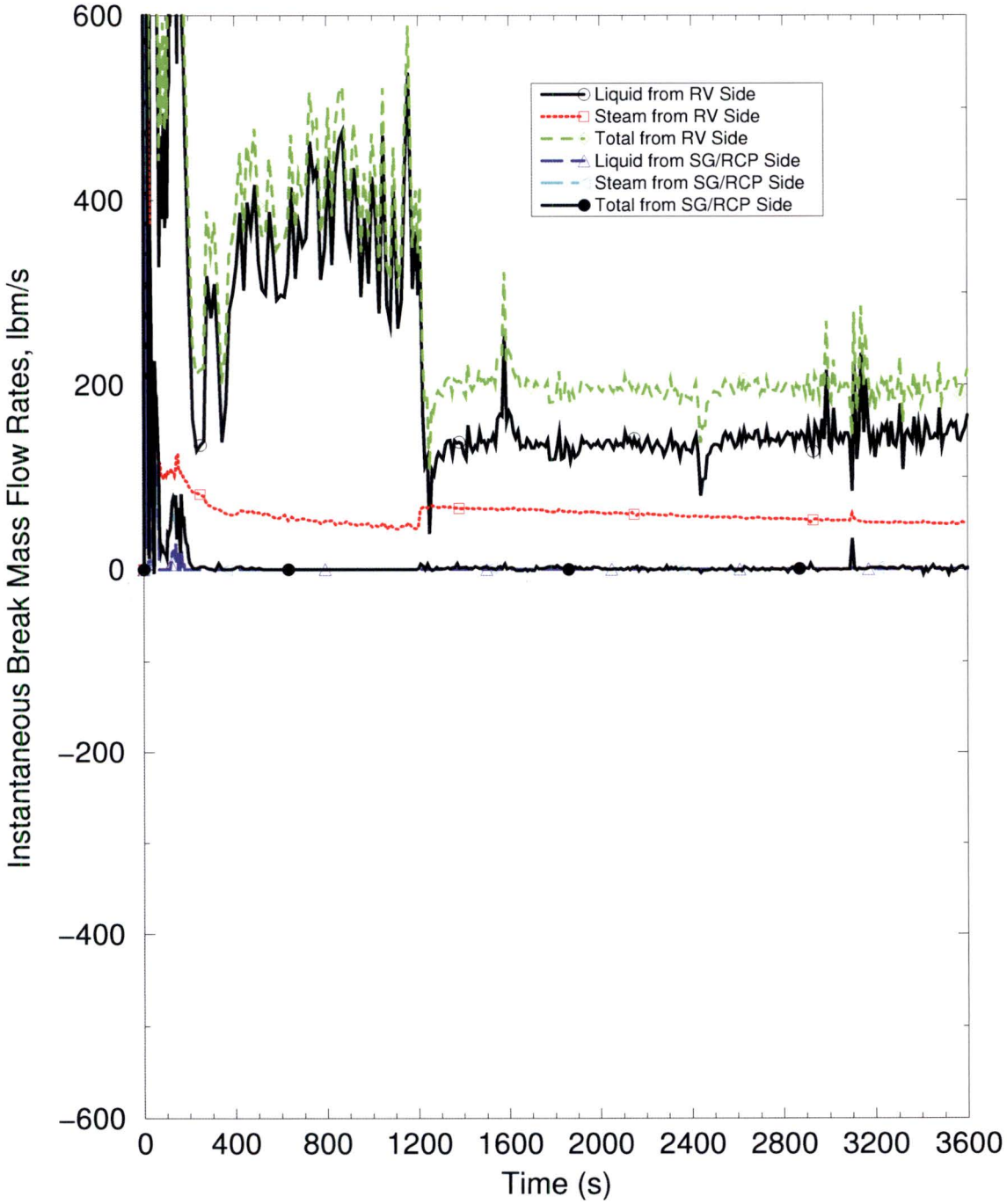

Figure RAI-4.17-2: ECCS Liquid Mass Flow Rates for B&W Analyses

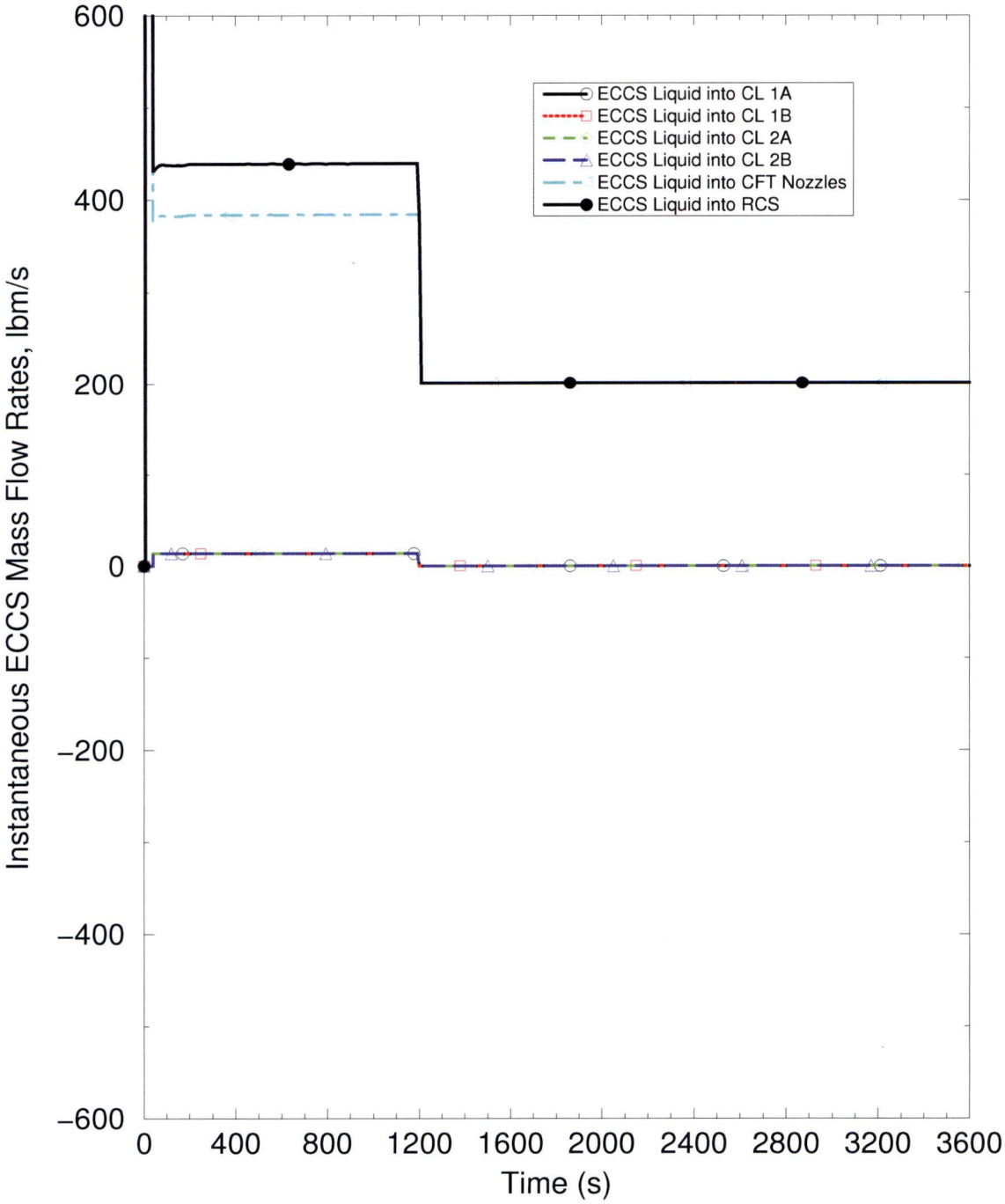

Figure RAI-4.17-3: Liquid Mass Flow Rates Entering RV through CLs for B&W Analyses

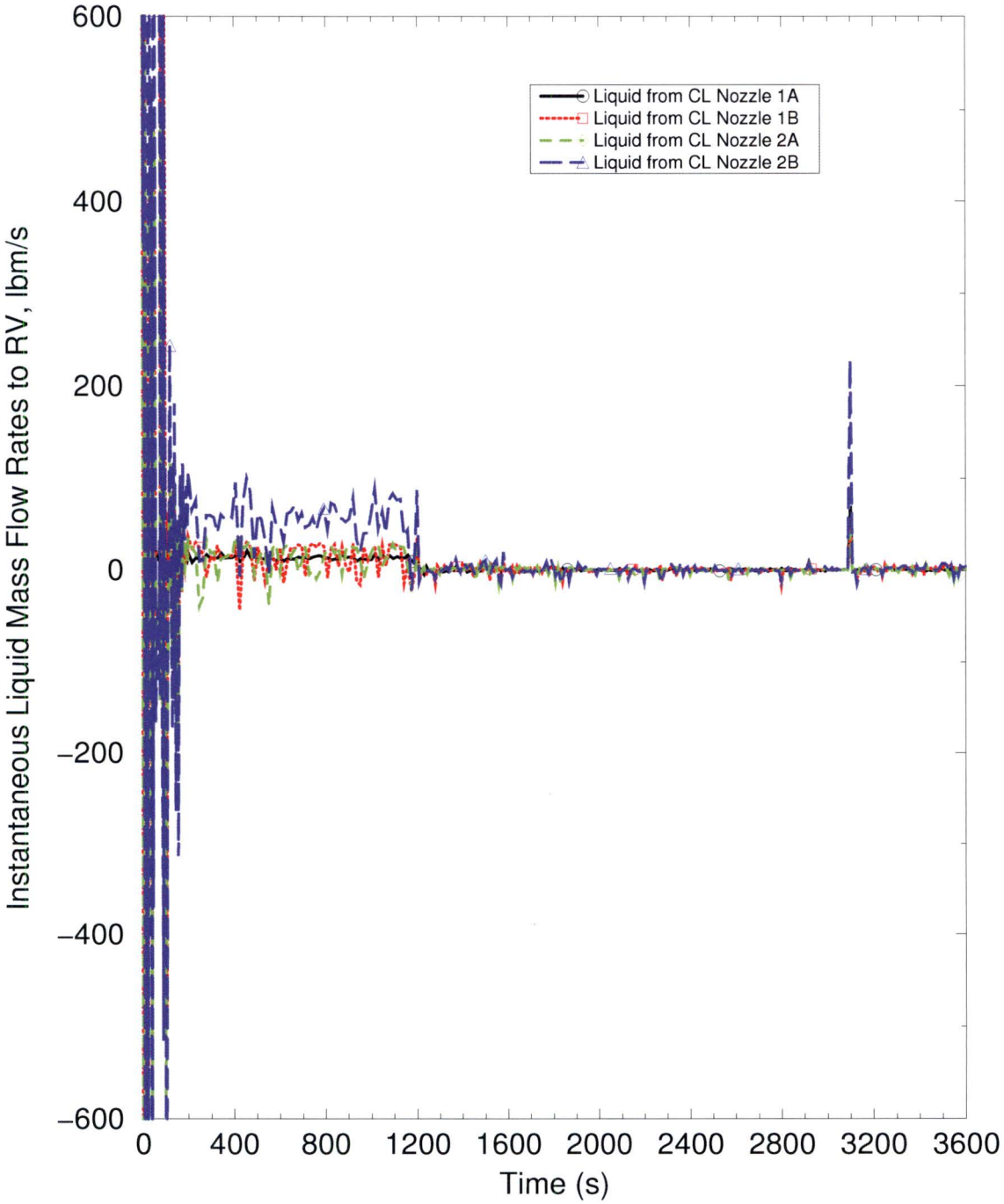

Figure RAI-4.17-4: Mass Flow Rates Entering RV through Intact HL for B&W Analyses

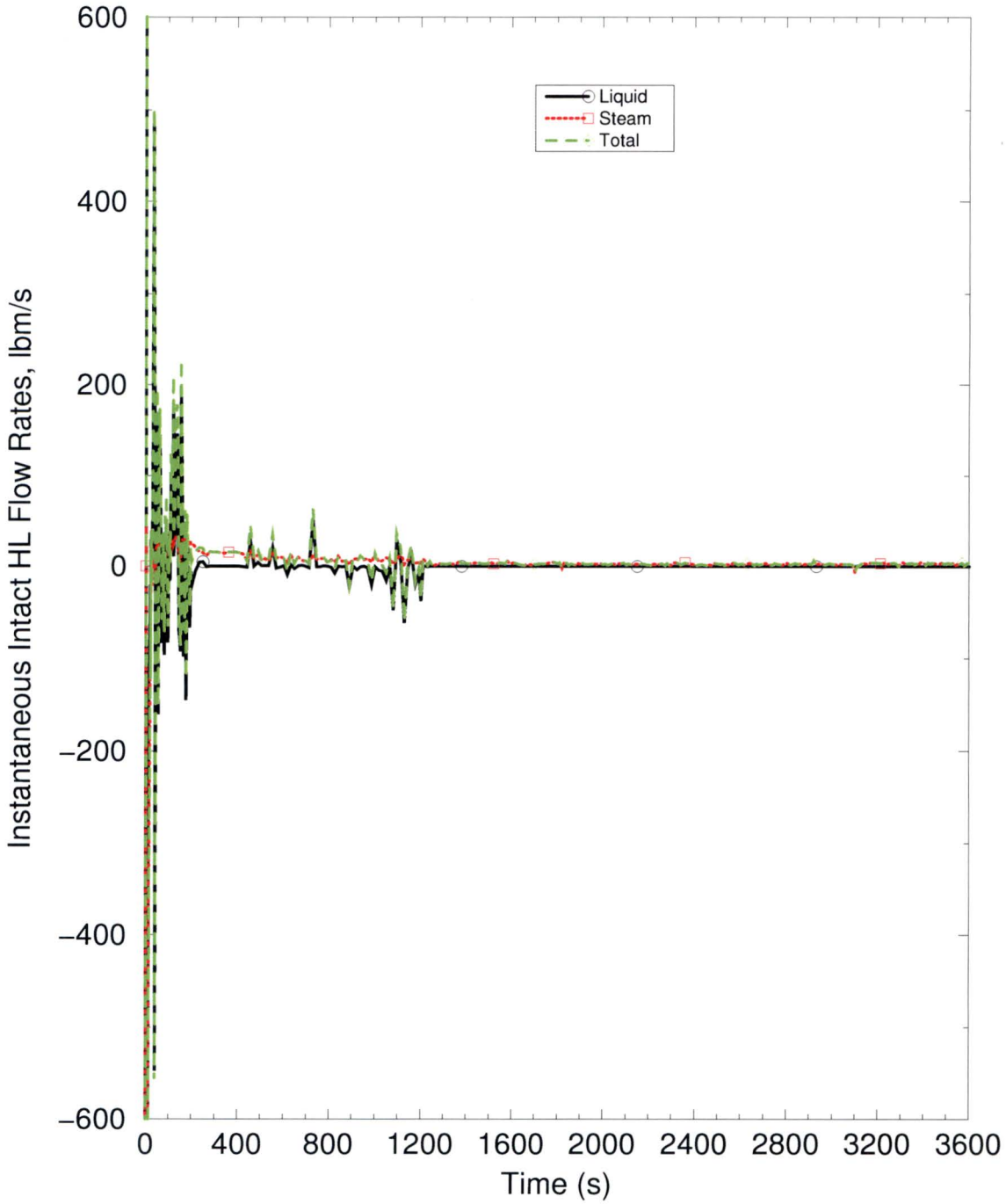

Figure RAI-4.17-5: Steam Flow Quality (RV Side of Break) for B&W Analyses

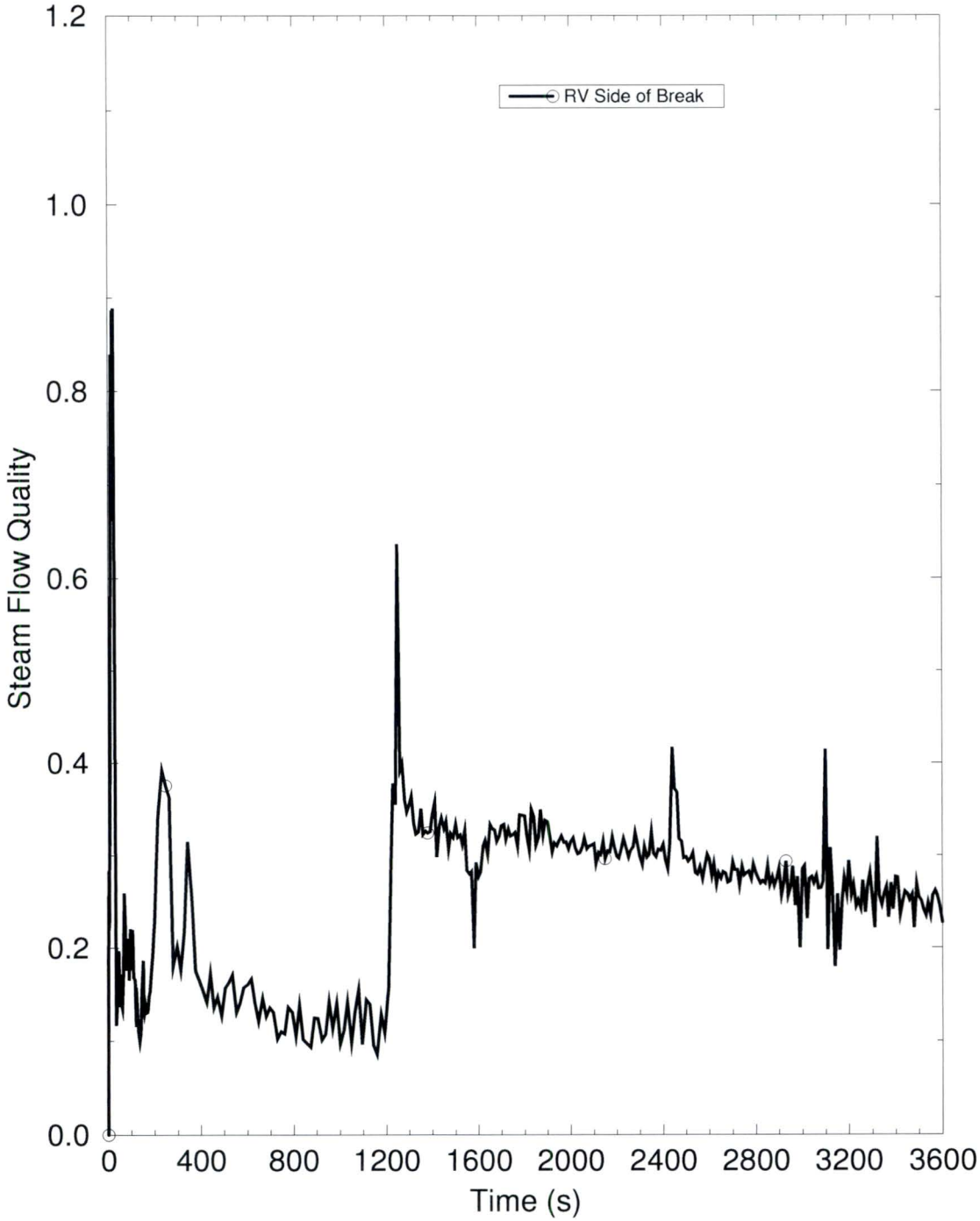

2.17.2.4 Part d

The requested information for the B&W t_{block}/K_{max} evaluation is provided in the following figures. These results are from the updated analyses described in RAI 4.22. The integrated break mass flow rates are provided in Figure RAI-4.17-6. The integrated ECCS liquid mass flow rates into the cold legs are provided in Figure RAI-4.17-7. The integrated liquid mass flow rates into RV from the cold legs are provided in Figure RAI-4.17-8. The integrated mass flow rates into RV from the intact HL are provided in Figure RAI-4.17-9.

Figure RAI-4.17-6: Integrated Break Mass Flow Rates for B&W Analyses

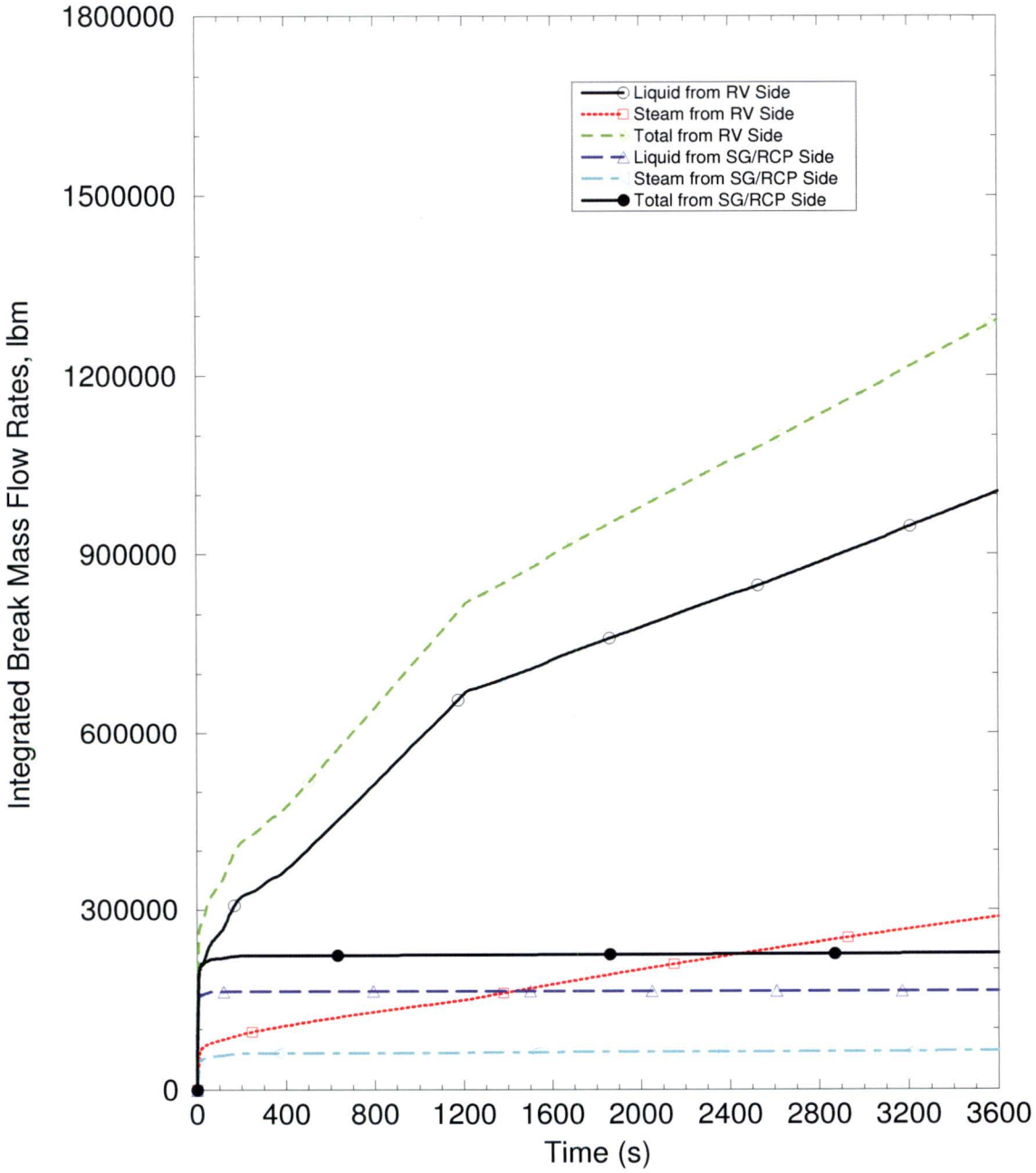

Figure RAI-4.17-7: Integrated ECCS Liquid Mass Flow Rates for B&W Analyses

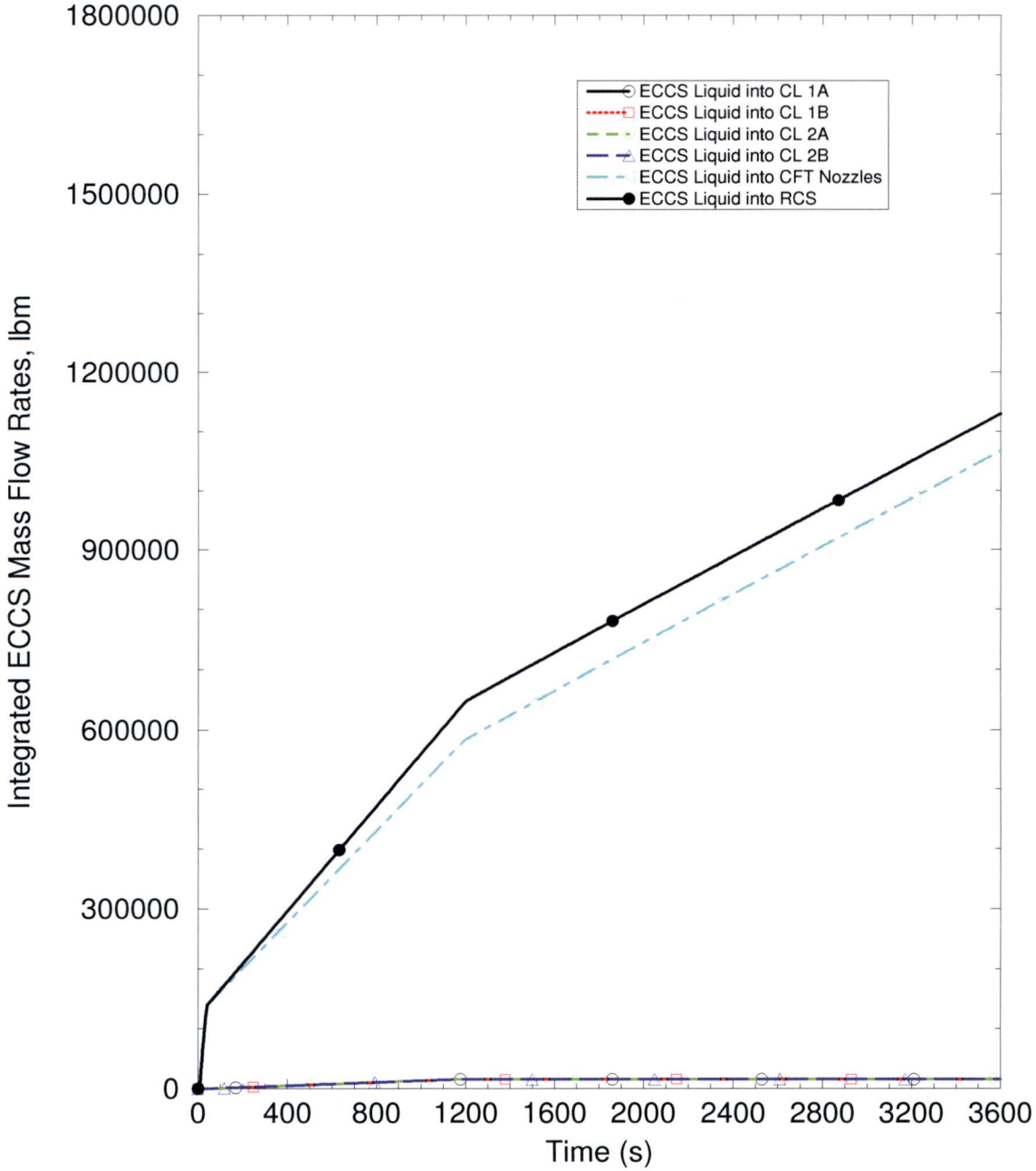

Figure RAI-4.17-8: Integrated Liquid Mass Flow Rates Entering RV through CLs for B&W Analyses

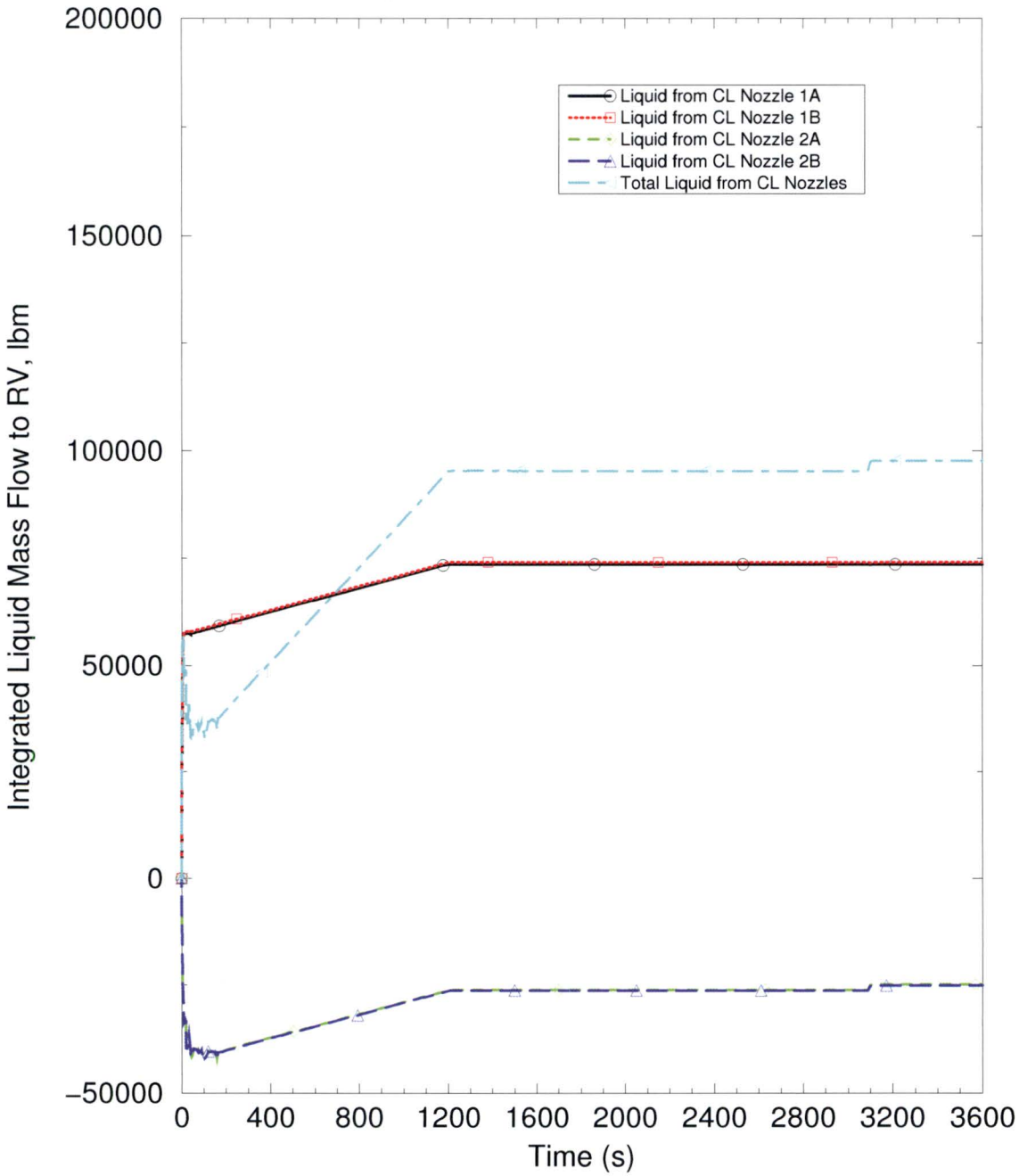

Figure RAI-4.17-9: Integrated Mass Flow Rates Entering RV through Intact HL for B&W Analyses

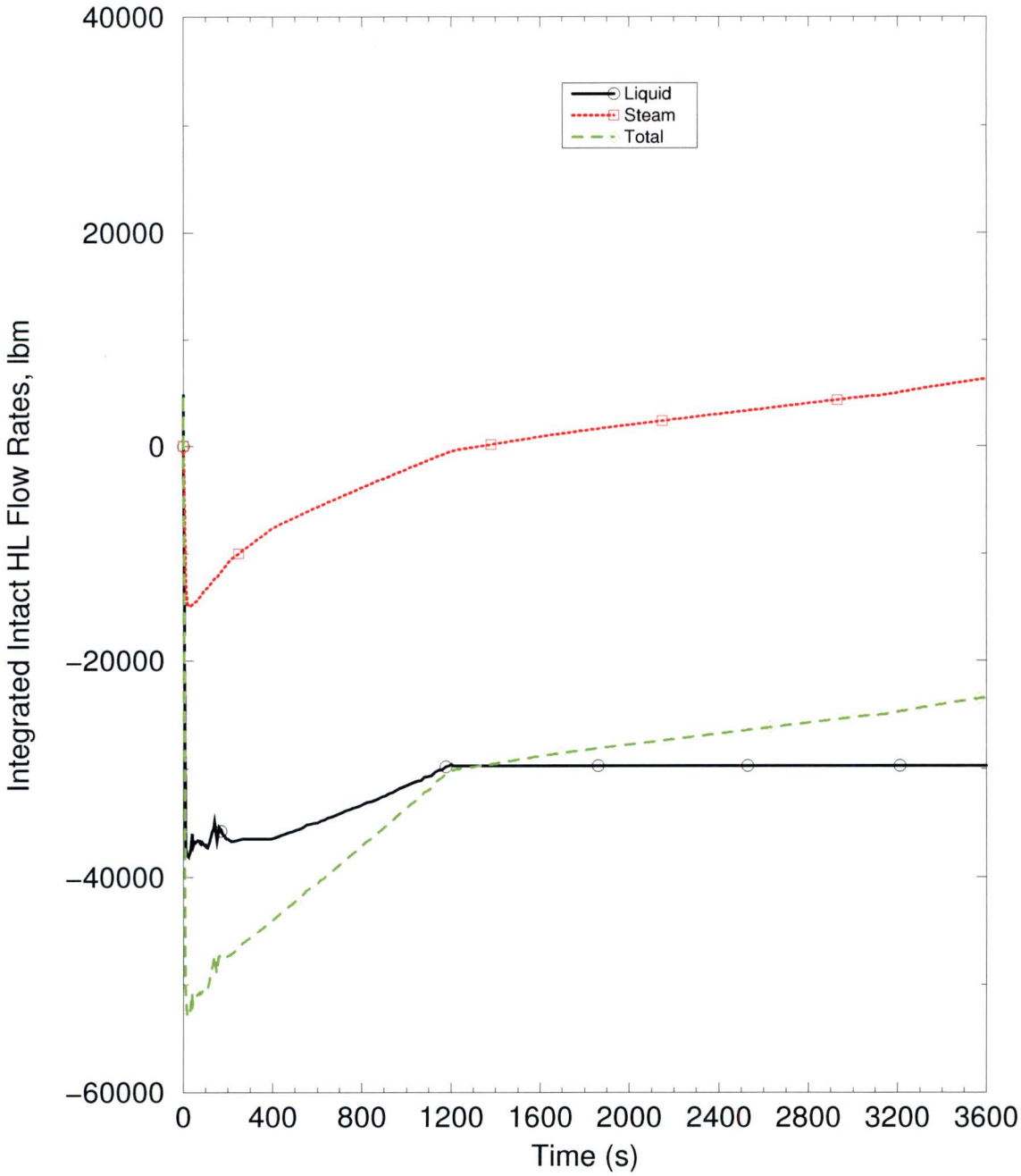

2.18 RAI 4.18

2.18.1 Statement of RAI 4.18

The HLB T-H cases analyzed for the Westinghouse upflow plant category presented in Section 8 include Case 5, which simulated debris blockage for determination of K_{split} and m_{split} at an ECCS recirculation flow rate of 8 gallons per minute per fuel assembly (gpm/FA). As seen in Figure 8-44, following the SSO time, the downcomer and BB collapsed liquid levels decrease relatively rapidly and drop by about 8 ft and 3 ft, respectively, and reach their minimum levels at about 2,100 seconds before starting a gradual recovery. In contrast to all remaining cases presented in Section 8 (Cases 0A, 1B, 2B, 1, and 3), the result for Case 5 shows the predicted downcomer collapsed liquid level decreasing below the BB collapsed liquid level over a period of about 1,800 seconds. Explain the physical processes leading to this prediction based on the code results for this case. Specifically, explain whether liquid entrainment is among the processes. If necessary, implement modeling changes that correct any unacceptable code behavior and present updated results for Case 5.

2.18.2 Response to RAI 4.18

This RAI pertains to the Westinghouse Electric Company (WEC) plant categories and therefore requires no response for the B&W plant category.

2.19 RAI 4.19

2.19.1 Statement of RAI 4.19

The HLB T-H results for the Westinghouse upflow plant category presented in Section 8 include calculations for a single case without debris simulation (Case 0A) and five additional cases that simulate debris for determining t_{block} (Case 1B), K_{max} (Case 2B), and K_{split} and m_{split} (Cases 1, 3, and 5). Regardless of whether debris was simulated or not, the results exhibit a common response as reflected in the plots of collapsed liquid levels for the downcomer, BB, hot assembly, and some plots of predicted RV fluid masses. The response takes place around and following the SSO time. It is characterized by an initial increase in the magnitude of these parameters, which reach maximum levels followed by a relatively rapid decrease. From the predicted collapsed liquid levels, this response is seen taking place around 100 seconds following SSO at 1,300 seconds for Case 0A (Figure 8-7), and within about one minute of the SSO time for Cases 1B (Figure 8-18), 2B (Figure 8-27; it is not easily seen in Figure 8-28 due to core blockage simulated coincidentally with SSO), 1 (Figure 8-36, over a shorter time frame than in the other noted figures due to the high ECCS flow), 3 (Figure 8-40), and 5 (Figure 8-44). A similar response also occurs in Figure 8-17, which illustrates the effect on a predicted RV fluid mass (note that the response is masked in Figure 8-26 due to core blockage simulated coincidentally with SSO).

A similar observation applies to the results presented in Section 9 for the Westinghouse downflow plant category. Figures 9-6, 9-7, 9-17, 9-18, 9-29, 9-33, and 9-37 illustrate the response on predicted collapsed levels and Figures 9-16 and 9-22 show predicted RV fluid masses.

(a) Explain the physical processes leading to this behavior based on the code results for the analyzed cases. This response reflects the system manometric balances and related contributing pressure losses experienced across the core inlet and other simulated flow passages and regions. Describe the effects of each process and explain whether the observed impact from such effects was considered acceptable. Specifically, explain whether liquid entrainment is among such processes. If liquid entrainment has an effect, analyze the degree to which it had an effect on key results from the simulated cases and justify the acceptability of the results.

(b) The maximum resistance, K_{max}, results for the Westinghouse upflow and downflow plant categories are obtained from analyses in which the core blockage is applied simultaneously with SSO. The NRC staff needs assurance that K_{max} results are not affected by processes associated with the above described system response occurring around the SSO time. The NRC staff recommends performing a

re-analyses for the cases presented in Sections 8 (Case 2B) and 9 (Case 2B) used to determine K_{max} with the only change being that the core inlet blockage is applied 200 seconds following the SSO time instead of coincidentally with the SSO time.

2.19.2 Response to RAI 4.19

2.19.2.1 Part a

This RAI pertains to the Westinghouse Electric Company (WEC) plant categories and therefore requires no response for the B&W plant category.

2.19.2.2 Part b

While the RAI specifically pertains to the WEC plant category, an explanation of the process followed in the B&W plant category analyses is presented. In the B&W plant analyses, Sump Switch Over (SSO) is modeled to occur at 1200 seconds as described in WCAP-17788, Volume 4, Section 4.2. Coincident with SSO, debris is assumed to completely block the core inlet such that K_{max} is $1x10^8$. As discussed in detail in RAI 4.22, the baffle region of the B&W plant design has a very low hydraulic resistance. When the blockage is applied, flow previously passing through the core inlet is redirected into the baffle, and enters the core through the LOCA holes and baffle slots. The effect on the system response due to the abrupt application of the blockage is minimal. Instead, the system response shown in the new base case (RAI 4.22) is clearly related to the significant reduction in Emergency Core Cooling System (ECCS) flow rate that occurs at SSO. Given the low resistance of the baffle region in the B&W plant design, delaying the blockage of the core inlet would not change the system response.

2.20 RAI 4.20

2.20.1 Statement of RAI 4.20

The T-H analyses for the large HLB LOCA scenario are used to determine four key parameters, t_{block}, K_{max}, K_{split}, and m_{split}, which are used as inputs to the overall HLB methodology described in Volume 1.

Implementing the high-level process outlined in Figure 4-2, "Overview of Hot Leg Break Methodology," Section 6.5 provides an algorithm that uses K_{split} and m_{split} for calculating in vessel fiber loads and verifying that they comply with the applicable limits for core inlet, in core, and total RV fiber. In particular, the core inlet fiber load is used to determine the core inlet resistance, based on the subscale head loss testing in Vol. 6, so that it can be compared against the applicable K_{max} limit as the accident progresses. This important check is performed in Step 10 of the algorithm. As stated in Step 10, "if the core inlet K factor is greater than K_{max} before the time of t_{block}, then the calculation does not meet the acceptance criteria defined by the TH analyses". The core inlet flow and fiber load after SSO are calculated using both K_{split} and m_{split}. When the core inlet resistance is less than or equal to K_{split}, the flow into the RV passes only through the core inlet where it deposits fiber. When the core inlet resistance is greater than K_{split}, the flow into the RV is split between the core inlet and the alternate flow path (AFP) based on m_{split}. The current core inlet resistance is compared against K_{split} at Step 9 of the algorithm.

The K_{split} and m_{split} critical inputs are determined in Vol. 4 from T-H analyses, which were performed using minimum BB flow resistances "for all plant categories with an upflow BB configuration". Section 4.2 states that "selecting the minimum resistance will minimize the resistance due to debris (and hence the amount of debris at the core inlet) that will begin to divert flow to the AFP". It explains that "minimizing the debris at the core inlet required to divert flow to the AFP will maximize the amount of debris predicted to bypass the core inlet and transport to the core region through the AFP". Section 4.2 further explains that a minimum UHSN resistance "will be applied for cases that are used to determine K_{split} and m_{split}" for the Westinghouse downflow plant category.

Explain if the use of maximum AFP flow resistances result in a conservative mass of debris at the core inlet for all cases. Evidently, using thus determined K_{split} and m_{split} parameters will result in the earliest time of flow diversion through the AFPs and the maximum fraction of ensuing ECCS flow through the AFPs, which will maximize the predicted amount of debris transported to the core region and minimize the amount of debris accumulated at the core inlet. Accordingly, the calculated core inlet debris amount can allow the calculation process to continue, unless stopped due to exceeding the in-core or total RV fiber limits, both of which can be significantly higher than the core inlet fiber limit, and eventually produce an acceptable overall analysis outcome without

detecting possible violation of the applicable core inlet debris limit. Therefore, the generic HLB methodology, using the K_{split} and m_{split} critical inputs established in Vol. 4, could result in non-conservative results for the Westinghouse upflow, Westinghouse downflow, and CE plant categories.

It is possible that an approach based on maximized, as opposed to minimized, AFP resistances for the determination of K_{split} and m_{split} can be considered for implementation in the HLB methodology for assuring satisfaction of the core inlet fiber limit. Provide additional information to justify how the HLB methodology described in WCAP-17788 can be applied to assure satisfaction of the established core inlet fiber based on the t_{block}, K_{max}, K_{split}, and m_{split} results established in Vol. 4. The justification could include sensitivity studies where AFP resistance is minimized for each plant category and plant-specific guidance on this matter.

2.20.2 Response to RAI 4.20

As described in RAI 4.4, all of the baffle designs for the operating Babcock & Wilcox (B&W) plants are identical. To that end, the appropriate baffle resistance was used to establish the K_{split} and m_{split} parameters described in WCAP-17788, Volume 4, Figures 11-3 and 11-4 (and replicated in WCAP-17788, Volume 1 Figures 6-7 and 6-8). However, it can be argued that the curve fits provided for both sets of data are non-conservative.

The basis for developing K_{split} and m_{split} was established early in the development of WCAP-17788 as a way to track where and how much debris is deposited between the core inlet and the heated region of the core. The method was applied universally among all of the plant categories analyzed. As the methodology progressed, decisions were made that could have influenced the calculation of K_{split} and m_{split} although the method was not revisited. This RAI is an outcome of that oversight. Further investigation into the method for the operating B&W plants indicates that the use of K_{split} and m_{split} can be greatly simplified.

The RAI also correctly describes that if the core inlet K factor is greater than K_{max} before the time of t_{block}, then the calculation does not meet the acceptance criteria defined by the TH analyses. For the operating B&W plants, K_{max} is $1x10^8$, which exceeds the K factor determined from testing for the core inlet (WCAP-17788, Volume 1, Tables 6-3 and 6-5). Further, t_{block} is 20 minutes, which corresponds to the first time that debris could reach the core inlet. Clearly, K_{max} will not occur before t_{block} even if K_{max} could be reached.

As described in RAI 4.4, the baffle k/A^2 for the operating B&W plants is less than [ ] from bottom to top. However, the TH analyses show that once the core inlet is blocked, the flow need only traverse the lower grid rib and two former plates before it has

the opportunity to enter the core via a row of LOCA holes in the baffle plates (see Figure RAI-4.4-1). The k/A^2 for this flow path is less than half of the total for the entire baffle region. The TH analyses confirm that complete core inlet blockage can instantaneously occur 20 minutes after the LOCA without resulting in a core heatup. The flow through this low resistance path is able to continue to provide decay heat removal even if the core inlet is completely blocked.

The methodology described in WCAP-17788, Volume 1 for the hot leg break defines the in-vessel fiber limit as the sum of fiber that accumulates at the core inlet and the fiber that reaches the heated region (WCAP-17788, Volume 1, Section 4.1). The core inlet debris limit is defined by fuel assembly testing and ranges from [ ] (WCAP-17788, Volume 1, Section 6.3). The in-core debris limit is limited to [ ] as described in WCAP-17788, Volume 1, Section 6.4. The total in-vessel fiber limit is further restricted to [ ] as described in WCAP-17788, Volume 1, Section 6.5.5, Step 10.

While it is not possible to completely block the core inlet without any fiber buildup, the parameters provided above and the results of the TH analysis demonstrate the operating B&W plants will all have fiber limits [ ]. If zero fiber builds at the core inlet, then all of the fiber will transport to the heated core. If any amount of fiber builds up at the core inlet, the total amount of fiber possible in the RV would exceed this value, but the total fiber load in the RV [ ].

Given the above discussion, it is clear that the fiber limit for the operating B&W plants will be the [ ] and that K_{split} and m_{split} are not needed to determine this limit. That is, within the context of the hot leg break methodology described in WCAP-17788, Volume 1, K_{split} can be set to 20 minutes regardless of ECCS flow rate and m_{split} set to 1.0 for all times after K_{split}. The result will be a fiber limit of [ ], which is what would be calculated if more reasonable values for K_{split} and m_{split} were calculated.

WCAP-17788-P, Volumes 1 and 4 will be updated to reflect the new analyses presented in this RAI response.

2.21 RAI 4.21

2.21.1 Statement of RAI 4.21

The T-H analyses determine four key parameters, t_{block}, K_{max}, K_{split}, and m_{split}, which are used as input to the overall methodology described in Vol. 1. The K_{split} results are presented in Figures 8-4, 9-3, 10-4, and 11-3 and the m_{split} results are presented in Figures 8-5, 9-4, 10-5, and 11-4 in Vol. 4. Fitting curves to the predicted K_{split} and some m_{split} results are shown in each of these plots. The same plots are reproduced in Figures 6-1 through 6-8 in Volume 1.

The T-H analyses do not provide a basis for extrapolation or interpolation of the calculated K_{split} results as a function of the ECCS recirculation flow rate. Provide the applicability of extrapolating the calculated K_{split} values outside of the analyzed range of ECCS rates for the fitting expressions in Figures 8-4, 9-3, 10-4, and 11-3. Justify the ability to interpolate the expressions to reproduce the calculated K_{split} values between the calculated points.

Similar to the case with the calculated K_{split} inputs, the m_{split} results and the supporting T-H analyses in Vol. 4 do not provide a basis for justifiable extrapolation or interpolation of the calculated m_{split} results documented as a function of the core inlet resistance reduced by K_{split} and the ECCS flow rate. Provide the basis for extrapolating the calculated m_{split} results beyond the maximum core inlet resistances analyzed for each assumed ECCS rate to produce the m_{split} results shown in Figures 8-5, 9-4, 10-5, and 11-4. For the Westinghouse upflow category, the largest core inlet resistance of about 4.0×10^4 was reached in the case of 8 gpm/FA, whereas the applicable K_{max} is 5.0×10^5; for the Westinghouse downflow category the largest core inlet resistance of about 1.2×10^5 was reached in the case of 8 gpm/FA whereas the applicable K_{max} is 6.0×10^5; for the CE category the largest core inlet resistance of about 5.4×10^5 was reached in the case of 800 gpm, whereas the applicable K_{max} is 6.5×10^6; and for the B&W category, a core inlet resistance of about 1.8×10^4 was reached for each ECCS rate, whereas the applicable K_{max} is 1.0×10^8. Figures 8-5 and 9-4 each document two fitting expressions for the cases with the lowest and highest ECCS rates for the Westinghouse upflow and downflow categories, whereas Figures 10-5 and 11-4 each show a single fitting curve presumably intended to bound the calculated m_{split} results. Describe how the m_{split} results can be justifiably interpolated to obtain a valid m_{split} input at ECCS flow rates that do not match any of the values analyzed for the Westinghouse upflow and downflow categories (8, 12, 18, 30, and 40 gpm/FA) or for the B&W category (7.5, 12.5, 17.5, 22.5, 27.5, and 43.5 gpm/FA). Also, the significant degree of scatter in the plotted m_{split} points in Figure 10-5 makes the information on the plot hard to interpret.

The NRC staff needs confidence that reliable and valid K_{split} and m_{split} inputs were

obtained. If such assurance is not reached generically, additional T-H calculations to produce applicable K_{split} and m_{split} inputs, including supporting analyses, will be requested on an as-needed plant specific basis.

2.21.2 Response to RAI 4.21

As described in RAI 4.20, the use of K_{split} and m_{split} is not needed to determine a fiber limit for the operating B&W plants. That is, within the context of the hot leg break methodology described in WCAP-17788, Volume 1, K_{split} can be set to 20 minutes regardless of ECCS flow rate and m_{split} set to 1.0 for all times after K_{split}. The result will be a fiber limit of [ ], which is what would be calculated if more reasonable values for K_{split} and m_{split} were calculated. Therefore, extrapolation of the data is not needed.

2.22 RAI 4.22

2.22.1 Statement of RAI 4.22

The small-break LOCA analysis approach applied for the B&W plant category and the plant analysis results for a 0.5 ft^2 small HLB LOCA presented in Section 11 may not meet the requirements of 10 CFR 50.46(a)(1)(i), which states, "ECCS cooling performance must be calculated in accordance with an acceptable evaluation model and must be calculated for a number of postulated loss-of-coolant accidents of different sizes, locations, and other properties sufficient to provide assurance that the most severe postulated loss-of-coolant accidents are calculated". Specifically, it is questionable whether the RCS T-H conditions, predicted at the time of core inlet blockage and thereafter for a 0.5 ft^2 small HLB LOCA, remain applicable to a DEG HLB LOCA, which represents the limiting scenario as stated in the TR. The three arguments provided in Section 6.4 of Vol. 4 in support of the selected 0.5 ft^2 break size do justify extrapolation of the calculated small-break LOCA results to a full-size DEG HLB LOCA transient considered as the limiting scenario.

Provide additional LOCA calculation results for the B&W plant design category, including results for predicted safety criteria, figures of merit, and supporting analysis results, which demonstrate quantitatively that the requirements of 10 CFR 50.46(a)(1)(i) are met. T-H LOCA calculations should be performed using applicable and appropriately assessed EMs.

2.22.2 Response to RAI 4.22

The base plant model selected for the B&W analysis is described in WCAP-17788-P, Volume 4, Section 6.4. The break size analyzed was a 0.5-ft^2 break in the bottom of the pipe adjacent to Hot Leg (HL) nozzle. It was stated that this break size suitably represents a Double-Ended Guillotine (DEG) break in the same location for the purposes of evaluating GSI-191 in-vessel effects. As identified by this Request for Additional Information (RAI), the reasons as stated were not sufficient to address all break sizes and provide assurance that the results are bounding for the application of all HL Loss of Coolant Accidents (LOCAs) for GSI-191 Long Term Core Cooling (LTCC) analyses with core inlet blockage. Further justification of the selection of this break size for the analysis is provided in this RAI response.

The 0.5-ft^2 break results performed and described in WCAP-17788 Volume 4 results in a Reactor Coolant System (RCS) pressure during the LTCC phase that is approximately 20 psi higher than the containment pressure. This result was obtained using a minimum Emergency Core Cooling System (ECCS) flow rate that was conservative by more than

a factor of two as compared to the single train Low Pressure Injection (LPI) flow for the hot leg break location (see response to RAI 4.5a). A larger break size or more ECCS injection would reduce the RCS pressure such that it would be closer to containment pressure, as would be expected with a DEG break. However, conservatively, the higher pressure minimizes core voiding or level swell. The smaller break size also has the potential to achieve more core inlet subcooling, which also reduces the core steam production and overall core level swell. In addition, the time for sump switchover would have been much later with the minimum ECCS flow rates modeled as it takes longer to empty the Borated Water Storage Tank (BWST). The core decay heat would be much lower if the sump switchover time was increased, however, it was held at the earliest time determined with ECCS and reactor building spray maximized (see response to RAI 4.5a). The high decay heat associated with the highest plant power level and low ECCS flow increased the likelihood of core uncovering after the core inlet blockage (based on debris quantities and transport from a DEG break) is imposed. The only potential adverse effects relative to use of a smaller break size is a different minimum liquid mass inventory in the core at the time of sump switchover and slightly more stored energy allowed in the fuel and Reactor Vessel (RV) metal as the saturation temperatures are higher than they would be with a DEG break with the containment at a lower bound of 14.7 psia.

To further support the qualitative assessment provided above, and to provide further demonstration that the requirements of 10 CFR 50.46 are met, additional analyses are presented. Specifically, DEG Hot Leg Break (HLB) LOCA analyses were performed using both Large Break Loss of Coolant Accident (LBLOCA) and Small Break Loss of Coolant Accident (SBLOCA) Evaluation Models (EMs). These analyses are provided for two purposes: (1) demonstrate that the 0.5-ft^2 SBLOCA analysis provided in Volume 4 was a reasonable choice and (2) demonstrate that the use of the SBLOCA EM is appropriate for LTCC applications. While both of these objectives were met (as described below), the decision was made to make the DEG SBLOCA analysis the new Analysis of Record (AOR) for GSI-191 applications. Use of the DEG break for the B&W plants provides consistency with the break size used for the Combustion Engineering (CE) and Westinghouse Electric Company (WEC) plant types and provides a more appropriate analysis for the operating B&W plants as described in the following material.

The analysis described in Volume 4, Section 11 was performed using the Crystal River-3 (CR-3) plant model at a proposed uprated power level plus uncertainty (3026 MWt), because this was the highest analyzed power of all B&W-designed plants that were operating at the time that the original analyses for GSI-191 were performed. The CR-3 plant has since closed. The next highest powered plant including uncertainty (2827.4 MWt) that is operating is the Davis-Besse (DB) plant. Therefore, the Cold Leg Pump Discharge (CLDP) AOR LBLOCA plant model for DB was used as a starting model from which the inputs were modified to have a consistent basis with the assumptions used in the base GSI-191 analysis documented in WCAP-17788-P, Volume 4.

Two analyses of a DEG hot leg break were performed to support the new AOR for GSI-191. The first analysis used an SBLOCA model that conformed to the guidance described in BAW-10192, Volume 2 (Reference 4.22-1). The additional changes described in WCAP-17788-P, Volume 4, Section 6.4 were made to the DB model with the exception of the break size. For this new analysis, a DEG break model was specified. The second analysis used an LBLOCA model that conforms to the guidance described in BAW-10192, Volume 1, Section 4.3.7. Modifications were made as described in WCAP-17788-P, Volume 4, Section 6.4 for the GSI-191 scenario.

In both cases, a DEG break in the hot leg at the elevation of the core exit nozzle was analyzed up to the earliest sump switchover. The approximate earliest time of Sump Switch Over (SSO) for any B&W plant with maximum ECCS flow and with both reactor building spray pumps in service was defined as 20 minutes (see response to RAI 4.5a). While the complete switchover process takes five minutes or more to complete, the analyses assumed the transfer was instantaneous and with sufficient debris to totally block the core inlet paths simultaneously at 20 minutes in the simulation. Simulating these actions at 20 minutes maximizes the core decay heat and requires the highest ECCS flow to the core to remove the energy. Therefore, the combination of minimum ECCS flow rates and earliest SSO time provides the most severe challenge to demonstrating continuous LTCC.

The large, HLB methodology (described in BAW-10192, Volume 1, Section 4.3.7) (hereafter referred to as the LBLOCA method) was developed specifically for the Short Term Core Cooling (STCC) period, which typically ends at the time of average channel core quench. After this point, conservative modeling choices required by Appendix K to maximize Peak Cladding Temperature (PCT) severely limit the ability of the model to complete the quench of the hot channel and provide meaningful core internal circulation rates following core quench. [

] Therefore, alternate modeling is needed for simulation of the LTCC phase of the event, especially when using the LBLOCA modeling after the core inlet is completely blocked.

[

]

[

]

Several options were considered for addressing the analytical modeling choice used for the DEG GSI-191 analyses. The option selected uses an alternative calculation that uses the SBLOCA model throughout the DEG HLB transient. The SBLOCA modeling has a sufficient number of fuel assemblies to allow the recirculation to be unencumbered by axial flow areas. This approach is validated for the LTCC phase via comparisons to the STCC results from the approved HLB LBLOCA EM method to those of the DEG HLB SBLOCA model with some appropriate modifications to make it consistent with the LBLOCA EM.

The modifications to the STCC SBLOCA EM model, which was developed to analyze the limiting peak clad temperature PCT break sizes in the CLDP piping, are simple and straightforward. The following changes were made:

1. Break size and location with the containment pressure set to 14.7 psia,
2. HL break modeling from a split arrangement to a DEG modeling with smaller volumes identical to those used in the LBLOCA model,
3. Disable the departure of nucleate boiling (Departure from Nuclate Boiling (DNB)) termination trip (e.g. allow DNB and subsequent rewet and quench),
4. Core volume and junction modeling to that used in the post-reflood phase, and
5. Various other control variable additions and minor changes to facility the extended LTCC phase calculations.

Of these changes, the two primary variations in the SBLOCA methods to allow the analysis to continue following DNB were to allow rewet and quench (Item 3) and the use of different control volume core modeling options (Item 4). The core modeling options are made to simulate the LTCC phase of the transient.

The EM requires that the SBLOCA model be stopped if DNB occurs or the Critical Heat Flux (CHF) is exceeded. This restriction is imposed for the STCC PCT predictions only, but since the focus of the GSI-191 efforts is the LTCC phase, it is acceptable to allow DNB to occur with a return to transition or nucleate boiling in the model to get to the LTCC phase of the accident that is the area of focus. By the time of sump switchover, the core has been refilled and the fuel pins rewetted and quenched. Provided the thermal-hydraulic conditions and system inventories are appropriate at the time of sump switchover between the LBLOCA and SBLOCA models, there is no reason why the SBLOCA model should not be used to assess the core response to the inlet blockage.

The SBLOCA EM uses equilibrium core control volumes during the STCC phase, similar to the LBLOCA model during the blowdown phase of the event. The EM heat transfer package uses heat transfer correlations developed for application with two-phase fluids in an equilibrium state. Use of equilibrium for the STCC PCT predictions in SBLOCA analyses is appropriate because the smaller LOCAs evolve into a boiling pot phase, where there are two fluid phases present in the core region are near saturated conditions. The fluid in the core remains effectively in an equilibrium state during the violent blowdown phase of a LBLOCA; however, it becomes non-equilibrium during the refill and reflooding phases as highly subcooled water from the Core Flood Tanks (CFTs) enters the core creating the potential for non-equilibrium from subcooled nucleate boiling in the pool or quenched region of the core. Above the quenched region, the steam can be superheated with entrained saturated liquid droplets. Therefore, the core control volumes are modeled as non-equilibrium for the refill and reflood phases of the event for the LBLOCA transient.

The SBLOCA method analysis of a large HLB for GSI-191 purposes is most focused on the post refill portion of the event, where non-equilibrium in the pool can occur. The blowdown phase of the event is over in less than 20 seconds. Given this short duration of the blowdown phase for which the SBLOCA model is not used to establish PCT results, it is acceptable for the entire event can use non-equilibrium in the core of the SBLOCA GSI-191 HLB model.

The DEG HLB was modeled at the reactor vessel hot leg nozzle exit elevation by splitting the first hot leg control volume into three volumes based on the methods described in the EM. The broken hot leg was modeled in the loop that did not contain the pressurizer. The approved EM method calculates a minimum containment pressure near the end of blowdown (EOB) that is typically in the range of 40 to 50 psia and decreasing to 25 to 35 psia by five minutes, which covers the STCC phase of the LBLOCA for the B&W-designed plants. However, because of continued fan cooler heat removal along with reactor building spray flow from the BWST, the containment pressure will decrease. The containment pressure later during the LTCC phase can approach atmospheric values. Rather than compute a containment pressure for the GSI-191 application, the containment pressure was conveniently and conservatively set to 14.7 psia for the entire duration of the event.

The approved LBLOCA HLB model was used to perform a DEG analysis of the hot leg piping at the elevation of the RV outlet nozzle. The RCS pressure quickly approaches the containment pressure for a DEG break. [

]

[

]

The key comparison parameter between the two methods is the liquid inventory in the core, core baffle, core bypass and upper plenum at the time of sump switchover when a complete core inlet blockage is imposed. The inventory in this region is not explicitly part of the reported parameters however the total liquid volume in the RV (Figure RAI-4.22-1, which includes the Downcomer (DC) volume in addition to the above volumes) and the collapsed level in the DC (Figure RAI-4.22-2) are available. The downcomer collapsed levels have similar trends. After 300 seconds the collapsed liquid levels are effectively the same. Since the downcomer collapsed liquid levels are the same, the RV liquid inventory can be used to compare the liquid inventory in the core and upper plenum. The two methods produce very similar results of the minimum RV inventory prior to refill and maximum inventory from CFT discharge. Slight differences in carryout change the volumes in the first 600 seconds (10 minutes), but after that time until the time of sump switchover, both models are nearly identical.

Table RAI-4.22-1 gives some of the key sequence of events and results comparisons between the two cases. This table shows a considerable difference in the STCC PCT which is not unexpected between the two methods. The SBLOCA analysis model does uncover the core early (before SSO) and show fuel pin heatup similar to the LBLOCA results; however, the hot pin and average core quench sooner with the SBLOCA method, because the mixture level swell was higher for this methodology during the STCC phase of the transient. The largest timing difference shown in the table is the time for the hot channel quench. The LBLOCA method quenched the average core at 400 seconds but the hot channel did not quench until approximately 1125 seconds. The delayed quench is primarily an artifact of the model [

]

While this is conservative for STCC PCT predictions it is not realistic for the boiling pot phase that exists during LTCC. The SBLOCA model has been designed to handle these conditions and its quench timing and results are more realistic and appropriate for LTCC calculations.

Comparisons of the DEG HLB LOCA using the LBLOCA EM and the SBLOCA EM methods described show that the RV liquid inventory is effectively the same at the time the BWST empties (SBLOCA 1584 ft^3 versus LBLOCA 1588 ft^3). Based on the similarity of the two comparisons, plus the fact that the SBLOCA EM did quench the core at the time that considerable liquid discharge began to occur from the RV side of the break, it is concluded that the SBLOCA EM is the appropriate tool to use for this analytical work and

to extend the analysis longer in the LTCC phase following sump switchover and imposition of complete core inlet blockage at 20 minutes.

The 0.5 ft^2 SBLOCA EM HLB analysis was performed for the B&W plants in Volume 4 of WCAP-17788-P. The minimum ECCS flow used in that analysis calculated the RV liquid inventory to be 1546 ft^3 at the time of sump switchover. While the spectrum of break sizes was not explicitly addressed, the analysis that was performed resulted in a RV liquid volume at the time of sump switch that was similar to but slightly less than that obtained by a DEG HLB LOCA. Therefore, the selection of a high core power and low ECCS flow for the prior WCAP-17788 analyses was reasonable to conservative based on the new DEG HLB analyses. Together these two cases demonstrate that different ends of the large break spectrum have been considered.

The results of the DEG HLB SBLOCA EM model GSI-191 analyses will be used as the new AOR for GSI-191 and will be used to address the RAI responses for the B&W-designed plants. This break size is consistent with the one that generates the maximum core debris and sets the earliest time for sump switchover. It is also consistent with the break sizes considered and analyzed by the WEC and CE plants. Further, Volume 4 will be updated to reflect this new AOR for the B&W plant categories.

Table RAI-4.22-1: Sequence of Events and Results of the DEG HLB LBLOCA vs. SBLOCA Method

Description	Large Break EM - DEG	Small Break EM - DEG
Break Opens, sec	0.0	0.0
CFT Injection Starts, sec	7.9	8.4
Core Reflood Begins, sec	12.9	NA
CFT Injection Ends, sec	39.0	40.5
ECCS Actuation, sec	40.1	40.7
Average Channel Quenched, sec	~400	~50
Hot Channel Quenched, sec	~1125	~75
Average Channel PCT, °F	952	700
Average Channel PCT Time, sec	100	16.3
Hot Pin PCT, °F	1584	1279
Hot Pin PCT Time, sec	228	13.6
Liquid Volume available to RV at 600 sec, ft^3	1472	1474
Liquid Volume available to RV at 1200 sec, ft^3	1588	1584
Time of SSO, sec	1200	1200

Figure RAI-4.22-1: DEG HLB Comparison of RV Liquid Volumes with the Large and Small LOCA Models

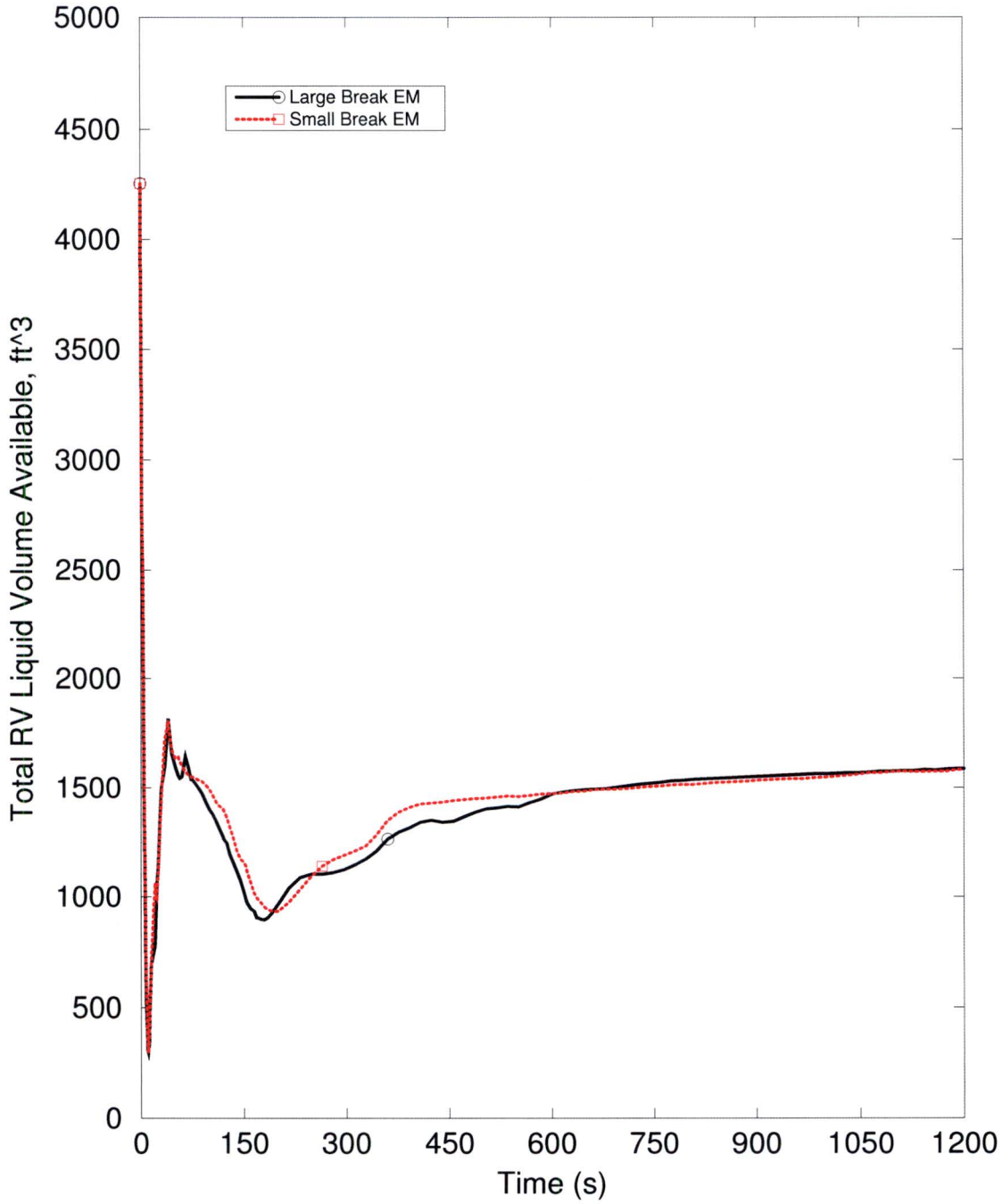

Figure RAI-4.22-2: DEG HLB Comparison of RV DC Collapsed Liquid Levels with the Large and Small LOCA Models.

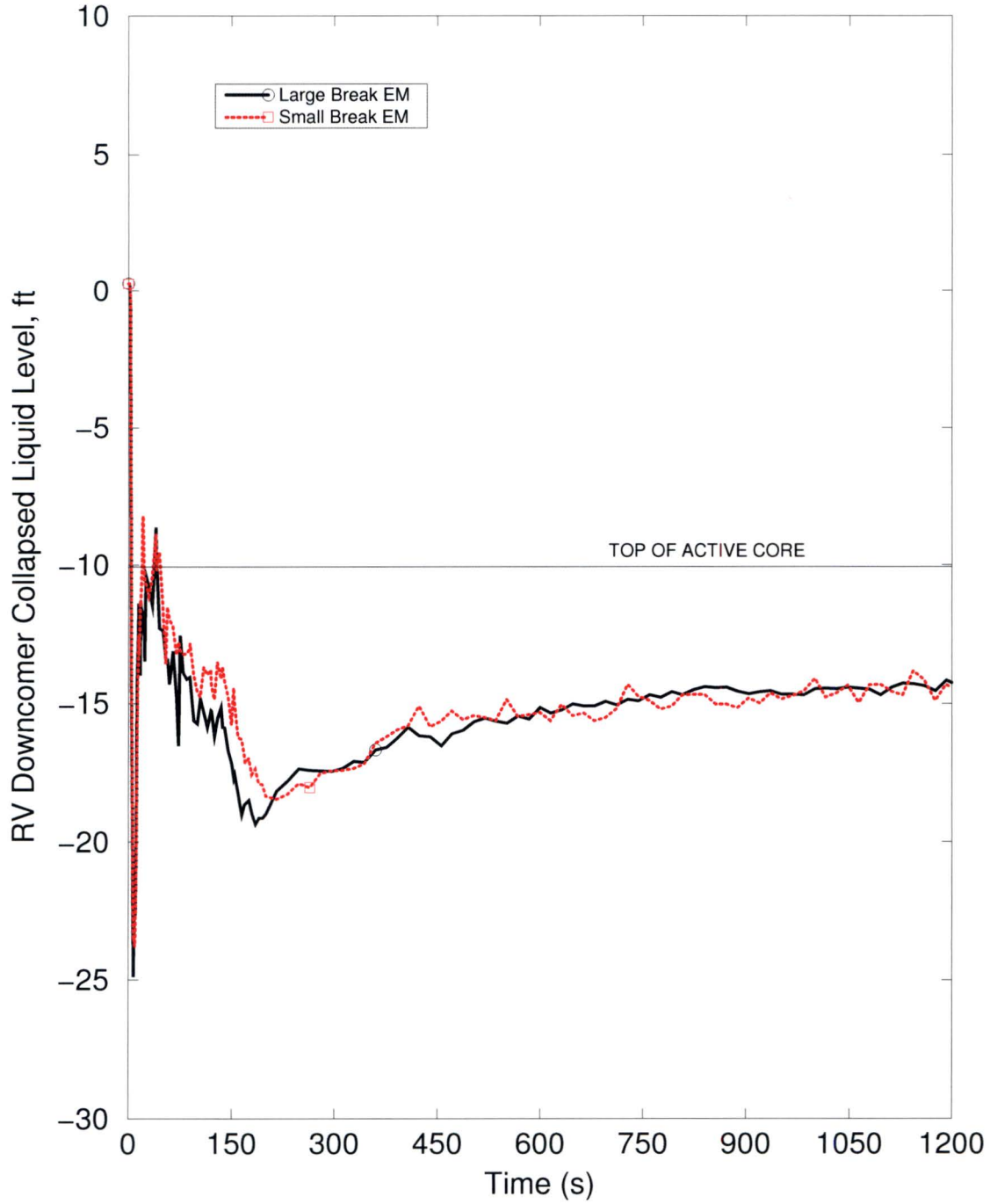

References - RAI 4.22

4.22-1 AREVA Document BAW-10192PA, Revision 0, *BWNT LOCA - BWNT Loss-of-Coolant Accident Evaluation Model for Once-Through Steam Generator Plants.*

2.23 RAI 4.23

2.23.1 Statement of RAI 4.23

To assist the NRC staff evaluation of liquid discharge through the break for the large HLB LOCA scenario, provide the following information for each of the four analyzed plant categories for the limiting break size.

(a) Identify key transport mechanisms of liquid discharge through each side of the break that can occur during transient phases of relevance to the T-H analyses. Explain how liquid transport mechanisms caused by liquid spillover under elevated two-phase mixture levels in the reactor upper plenum due to carry-out of dispersed liquid by entrainment under depressed mixture level conditions are accounted for and modeled in the applied codes. Describe whether the liquid transport models are reflective of and dependent on the upper plenum two-phase mixture level and explain how the performance of these models, in terms of their accuracy and sensitivity, depends on the code capabilities to predict the two-phase mixture levels in the reactor upper plenum under conditions representative of the LTCC phase of a large HLB LOCA.

(b) Describe code assessments, including analyses and results, which demonstrate the capability of the codes used in the T-H analyses to adequately predict transport mechanisms that result in liquid discharge through the break during LTCC. Consideration should be given to contribution from mechanisms accounting for both entrainment and deposition (de-entrainment) of liquid that can take place in participating RV regions including the upper plenum and connected broken hot leg piping. Include information identifying test facilities, test runs, and test conditions used in the code assessments. Provide comparisons of code predictions against relevant test data, as available.

(c) Explain if any special liquid entrainment models, modeling options, and related flags were available in the applied codes and if any such features were activated in the T-H analyses to account for liquid entrainment. Examples of such modeling features can be related to special upper plenum entrainment models, mixture level models, and related special interfacial drag models. State whether any break flow multipliers were applied in the analyses. Provide the multiplier values, and explain if the selected inputs were examined for impact on the predicted break liquid discharge.

(d) Identify key models used and the underlying correlations related to the predicted break liquid discharges. Provide the ranges of applicability of these correlations,

and compare them against the conditions predicted in the analyses documented in Sections 8 through 11. Provide the information in a table format for each of the cases analyzed to determine t_{block} and K_{max} in Section 8 (Cases 1B and 2B), Section 9 (Cases 1A and 2B), Section 10 (Cases 1 and 2), and Section 11.

(e) If not provided elsewhere, include plots showing the following sets of parameters for the cases documented in Sections 8 through 11 as a function of transient time:

(i) Mass flow rates of liquid, steam, and total fluid (liquid and steam) discharges through each opening of the DEG break. Include integrals of the identified break mass flow rates.

(ii) Two-phase mixture level on the core side of the RV

(iii) Steam flow quality calculated as a ratio of the steam mass flow rate to the total (liquid and steam) mass flow rate for the RV-side opening of the DEG break

(iv) Predicted pressure difference between the upper plenum cell connected to the broken hot leg pipe and the containment backpressure.

(f) Figure 1 below compares predicted exit qualities for the original analysis of Case 1 used to determine t_{block} for the CE plant category as documented in Section 10 and the revised analysis in Erratum, submitted with the February 12, 2016, letter OG-16-42 (t_{block}=20,000 seconds). It is noted that the results are significantly different following the simulated blockage time in each analysis. The results also differ during some time periods prior to 15,000 seconds, which is the earlier of both simulated t_{block} times. Describe why the results prior to 15,000 seconds are not consistent between the two cases and state which case presents the correct values. Provide similar information for the time period after blockage is simulated. Please describe why the results fluctuate significantly and justify that the code performance provides a valid representation of the system.

(g) During the NRC audit of the AREVA T-H analyses for the CE plant category, entrainment predictions using S-RELAP5 were presented to the NRC staff. Explain whether any code and/or plant input model changes were found necessary to address the code performance. If they were needed, identity and describe any modeling changes that were implemented along with their supporting validation bases. Justify the break liquid carry-out predictions for each of the analyses for the CE plant category in Section 10 including any revisions to these analyses. If necessary, provide updated T-H analysis results.

(h) Investigate whether the substantial scatter in the m_{split} results shown in Figure 10-5 is related to the behavior of the break liquid carry-out result. Note that if the liquid carryover is incorrect, it can render the m_{split} result unacceptable. Describe whether correction of the m_{split} results was found necessary to address the observed scatter

if it was determined that effects from deficiencies in the predicted liquid entrainment were a contributing factor. Provide any updated result if applicable.

(i) Provide assessments demonstrating that t_{block}, K_{max}, K_{split}, and m_{split} results, as obtained from the analyses in Sections 8 through 11 for compliance demonstration with regard to the acceptance criteria, are accurate and not influenced unduly by deficiencies in the entrainment predictions that can be attributed to various factors such as those discussed above in Items a through h. Include consideration of the effects that the ECCS temperatures, both prior and following SSO, and modeling assumptions related to this parameter can have on the prediction results for entrainment.

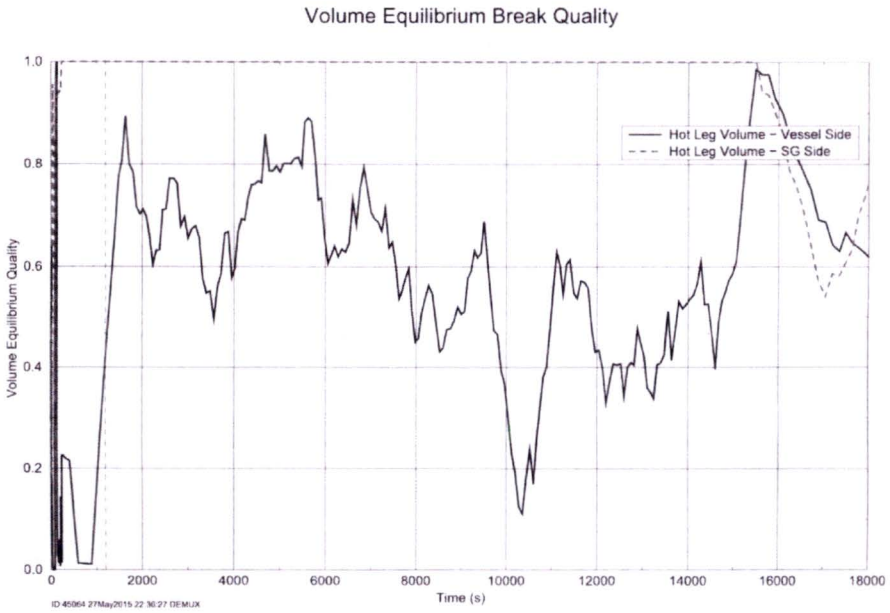

Figure 10-22 Case 1 – Break Exit Quality

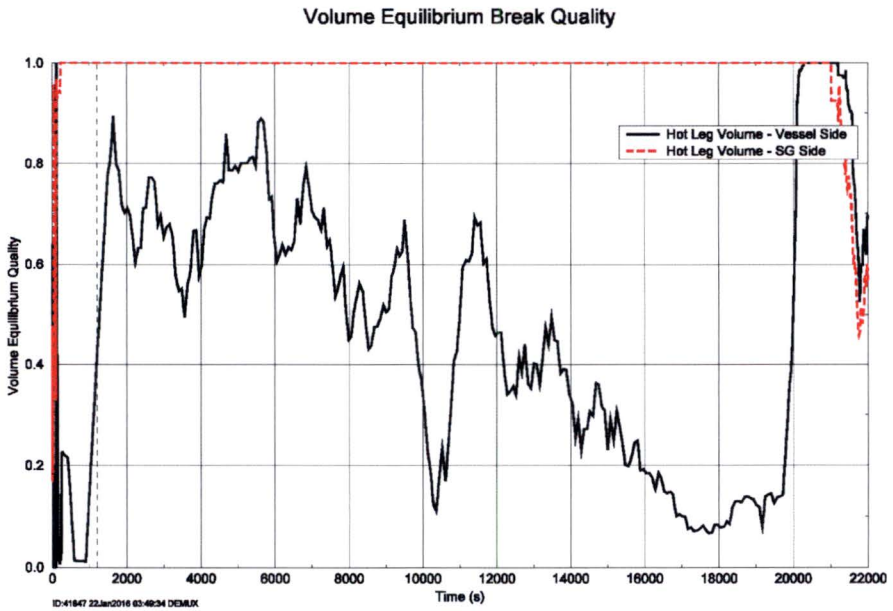

Figure 10-22 Case 1 – Break Exit Quality

Figure 1: Predicted Break Exit Qualities for Case 1 to Determine t_{block} for the CE Plant Category (Top: original result from WCAP-17788 Rev. 0 with t_{block}=15,000 s = 250 min Bottom: corrected result from WCAP-17788, Erratum, OG-16-42 with t_{block}=20,000 s = 333 min)

2.23.2 Response to RAI 4.23

2.23.2.1 Part a

During the blowdown and reflooding phases of Short Term Core Cooling (STCC), entrainment of liquid droplets within the steam flow field is important as it controls the core pool region liquid mass, core quench times, and cladding temperature response above the quench front. Extensive reflooding phase benchmarks (UPTF, SCTF, CCTF, FLECHT, REBEKA and G2) are performed to confirm the validity of the code models to predict these key facets of this Thermal Hydraulic (TH) behavior during the STCC. Once the core is quenched STCC ends and Long Term Core Cooling (LTCC) begins. The additional steaming contribution from the stored energy in the fuel and metal structures is lost and the only steam production is created by the boiloff of liquid to remove the decay heat. As the time after reactor shutdown increases during the LTCC phase of the transient, the decay heat decreases and the substantial entrainment mechanism ceases.

The core and upper plenum mixture level is controlled during LTCC by the decay heat rate, core inlet flow and subcooling, pressure, and core axial power shape. The level swell is lower but the core liquid inventory is higher for smaller decay heat rates, high inlet flows and subcooling, higher pressures, and top skewed axial power peaks. By the time of Sump Switch Over (SSO) for a Hot Leg Break (HLB) Loss of Coolant Accident (LOCA), the core and upper plenum region have refilled with a two phase mixture level to roughly the elevation of the break. From this point onward, the entrainment has diminished to nearly nothing as it is effectively replaced by mixture level spilling out of the break. While the Reactor Vessel (RV) side of the break active, the steam generator side of the Double-Ended Guillotine (DEG) is quiescent. The steam generator side conditions are all steam and it is superheated to roughly that of the secondary side saturation temperature. The steam flow rates are small but oscillatory with a magnitude in the order of a few lbm/s.

With respect to the potential for core uncovering when a complete core inlet blockage is applied, the highest decay heat rates, saturated minimum core inlet flows, lowest pressure, and top skewed power peaks minimize the core liquid inventory. Therefore, this combination of inputs is used as it maximizes the severity should core uncovering occur. If core uncovering does not occur with this combination of inputs then no other variation of these parameters will cause core uncovering and additional sensitivity studies are not needed. By minimizing the Emergency Core Cooling System (ECCS) flows, the time it takes for the Alternate Flow Path (AFP) to begin to deliver flow to the core is lengthened. Low pressure and low subcooling maximizes the boiling contribution and require the largest AFP flow to offset the boiloff and a core exit peak maximizes the cladding heat-up should the core uncover.

The B&W plants have two unique features (compared to the Combustion Engineering

(CE) and Westinghouse Electric Company (WEC) plant designs) relative to GSI-191 analyses. First, the barrel/baffle region of the core has a very low resistance with a "shortcut" from the baffle region to the core via the LOCA holes in the core baffle plates (see response to RAI 4.4 for details). As extensively discussed elsewhere in the RAIs for the B&W plants, this feature allows a continuous flow of ECCS into the baffle and through the first row of LOCA holes and into the core even after the core inlet is completely blocked.

Second, the B&W plants have a unique upper plenum geometry as was shown in Figure 3-6 of WCAP-17788-P, Volume 2 and provided in Figure RAI-4.23-1 for convenience. The upper plenum is divided into two regions by the plenum assembly. The control rod housings reside on the inside of the cylinder. The space between the outside the cylinder and the core support shield or core barrel wall is called the "outlet annulus". The plenum cylinder has a series of moderately sized holes adjacent to each of the RV exit (hot leg) nozzles. It also has multiple larger holes at a higher elevation in the plenum cylinder to promote mixing of the core exit fluid during normal operation prior to exiting the hot leg nozzles. This region is an effective steam water separator during LOCAs with the Reactor Coolant Pumps (RCPs) tripped.

During the core refill, the majority of the steam flows up into the upper plenum and out of the larger holes higher in the plenum assembly. After the core refills completely, the excess ECCS not boiled off continues to flow upward creating a mixture level that rises into the middle region of the upper plenum. Once the level reaches the lower set of moderately sized holes in the plenum assembly adjacent to the hot leg nozzle, the liquid not boiled off flows through the holes into the outlet annulus region. The liquid separates from the steam and fills the bottom of the outlet annulus until the liquid level approaches the bottom of the Hot Leg (HL) nozzle. Once the outlet annulus is nearly full, the acceleration of the steam velocities coming down from the upper holes in the plenum assembly can sweep liquid off of the top of the mixture in the outlet annulus and out the broken hot leg.

When the mixture level in the RV Upper Plenum (UP) has reached this configuration, the ECCS liquid not needed to replace that which is boiled off by the core decay heat will flow out of the hot leg and to the break. As demonstrated in the thermal-hydraulic analyses presented in the response to RAI 4.22, this plant condition is reached well before the time of SSO (and the application of a blockage at the core inlet).

Once the core inlet blockage is assumed at 20 minutes, the ECCS flows are delivered to the core from the baffle via the AFP. The low resistance of the AFP in the B&W plants allows sufficient core cooling flows from the ECCS. The core Decay Heat (DH) can boil off roughly 71 lbm/s (532 gpm) of saturated water at this time. The ECCS injection following sump switchover will be between 1500 and 5000 gpm. Given these flow ranges, there is always an excess flow after SSO.

In order to visually show the mixture levels in the core and downcomer after SSO, colored overlays were put on top of the reactor vessel (Figure RAI-4.23-2). The mixture levels in the core and upper plenum was shown by a graduated pink overlay, while the downcomer and lower plenums collapsed levels were shown in blue. The lower portion of the baffle region is also shown in blue as the core inlet blockage, shown in dark brown, interrupts the flow through the fuel inlet region causing it to be diverted into the baffle as an AFP. Prior to core inlet blockage, the core flow enters through the core inlet and the baffle flow is downward. The core levels are the same, but the downcomer level will be slightly lower than those depicted. A high level flow pattern is provided in Figure RAI-4.23-3 for a B&W plant with holes in the baffle when the core inlet is completely blocked and the AFP is providing ECCS flow to the core.

When the blockage is instantaneously imposed, the core inlet resistance through the baffle requires an increased elevation head in the downcomer to overcome the higher flow losses in the lower baffle and the first row of holes in the baffle plates. Based on a simple Bernoulli calculation, it takes an additional 1.5 ft of elevation head difference to force a minimum ECCS flow of 1500 gpm through the AFP versus though an unblocked core inlet. Figure RAI-4.23-4 shows how much the downcomer elevation head must change to provide the different ECCS flow rates through the AFP and into the core.

The 1500 gpm minimum ECCS flow used in the example provided can raise the Downcomer (DC) level by 1.5 ft in less than 30 seconds. So within 30 seconds of imposing the instantaneous blockage, the elevation head needed to flow 1500 gpm of ECCS to the core is established. The short duration prior to when the AFP is established does not allow time for the core inventory to decrease and uncover the core, therefore the B&W reactor designs allow for continuous core cooling without any uncovering at the time that an instantaneous blockage is imposed. There is even less of a delay in establishing the sufficient AFP flow if the blockage forms more slowly or at a later time when the decay heat is lower.

The elevation head across the AFP is also augmented by a boiloff reduction of the core collapsed level. When the core inlet flow stops, the liquid in the core boils off off until the ECCS delivery can be reestablished. For the B&W plant geometry it takes a fraction of a minute before the lower baffle flow direction reverses and this AFP flow provides adequate flow to the core to match or exceed boiloff. The rate of core collapsed liquid level reduction at 20 minutes due to boiloff is roughly 1 foot in 45 seconds. When the core and DC rates of change are considered together, the elevation head of 1.5 feet is obtained in roughly 20 seconds following complete core inlet blockage for an ECCS flow rate of 1500 gpm. At higher ECCS flow rates, this time will be shorter. The ranges of possible ECCS flow rates following SSO are well in excess of the boiloff rate. Given this large surplus of ECCS and the low AFP resistance, there is no challenge to the conclusion that the AFP in the B&W plant can reverse flow rapidly and maintain adequate to abundant core cooling with excess ECCS liquid spilling out of the break.

The effects of Reactor Coolant System (RCS) pressure, decay heat, axial power shapes, and ECCS subcooling can slightly impact the mixture level swell in the core and upper plenum regions when determining the time when the excess ECCS spills out of the broken HL. If the pressure was higher, the core inventory would be greater; however it is supported with the requisite DC level that is established prior to the time of sump switchover. Lower decay heat also increases core inventory, but like the pressure effect, the DC level to support additional liquid in the core and upper plenum is established prior to sump switchover. Excess ECCS was spilling out of the break within 10 minutes into the transient, so any small variation in the mixture level will adjust well before the time of SSO. A core inlet axial shape can also increase the void fraction in the core, which reduces the liquid inventory. A lower DC level is needed to support the collapsed level in the core and upper plenum that swells to the elevation of the break where it spills out continuously. More ECCS subcooling, reduces the core boiling and decreases the level swell. However, the excess ECCS flow simply increases the liquid volume in the core, upper plenum and DC regions based on the manometric balance through the AFP until the level swell in the upper plenum reaches the break elevation and the excess ECCS fluid not boiled off exits the break.

The excess ECCS flow into the core for the B&W plants maintains a mixture level that resides continuously above the top of the core during the LTCC phase and within the elevation of the hot leg nozzle. The excess ECCS liquid not used for core boiloff will flow out of the break with the core steam that does not flow through the Reactor Vessel Vent Valves (RVVVs) or around the loop if the loop seals are cleared to be condensed on the subcooled ECCS that is injected in the cold legs and upper DC. This continuous core liquid throughput, keeps the concentration of the boric acid or sodium-borate compounds at low values such that will not reach the solubility limit and precipitate in any location of the RV. The sodium-borate is formed when the sump pH additives that are mixed in the containment with the Borated Water Storage Tank (BWST) and RCS fluid expelled from the break. This mix is injected into the RV following sump recirculation.

Given the above discussion, liquid entrainment in the RV upper plenum is not an issue for LTCC for the B&W plants. The core mixture level resides continuously at the level of the break for the B&W plant design and liquid spills out of the break due to the level versus from entrainment. While there can be some small liquid droplet entrainment off of the top of the outlet annulus mixture level, there is no substantial core or central upper plenum region entrainment of liquid by the steam flow during the LTCC. The RELAP5/MOD2-B&W code and B&W plant models have been shown to appropriately predict this behavior.

Figure RAI-4.23-1: B&W 177 FA Reactor Vessel and Internals Arrangement

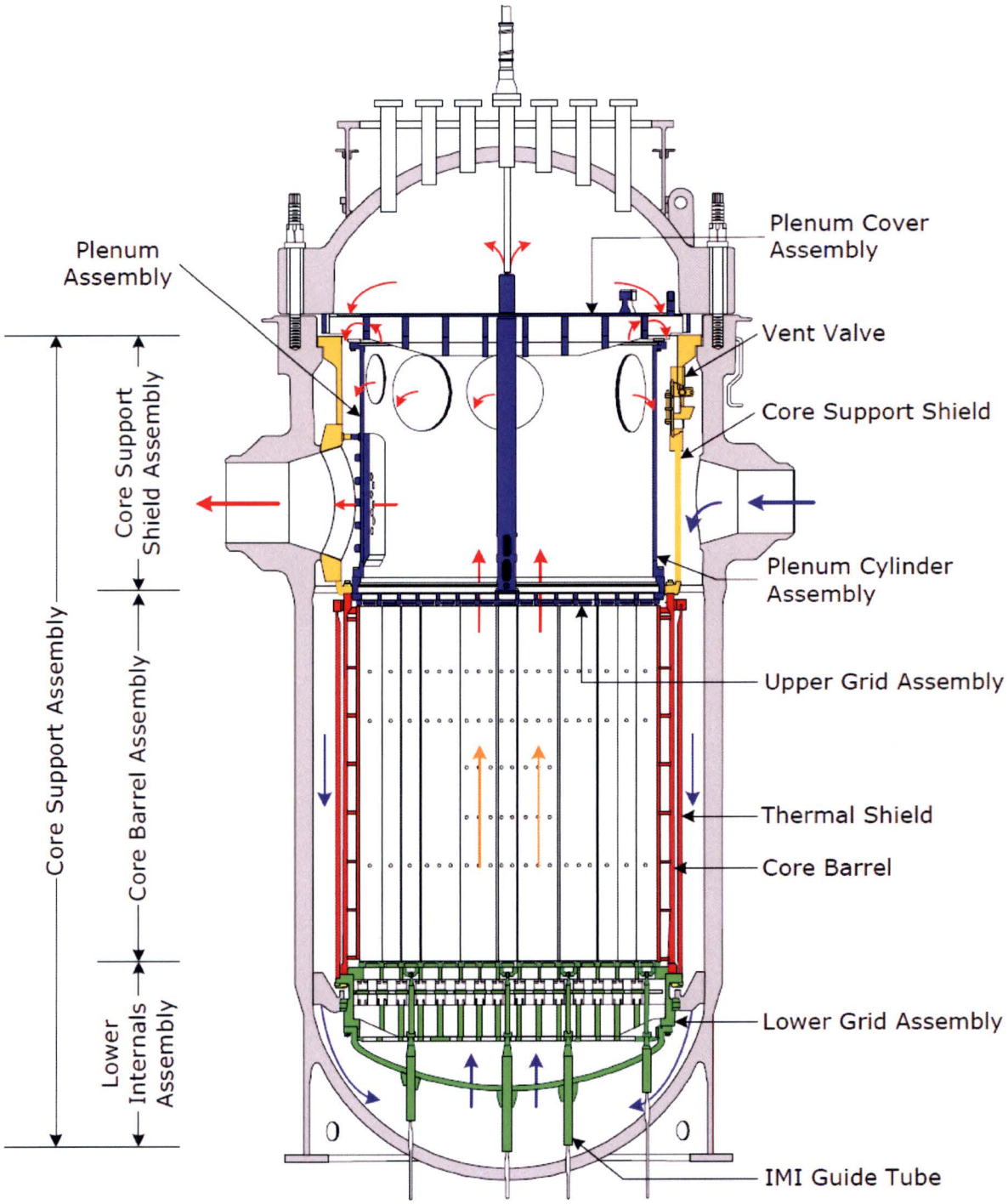

Figure RAI-4.23-2: B&W 177 FA Reactor Vessel and Internals Arrangement with Representative LTCC Levels

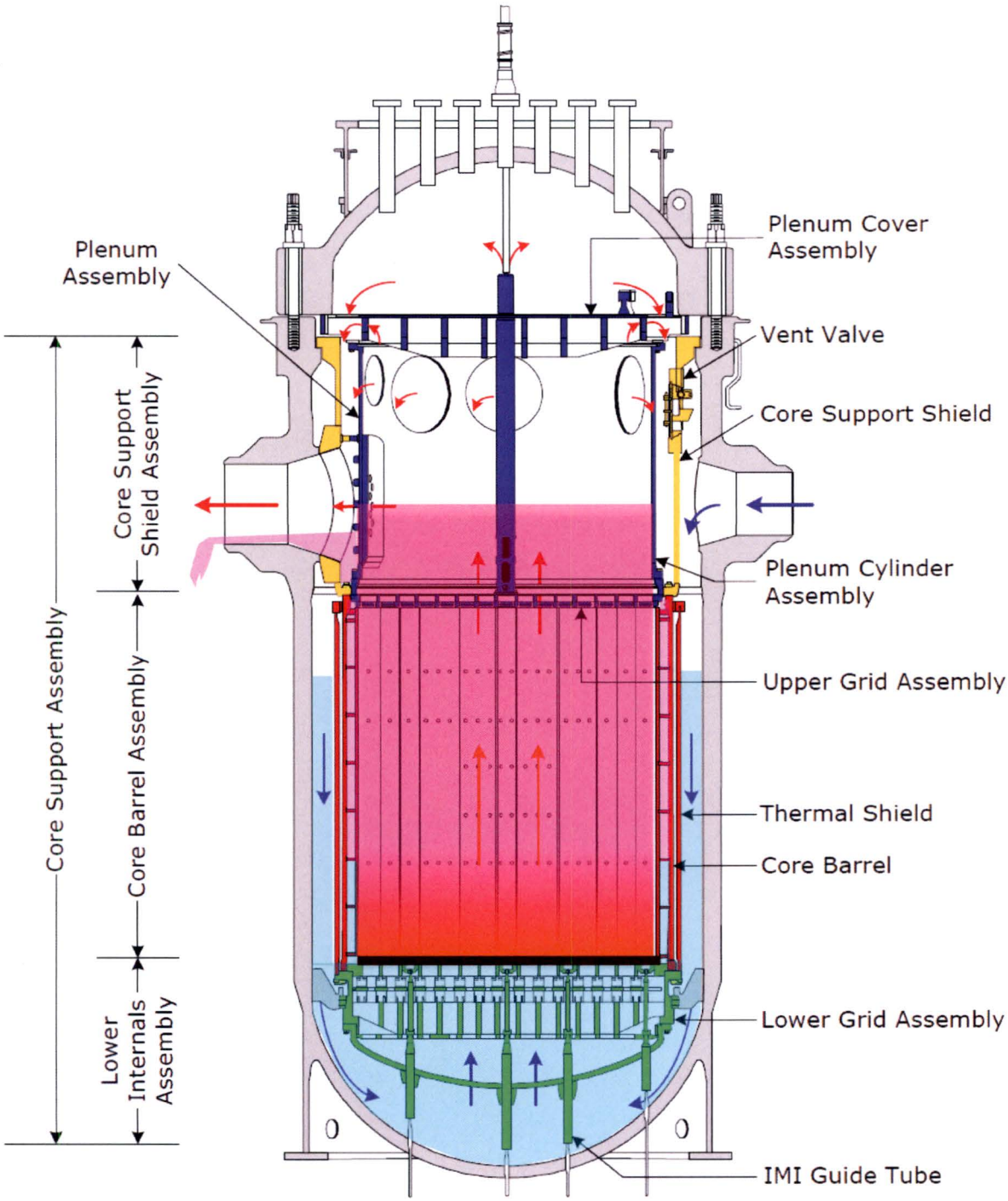

Note: Arrows depicting normal, steady-state pumps on operation were not removed from this figure

Figure RAI-4.23-3: B&W 177 FA Reactor Vessel Flow Patterns after Complete Core Inlet Blockage

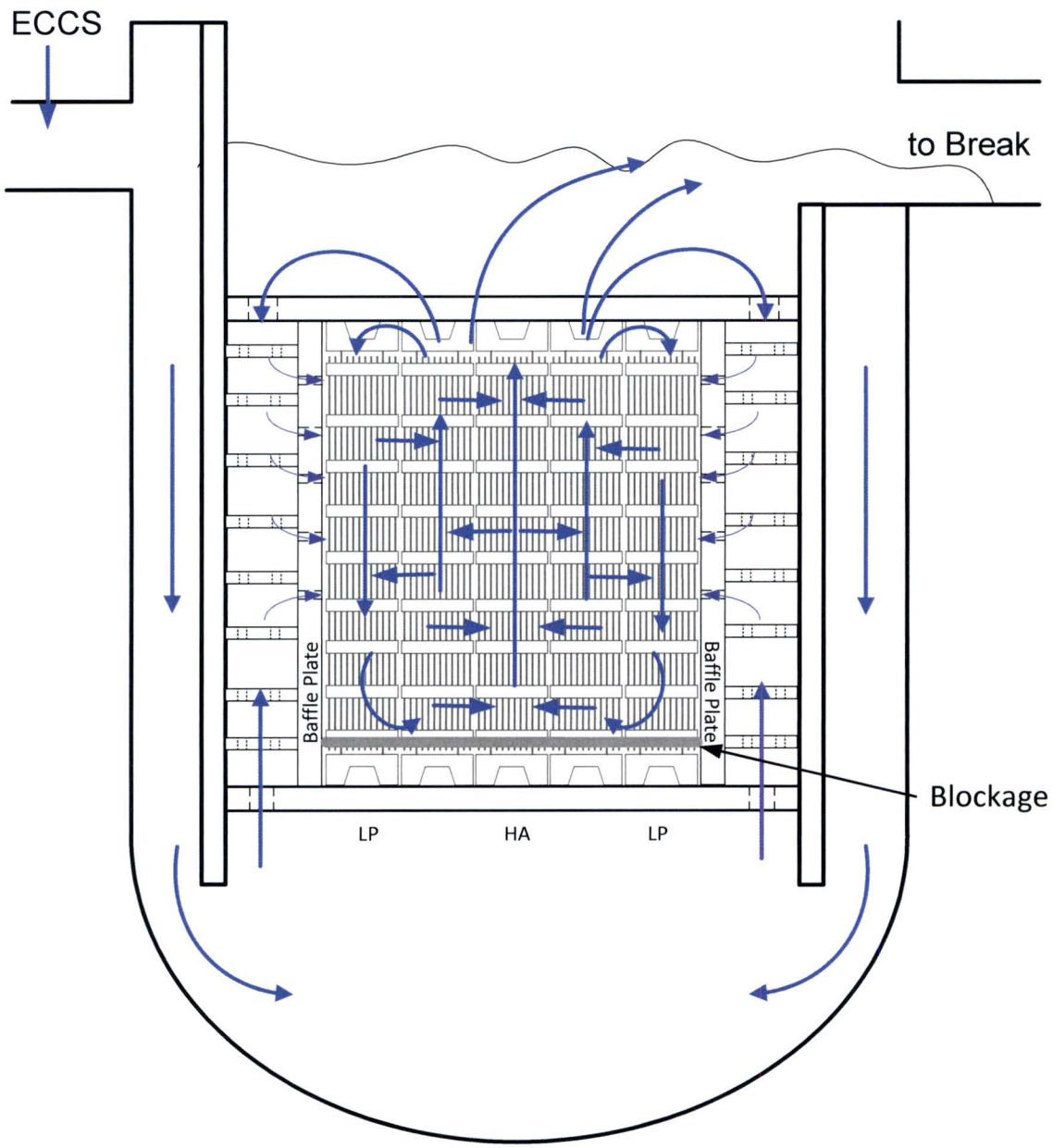

Figure RAI-4.23-4: B&W DC to Core Elevation Head Difference to Overcome AFP Resistance

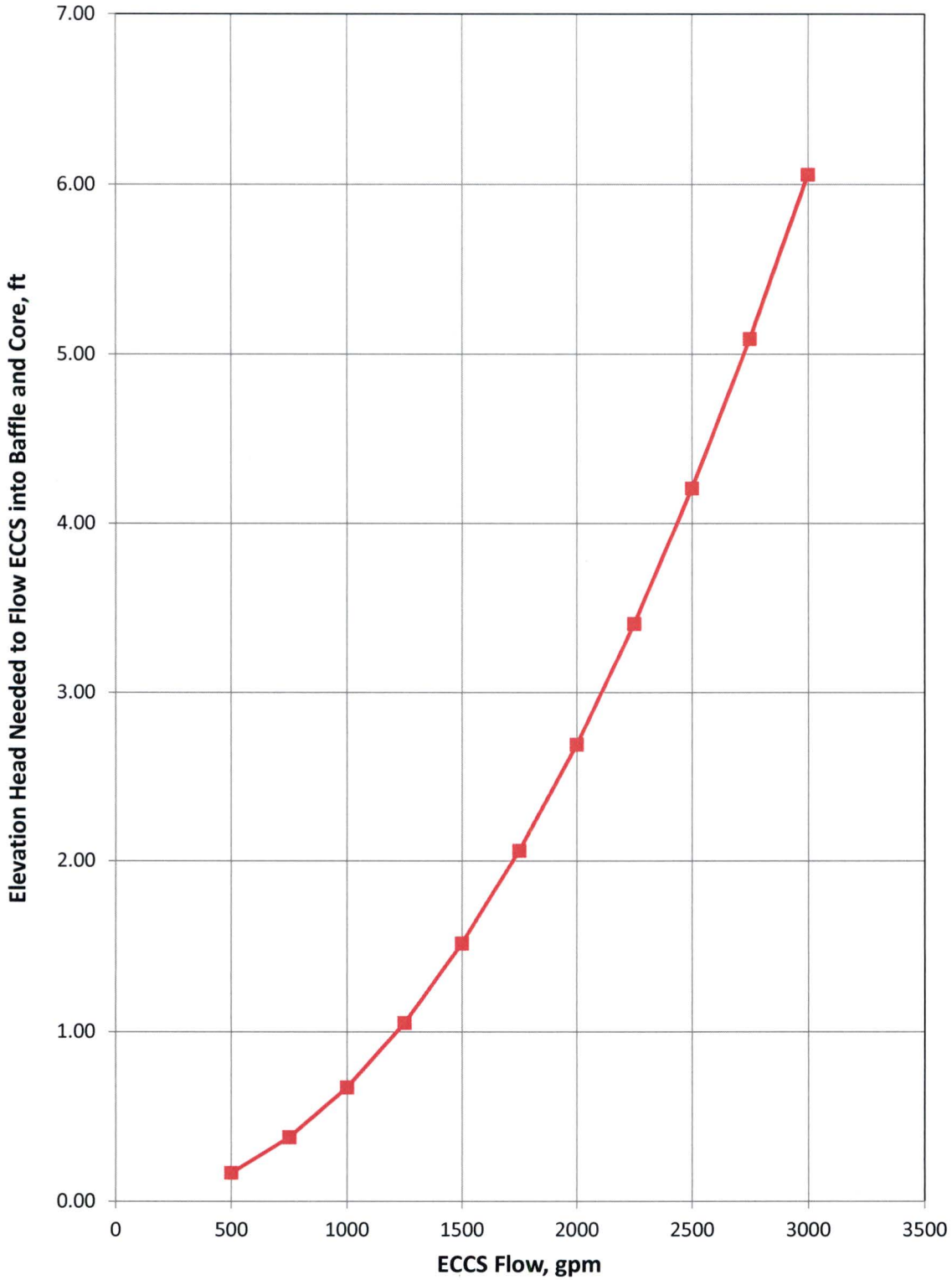

2.23.2.2 Part b

As described in the response to RAI 4.23a, entrainment is only applicable during the STCC phase of the event. Mixture level swell is the key factor that results in liquid discharge out of the break during the LTCC phase when the core inlet blockage is imposed.

A variety of code benchmarks have been performed to validate the core region void distributions during LTCC with and without core uncovering. With respect to prototypical low pressure with low DH during the LTCC phase, the most appropriate benchmarks are comparisons to tests in the Rod Bundle Heat Transfer (RBHT) facility. The emphasis for these benchmarks was to compare the calculated core void distribution to the measured values. Based on these comparisons in the core region (see Figure RAI-4.8-1), it is demonstrated that RELAP5/MOD2-B&W can predict the void distributions in the core. The similar models are used in the upper plenum and the void distributions are similar to those for the core exit. The excess ECCS fills the reactor vessel to the break elevation where liquid spills out continuously of the RV exit nozzle to HL break.

2.23.2.3 Part c

Core and upper plenum entrainment is only applicable during the reflood phase of STCC for a Large Break Loss of Coolant Accident (LBLOCA) transient when the combination of high decay heat and stored energy heat removal generate sufficient steam velocities to entrain liquid droplets. During the reflood phase, the core exit steam velocities are high and the unquenched core and upper plenum control volumes are in a mist flow regime. After the core quenches, the fuel pins rewet as do the upper plenum structures. Following rewet, the liquid fraction increases and flow regime transitions to an annular mist flow regime with higher liquid content volumes transitioning to the slug flow regime. Once the transition into the annular mist or slug flow regime occurs, upper plenum entrainment subsides. After this time, the mixture level swell is the key factor that controls the core and upper plenum void fractions which results in liquid reaching the hot leg elevation where it is discharge out of the break during the LTCC phase This is true prior to and after the core inlet blockage is imposed.

RBHT code benchmarks of the LTCC phase core void distributions from prototypical tests performed at high decay heat levels and low pressure conditions confirms the validity of the code void distribution and level swell predictions (see RAI 4.8). With the pedigree of the code established, it can be used for plant applications for hypothetical accidents that evolve to the conditions that could result in debris flow blockage of the core inlet.

The NRC-approved Small Break Loss of Coolant Accident (SBLOCA) option of

RELAP5/MOD2-B&W code includes a specialized version of the Wilson interphase drag model [ ] in the UP. This option allows for the void distribution in the upper plenum to be lower than that of the core exit. This model allows the void distributions to be discontinuous at the interface between the core and its small bundle hydraulic diameter and the upper plenum and its larger hydraulic diameter. The model is used in SBLOCA benchmarks and in plant applications using the SBLOCA methods. At higher pressures and lower decay heat levels, the void fraction in the upper plenum is typically lower than that of the core exit. However, at the low pressures and high decay heat levels for the DEG HLB, there is little difference between the core and upper plenum void fractions.

The break flow uses the Moody model to calculate the two phase choked flow discharge with discharge coefficients of 1.0 on both sides of the break. The choked phase slip is different with the LBLOCA and SBLOCA models, but both sides of the break unchoke and do not choke again after several minutes into the event, well before the sump switchover occurs. The unchoked break flow is calculated by the RELAP5/MOD2-B&W momentum equation using phase slip and the full pipe area with a constant containment pressure of 14.7 psia.

2.23.2.4 Part d

The RCS to containment pressure differential decreases rapidly for a DEG HLB such that the RV side break flow unchokes during the STCC phase, which is well before sump recirculation. RAI 4.29 states that there is no choking after 57 seconds on the RV side so the break flow is calculated by the RELAP5/MOD2-B&W momentum equation using phase slip and the full pipe area with a constant containment pressure of 14.7 psia. There are no limitations on the range of applicability for the momentum equation calculation of break flow.

2.23.2.5 Part e

The mass flow rates of liquid, steam, and total fluid discharges through each opening of the DEG break are provided in Figure RAI-4.17-1. The integrals of the identified break mass flow rates are Figure RAI-4.17-6.

The average channel mixture level is shown in Figure RAI-4.23-5.

The steam flow quality calculated as a ratio of the steam mass flow rate to the total mass flow rate for the RV-side opening of the DEG break is provided in Figure RAI-4.17-5.

The upper plenum to containment difference is shown in Figure RAI-4.23-6.

Figure RAI-4.23-5: DEG HL Break Core Mixture Level versus Time

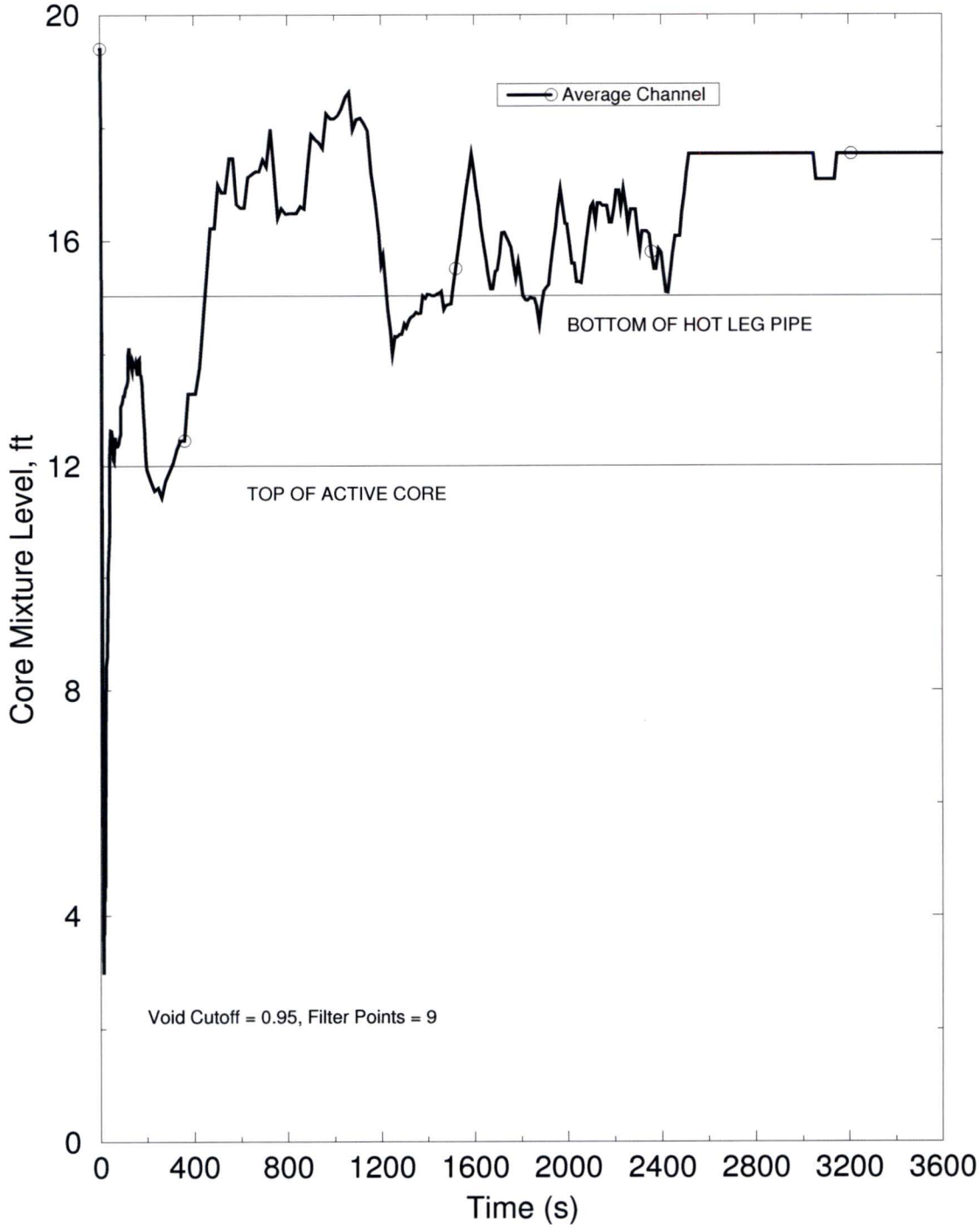

Figure RAI-4.23-6: DEG HL Break Upper Plenum to Containment Pressure Difference versus Time

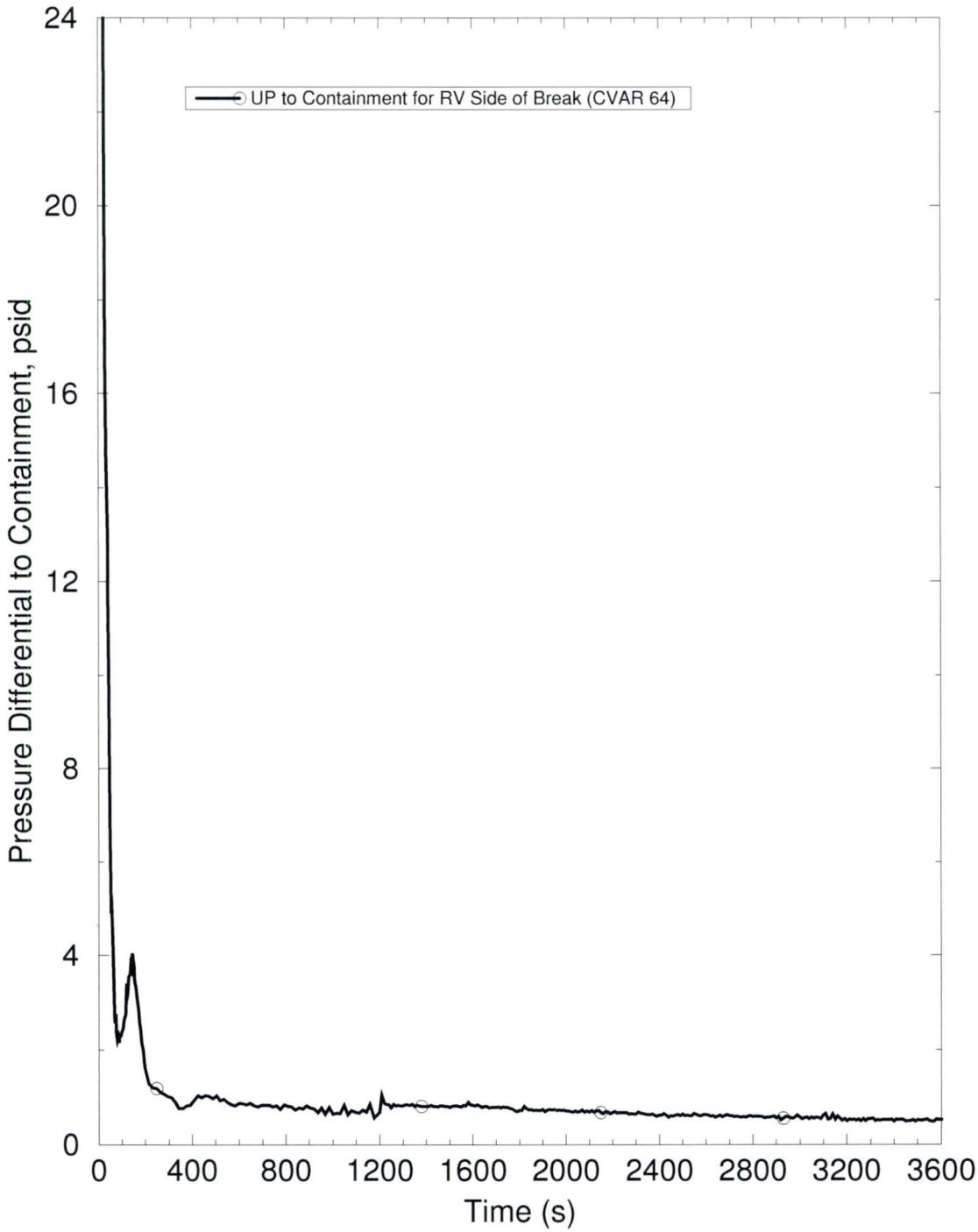

2.23.2.6 Part f

This RAI pertains to the CE plant categories and therefore requires no response for the B&W plant category.

2.23.2.7 Part g

This RAI pertains to the CE plant categories and therefore requires no response for the B&W plant category.

2.23.2.8 Part h

This RAI pertains to the CE plant categories and therefore requires no response for the B&W plant category.

2.23.2.9 Part i

As was documented in various parts of this RAI, core and upper plenum entrainment is only applicable during the reflooding phase of STCC, therefore the parameters or ECCS temperatures do not influence entrainment during LTCC. The core and UP entrainment predictions during this early time period are early in the event and will not impact the LTCC phase related to GSI-191.

As described in part c of this RAI, the mixture level is up to or above the bottom of the hot leg elevation. When the level is at this height, liquid can either run out or droplets or waves from the surface next to the hot leg can be entrained and swept out of the hot leg as the steam velocities accelerate to flow out of the break. Velocities of 100 to 200 ft/s are predicted in the HL prior to SSO and these velocities are adequate to entrain some liquid in this pipe. If entrainment did not occur, then the mixture level would rise and the liquid pool would flow out of the pipe. If entrainment was too high, the mixture level would decrease and the liquid flow out of the pipe would momentarily cease. However, the excess ECCS flow entering the core will raise the mixture level until liquid exits the break. The figures provided in part e of this RAI show this oscillatory but effectively a continuous liquid carryout behavior.

2.24 RAI 4.24

2.24.1 Statement of RAI 4.24

Figures 8-9 and 9-8 indicate that the total ECCS injected masses for the Westinghouse upflow and downflow design categories increase significantly at SSO even though the injection rates appear to be constant both prior to and after the observed stepwise change at SSO.

(a) Provide plots of the ECCS injection rates as a function of time for Case 0A for both Westinghouse upflow and downflow plant categories.

(b) Explain the way in which the simulated ECCS pump injection rates prior to and following SSO were determined and identify the factors and assumptions that were considered when determining the flows. Include any temporary safety injection (SI) impediment, single failure assumptions, and pump performance characteristics among the considered factors and assumptions. In the above identified cases, the ECCS recirculation flow rate is much different from the ECCS injection rate prior to SSO.

(c) Clarify if varying the ECCS injection mass flow rate upon SSO had an effect on the analysis results for both plant categories.

(d) Table 7-1 in the revised Section 7.1.1 of Vol. 1 describes the following ECCS performance for a Westinghouse three-loop plant following a large cold leg break. From 0 to 15 min: 1 residual heat removal and 2 high head SI (HHSI) pumps are described as typical injection phase modeling with single active failure; from 15 to 45 min: 2 HHSI pumps, typical SI phase modeling for this plant; from 45 to 47 min: no flow, interruption at cold leg recirculation; from 47 min to termination: 2 HHSI pumps. This represents an ECCS performance pattern, which appears opposite to the one described above (increase vs decrease in ECCS flow rate upon SSO). Clarify if varying the ECCS injection mass flow rate upon SSO following this opposite pattern would have an effect on the analysis results for both plant categories.

(e) Considering the results from Vol. 4, explain the applicable conditions and related requirements for adequately determining the values of ECCS flow. Consider injection and recirculation rates, including interruptions during switchover, on a plant-specific basis to ensure that ECCS performance is adequately represented.

(f) Provide the information requested in Items a through e for the CE and B&W plant categories. It is noted that Table 6-3 lists the "low pressure safety injection (LPSI)

flow rate" as a key input for the CE plant category and Table 6-4 identifies "low pressure injection (LPI) flow rate" as a key input for the B&W plant category thus linking this key input to the performance of specific ECCS components.

(g) Explain the reason for including Note 2 to Table 6-4 relevant to the B&W plant category stating that "the LPI flow rate followed a pump curve in the analysis. The value shown is the flow at run-out conditions". Provide the pump curve and the flow rates used in the analysis. Justify that these parameters are applicable to all plants in this category.

(h) Provide graphs of SI flow rates as a function of time for each individual reactor coolant primary loop for the entire duration of the analysis for the cases included in the case matrices in Tables 8-1, 8-2, 9-1, 9-2, 10-1, 10-2, 11-1, and 11-2. Show the contributions from both high and low pressure SI for the cold and hot legs. Describe all applicable assumptions related to the way in which these flow rates were established and simulated in the T-H analyses.

2.24.2 Response to RAI 4.24

2.24.2.1 Part a

Plots of Emergency Core Cooling System (ECCS) flow rates are included in the response to Request for Additional Information (RAI) 4.17b, 4.22 and part h of this RAI.

2.24.2.2 Part b

The basis for the ECCS injection before and after Sump Switch Over (SSO) is described in the response to RAI 4.5a.

2.24.2.3 Part c

As described in the response to RAI 4.5a, the ECCS flow rate before and after SSO is slightly different. Before SSO, automatic actuation of ECCS systems defines the amount of ECCS injection available. After SSO, the operators have the flexibility to throttle ECCS flow depending on the Reactor Coolant System (RCS) conditions with a minimum target of 2000 gpm to the RCS. The analyses presented modeled a 1500 gpm ECCS flow rate in an attempt to provide the biggest challenge to core cooling. However, these analyses demonstrated that the core remained covered for the Babcock & Wilcox (B&W) plants, mainly because upon core inlet blockage, flow into the core re-establishes via the low

resistance baffle region. Higher ECCS flow rates would change the observed core and downcomer levels but would provide similar results (i.e., core remains covered). Therefore, variations in the ECCS flow rate between before and after SSO will have no effect on the analysis conclusions that core uncovering will not occur even with a total instantaneous core inlet blockage.

2.24.2.4 Part d

This RAI pertains to the Westinghouse Electric Company (WEC) plant categories and therefore requires no response for the B&W plant category.

2.24.2.5 Part e

The basis for the ECCS injection before and after SSO is described in the response to RAI 4.5a.

2.24.2.6 Part f

The requested information for the B&W plant analyses are described in the pertinent sections of this RAI.

2.24.2.7 Part g

While the value provided was the flow rate at pump run-out conditions, the intent of Note 2 to Table 6-4 was to indicate that a variable flow rate based on the pump performance was used in lieu of a constant flow rate. The Low Pressure Injection (LPI) mass flow rates for each plant before SSO are provided in Figure RAI-4.5-1. After SSO, a constant LPI flow rate of 1500 gpm (200 lbm/s at 200 °F and 14.7 psia) was modeled. The small break Loss of Coolant Accident (LOCA) transient employs the Oconee Nuclear Station (ONS) LPI pump performance for the analysis, which bounds all of the B&W plants.

2.24.2.8 Part h

The requested information for the B&W t_{block}/K_{max} evaluation is provided in the following figures. These results are from the updated analyses described in RAI 4.22. The ECCS mass flow rates for each RCS loop are provided in Figure RAI-4.24-1. This figure also

includes the ECCS mass flow rate for direct injection to the reactor vessel. The assumptions used to develop these flow rates are described in the response to RAI 4.5a.

Figure RAI-4.24-1: ECCS Mass Flow Rates per RCS Loop for Small Break LOCA

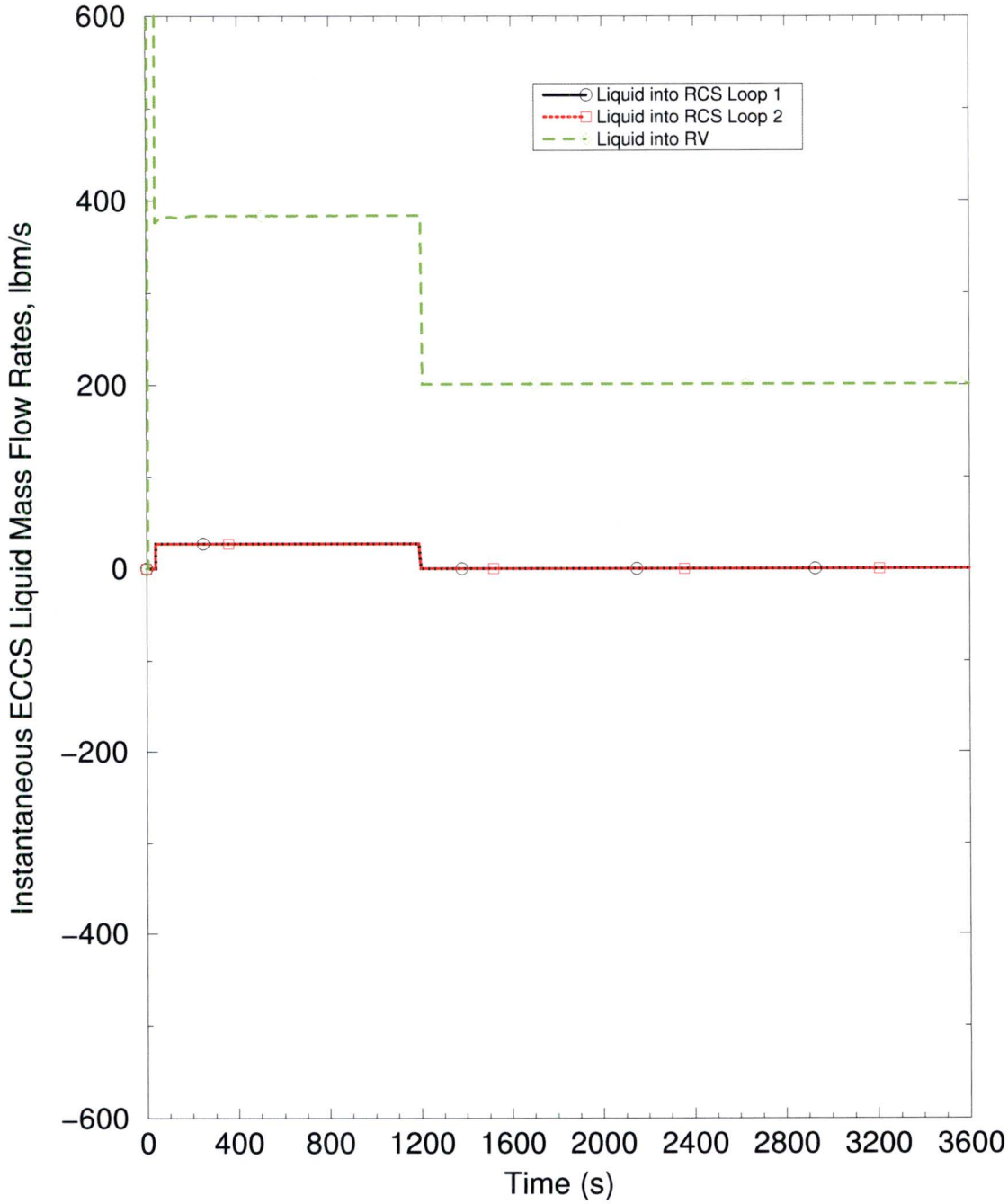

2.25 RAI 4.25

2.25.1 Statement of RAI 4.25

In determining the t_{block} and K_{max} inputs for the Westinghouse upflow category, Section 8.1 provides a simulation matrix of cases considering only two ECCS recirculation flow rates of 18 and 40 gpm/FA. Section 8.2 states that LTCC can be maintained if the time of complete core inlet blockage, t_{block}, occurs 143 minutes, or later, after the initiation of the LOCA event. This time is taken from Case 1B simulating the minimum ECCS recirculation flow rate of 18 gpm/FA and is stated to bound "the range of recirculation flows investigated". The K_{max} input is determined from Case 2B with the same simulated ECCS recirculation flow rate of 18 gpm/FA.

(a) Provide justification that the t_{block} criterion from Case 1B at 18 gpm/FA is valid for the range of flow rates from 8-40 gpm/FA as documented in Table 6-1 for this parameter.

(b) Provide justification that the K_{max} criterion from Case 2B with a simulated ECCS recirculation flow rate of 18 gpm/FA is valid for the range of flow rates from 8-40 gpm/FA as documented in Table 6-1 for this parameter.

(c) Provide justification for using only 18 and 40 gpm/FA flow rates for determining the t_{block} and K_{max} inputs as stated in Note 1 to Table 6-1 and documented in the simulation matrix of cases provided in Section 8.1.

(d) Define the range of ECCS recirculation flow rates for which the t_{block}, K_{max}, K_{split}, and m_{split} results, as obtained in Section 8, are considered applicable to the Westinghouse upflow plant category and provide a justification for this range.

(e) Provide similar responses to Items a through d for the other three plant categories to justify that the t_{block} and K_{max} inputs calculated using a single ECCS recirculation flow rate for each input are applicable to the range of flow rates defined for each plant category. For example, justify for the Westinghouse downflow category that t_{block} is determined from Case 1A simulating an ECCS recirculation flow rate of 40 gpm/FA and K_{max} is determined from Case 2B with a simulated ECCS recirculation flow rate of 18 gpm/FA.

(f) Sections 8-3 and 9-3 state that "the duration and magnitude of the heatup were heavily dependent on the timing of complete core inlet blockage and the ECCS flow rate". Considering the responses to items a through e above, demonstrate that the calculated parameters are valid for the ECCS flow rates and core inlet blockage times used in the analysis.

2.25.2 Response to RAI 4.25

2.25.2.1 Part a

This RAI pertains to the Westinghouse Electric Company (WEC) plant categories and therefore requires no response for the Babcock & Wilcox (B&W) plant category.

2.25.2.2 Part b

This RAI pertains to the WEC plant categories and therefore requires no response for the B&W plant category.

2.25.2.3 Part c

This RAI pertains to the WEC plant categories and therefore requires no response for the B&W plant category.

2.25.2.4 Part d

The basis for the Emergency Core Cooling System (ECCS) injection before and after Sump Switch Over (SSO) for the B&W plants is described in the response to RAI 4.5a. As described therein, the ECCS injection rate during the transient has a direct effect on the core mixture level and cladding temperature response. Higher flow rates will provide significant excess flow above core boiloff. Lower flow rates may be closer to the core boiloff rate such that when blockage is imposed, decay heat removal may be challenged while the flow through the core is reestablished via the barrel/baffle region instead of the core inlet. Studies presented in WCAP-17788-P, Volume 4 confirmed that lower flow rates are more conservative for the Thermal Hydraulic (TH) analyses. Therefore, a minimum flow rate for the B&W plants was targeted.

To that end, the B&W analyses to define t_{block} and K_{max} are valid for any ECCS flow rate that is higher than the flow rates analyzed and described in the response to RAI 4.5a. Note that this conclusion would also apply to calculations of K_{split} and m_{split}; however, the analyses to calculate these parameters are no longer needed as described in the response to RAI 4.20. Also note that the ECCS flow rate after SSO was increased in a study described in response to RAI 4.16a. The results of this study confirm that higher ECCS flow rates after SSO increase the core liquid level.

2.25.2.5 Part e

The requested information for the B&W plant analyses are described in the pertinent sections of this RAI.

2.25.2.6 Part f

The above responses demonstrate that the calculated parameters are valid for the ECCS flow rates and core inlet blockage times used in the analysis.

2.26 RAI 4.26

2.26.1 Statement of RAI 4.26

K_{max} for the CE plant category was determined by applying a gradual ramp in the simulated core inlet resistance starting from 0 at 1,800 seconds and reaching K_{max} of $6.5x10^6$ at 4,200 seconds as shown in Figure 10-2. The profile represents an increase in the resistance value by applying four different constant rates of resistance increase, which change in a stepwise manner with time.

(a) Justify that the K_{max} value of $6.5x10^6$, using the profile from Figure 10-2, represents a robust result and is not an outcome of tuning of the core inlet resistance profile to obtain a desired result. Results from sensitivity analyses can be used to provide the justification.

(b) In the case of the profile shown in Figure 10-2, the core inlet resistance was increased from 0 to $6.5x10^6$ within a time window of 2,400 seconds (40 min). As the result of $6.5x10^6$ for K_{max} was tied to the specific profile from Figure 10-2, justify the K_{max} input for the CE plant category by explaining how it can be assured that the K_{max} value will not be developed within a time window shorter than 40 minutes resulting in K_{max} occurring earlier than 70 minutes into the LOCA transient, which could lead to the PCT acceptance criteria being violated.

2.26.2 Response to RAI 4.26

This RAI pertains to the Combustion Engineering (CE) plant categories and therefore requires no response for the B&W plant category.

2.27 RAI 4.27

2.27.1 Statement of RAI 4.27

T-H code predictions to demonstrate adequate core coolability under conditions associated with blocked core inlet flow passages require reasonable assurance of adequate code performance under the simulated conditions. The examination of code results during the NRC audit of the Westinghouse T-H analyses in Sections 8 and 9 on January 27-28, 2016, indicates that flow patterns involving parallel cross-connected channels to model the core following a simulated complete core inlet blockage can be complex. It was determined that obstruction of lateral flow passages between fuel assemblies due to the presence of spacer grids was not accounted for in the modeling of the lateral cross-connections between parallel core channels, including the hot channel. In addition, potential effects on the axial flows due to possible localized accumulation of debris at the locations of spacer grids in regions above the core inlet were not modeled to assess such effects.

Cross-flows between parallel channels can be a contributing factor affecting code prediction of local fuel conditions, including PCT, due to their impact on fluid velocities, void fraction, and two phase flow patterns. Provide results from additional T-H analyses for a representative case analyzed in each plant category to assess the effects from the above identified factors related to lateral obstruction of cross-flow passages and impediment of axial flows on the PCT and t_{block} predictions. The analyses should be performed using core modeling changes that account for: (1) reduced flow area of cross-flow passages due to the spacer grids present in the active core region, (2) impact on resistances of cross-flow passages from the spacer grids present in the active core region, and (3) increase in the simulated spacer grid resistances in the axial direction at appropriately selected spacer grid locations, including impact for both axial directions, to simulate the effect from possible local fiber accumulation. Such modeling changes and modifications should be applied to the hot channel and all or some of the channels representing the entire core as found appropriate. If necessary to resolve the impact from the examined factors and processes on the PCT and t_{block} predictions, include sensitivity results related to specific factors and modeling assumptions as applicable. For each simulation, include sufficiently detailed results to explain effects on the predicted core T-H response, PCT, and t_{block} in comparison to the corresponding base cases. Include PCT, void fraction, fluid phase velocities, and two-phase flow patterns for appropriately selected hydraulic channels and cells, as well as integrated mass flows in both lateral and axial directions for selected critical flow passages. Include a description of the implemented modeling changes with a sufficient degree of detail to explain clearly how the physical processes and factors were accounted for in the model along with the introduced assumptions.

2.27.2 Response to RAI 4.27

In the B&W analysis, the core is modeled with two channels. The hot channel includes [ ]. The average channel contains the remaining fuel assemblies at the average core peaking. The channels are connected with crossflow junctions that allow flow between the average and hot channels as conditions permit. Flow from the baffle region to the average channel occurs through the Loss of Coolant Accident (LOCA) holes at the appropriate elevations (see response to RAI 4.4 for location and description of the LOCA holes). As described in the response to RAI 4.4, flow from the slots at the corners of the baffle plates near the middle of the core are separated and modeled at the locations of the rows of LOCA holes. The crossflow resistance modeled in the B&W plant analyses does not explicitly consider the reduction in flow area related to the presence of spacer grids.

The RCS state during the post-LOCA Long Term Core Cooling (LTCC) phase of the postulated accident is discussed in WCAP-17788, Volume 4, Section 7. Specifically, the Reactor Coolant System (RCS) conditions prior to and after the arrival of debris are discussed. The RCS state prior to the arrival of debris describes the conditions of the system at the point of switchover to sump recirculation, while the RCS state after debris arrival describes the system response after the application of core inlet blockage. The focus of the section is primarily on the Reactor Vessel (RV) and the core flow patterns that are present during the post-LOCA transient. The flow patterns before complete blockage are illustrated in Volume 4, Figure 7-1. The flow patterns after complete blockage are illustrated in Volume 4, Figure 7-3. The presence of the LOCA holes in the B&W plant design alter the flow patterns depicted in Volume 4, Figure 7-3 slightly in that flow from the baffle region enters the core periphery from near the midplane of the core instead of from the top of the peripheral core as shown in the illustration.

Downflow occurs in the lower power core periphery channels below the first row of LOCA holes. The downflow exceeds the boiloff occurring below the LOCA hole elevation in the entire lower average channel and also in the lower hot assemblies. The boiling process produces upflow in the hotter channels. This is true both before and after complete core inlet blockage occurs. Increased crossflow resistance due to the presence of spacer grids has the potential to affect the magnitude of the flow between assemblies near the spacer grids, but the overall flow pattern would not be altered, because the increase in effective resistance through the flow area reduction is not significant enough. The spacer grids are less than approximately three inches high. Over a span between grids of approximately 1.75 feet, the area reduction due to the spacer grids would be approximately 15 percent. Further, as described in this RAI, the presence of spacer grids is suitably represented in the B&W plant model.

The Small Break Loss of Coolant Accident (SBLOCA) crossflow between the average and hot channels is modeled using the rationale given in Section A.4 of Volume 2 of the

BWNT LOCA EM (Reference 4.27-1). The premise for this modeling approach is to produce representative two phase boiling pot thermal-hydraulic conditions in fuel bundles of varying power levels while achieving conservative Peak Cladding Temperatures (PCTs) during the core uncovering phase with a partially full boiling pot during a SBLOCA. The PCT conservatism is supported by use of a nominal to low crossflow resistance in the steam region to allow diversion of steam out of the hot channel. The resistance in the pool region is [

] to allow the power differences to create variations in the void distribution in the channels. [

] The crossflow form loss coefficient is [

] in the region that could be uncovered during the transient. The form losses from the hot-to-average channel flow direction [

]. This modeling approach was shown to give stable pool void distributions. In the uncovered core regions this crossflow scheme [

] ensure a conservative clad heatup should the core become uncovered.

In the SBLOCA model, the above logic is implemented via a special void-dependent form loss option of the full crossflow model. This option is described in detail in BAW-10164, Rev 6, Section 2.1.4.3 (Reference 4.27-2). It allows alteration of the user input, constant form loss coefficient based on the void fraction in the upstream volume and allows the regions of the core covered by a two-phase mixture or pool to have a resistance that is different from that in the uncovered or steam region as described in the preceding discussion. The crossflow resistance changes can alter the volume-average axial velocities that are used to determine the core surface heat transfer. In the B&W plant model described in the response to RAI 4.22, the crossflow resistance is specified as [

] in the heated region that connect the Average Channel (AC) to the Hot Channel (HC). The model uses the input form loss coefficients [

]

[

]

To better understand what this actually looks like, the results from the case described in RAI 4.22 from 1290 seconds (90 seconds after complete core inlet blockage) are shown in Table RAI-4.27-1. While the crossflow form-loss coefficient is input as the same value for all of the 20 junctions in the heated region of the core, [

] For GSI-191 applications, the high resistance in the pool region ([ ]) will restrict the flow from the average channel to the hot channel. While the spacer grids are not explicitly accounted for, the [ ] is more than adequate to account for their effect. In the steam region, neglecting the spacer grids in the crossflow resistance allows for more steam diversion from the hot channel to the average channel. Therefore, the crossflow model for the B&W plants is already sufficiently conservative and additional studies that vary the crossflow resistance to account for the spacer grids are unnecessary.

The effect of this crossflow resistance model on the core flow patterns can be seen by examining the core crossflows. Table RAI-4.27-1 provides a snapshot of the crossflow at 1290 seconds (90 seconds after complete core inlet blockage). In the lower portion of the core, the flow is from the average channel to the hot channel. Near the top of the core, the flow is out of the hot channel. These results confirm that the flow from the baffle region is directed downward in the average channel to the lower portions of the core and then into the hot channel to feed the boiling (as described in Volume 4, Section 7). Figure RAI-4.27-1 shows the crossflow below the first row of LOCA holes as a function of time, confirming that this flow pattern is stable after the core inlet blockage is applied.

The B&W plant design also features a relatively low resistance of the baffle region (see response to RAI 4.4). The conservatively low ECCS flow rate is still significantly higher than that required to remove core decay heat (see response to RAI 4.5a and 4.22). As shown in the analysis results in the response to RAI 4.22, this combination leads to a continuously covered core and continuous liquid flow out of the hot leg break. Unless the

Emergency Core Cooling System (ECCS) flow is unrealistically reduced even further to be close to or below the boiloff rate, the mixture level will persist at this location, and small variations in the core crossflow resistance to account for the spacer grid flow area obstruction will not alter this outcome.

Debris accumulation in the heated core region is described in Volume 1, Section 6.4.3.1. As described therein, the boiling process, in and of itself, precludes significant debris accumulation. While the general flow patterns in the core are well established by the TH analyses, the local flow patterns are quite complex due to the nature of the boiling process and uniqueness of the cycle specific bundle power distributions. Boiling at any given location in the core produces undulations in the void distributions that vary around a mean void faction. The instabilities of the boiling process introduce energy to the fluid that varies with time and location. In the event that debris begins to accumulate at the leading edge of a spacer grid, the perturbations of the local conditions will disturb the debris before a large accumulation can occur, therefore no contiguous bed can be established, and no significant interruption of the long-term core flow patterns will occur. Therefore, debris beds like those seen at the core inlet will not establish in the presence of boiling. These assertions are supported by the testing presented in Volume 1, Section 6.4.3.1.

As the transient progresses, the core decay heat will decrease, which decreases boiling in the core. In particular, boiling may decrease in lower power regions of the core (i.e., the core periphery) while the higher power assemblies continue to boil more vigorously. In any predominately liquid regions of the core, it may be possible to accumulate debris on the leading edge of a spacer grid. However, any debris bed that forms in the liquid region of the core will not extend across the entire core, because boiling continues in the higher power assemblies. The open lattice of the fuel design allows flow redistribution locally around any region than may develop additional blockages. Should the flow become stagnant near such a blockage, the fluid will heat up and eventually boil. The boiling will either dislodge a debris bed (if it formed on the top side or bottom of the spacer grid), or the decreased density of the boiling region will draw fluid in to replace the vaporized liquid. In all cases, the open lattice design of the fuel will ensure that the core is cooled and that localized regions with increased boron concentrations will not develop even for complete inlet core blockages and other limited size local blockages that may develop in small portions of the core.

While boiling precludes buildup at the leading edge of a spacer grid, the energy from the boiling process may force debris into internal grid locations such as the spring channels or dimples (see Volume 1, Figure 6-15). The limited size of these geometric features limits the expanse of the debris collection such that the effects would be localized and have little to no effect on the pressure drop across the spacer grid where they might occur. For the B&W plant response, all ECCS flow injected enters the middle of the core through the Alternate Flow Path (AFP) at a rate that is well in excess of the core boiloff

rate due to the low baffle resistance. As a result the core remains continuously covered with a two phase mixture level and cooled to within a few degrees of saturation. Even small increases in pressure drop at the spacer grids due to transient or localized buildup of material in the core periphery will not change the bulk internal circulation patterns that prevail within the core due to the assembly power differences, and thus would not impact the overall transient response.

Table RAI-4.27-1: Core Crossflow Resistance and Mass Flow Rates for B&W Plant Analysis at 1290 s

Figure RAI-4.27-1: Core Crossflow below the LOCA Holes

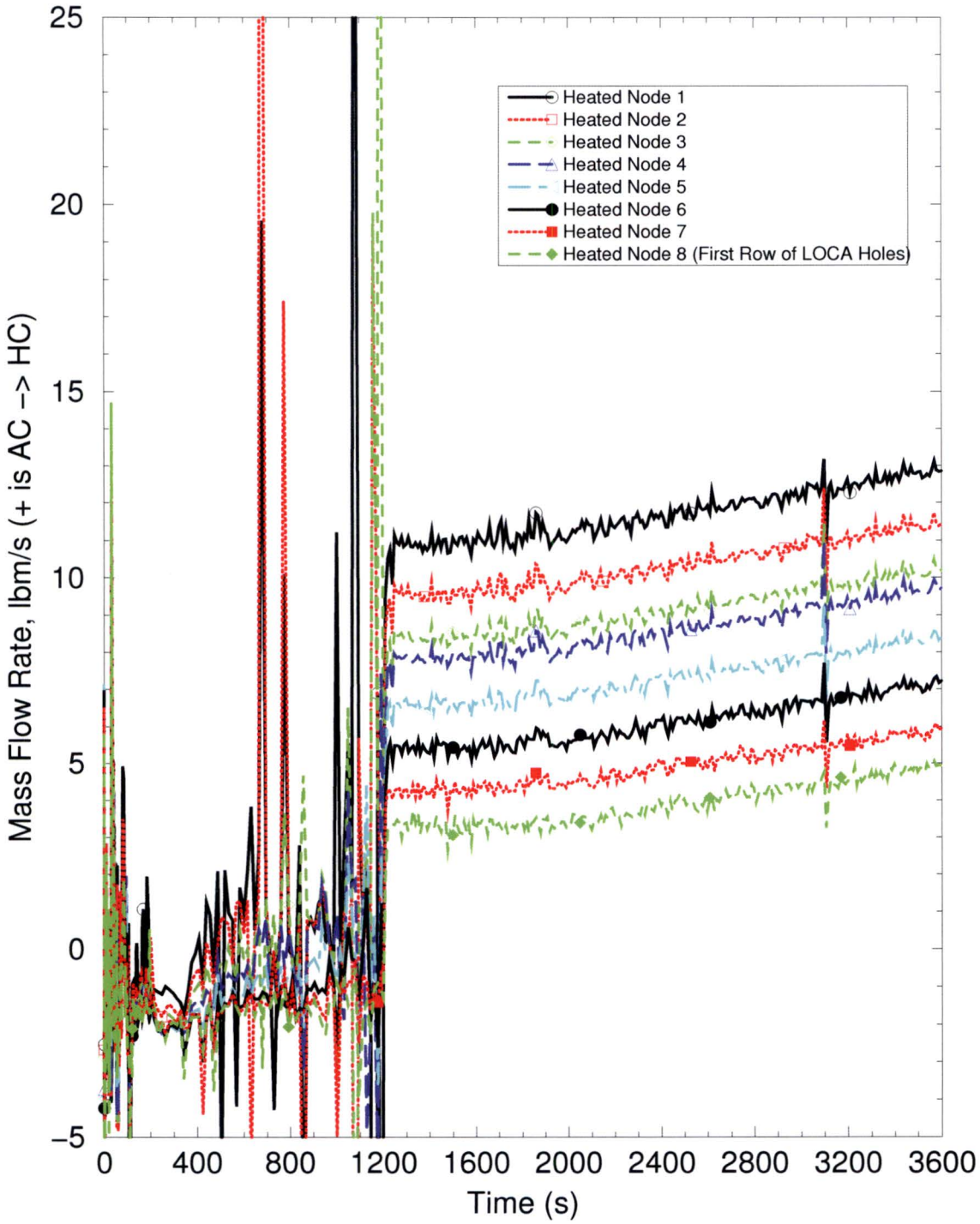

References - RAI 4.27

4.27-1 AREVA Document BAW-10192PA, Revision 0, *BWNT LOCA - BWNT Loss-of-Coolant Accident Evaluation Model for Once-Through Steam Generator Plants.*

4.27-2 AREVA Document BAW-10164PA, Revision 6, *RELAP5/MOD2-B&W - An Advanced Computer Program for Light Water Reactor LOCA and NON-LOCA Transient Analysis.*

2.28 RAI 4.28

2.28.1 Statement of RAI 4.28

The Westinghouse upflow, downflow, and CE base plant models were developed for best estimate (BE) PCT and clad oxidation analysis. As discussed in Section 6.1, many of the inputs from the BE models are set to nominal values. Some changes were made to bias the model toward an Appendix K analysis. The use of Appendix K type inputs is intended to add conservatism to the model to account for uncertainties associated with the LTCC phase following a LOCA.

Section 5 notes that the EMs used to analyze debris are based on NRC-approved EMs. For example, Section 5.1 notes that WCOBRA/TRAC MOD7A is used within the Code Qualification Document and ASTRUM EMs. However, the approach of nominal modeling with these codes has not been previously reviewed and accepted by the NRC.

Provide a table of all physical models and plant parameters that were considered in the uncertainty analysis for each computer code's most recently approved EM, and indicate how the uncertainty analysis has been adjusted to use a somewhat nominal, yet somewhat conservative analytic method. For each adjustment relative to the previously approved application, provide detail or justification that explains how the modified approach introduces an acceptable amount of conservatism. This table should expand on the information provided in, for example, Table 6-1, and should compare the current modeling approach to that previously approved for BE analysis.

2.28.2 Response to RAI 4.28

This RAI pertains to the Westinghouse Electric Company (WEC) and Combustion Engineering (CE) plant categories and therefore requires no response for the B&W plant category.

2.29 RAI 4.29

2.29.1 Statement of RAI 4.29

State whether the base plant models were submitted to the NRC to document safety analysis. Describe how the changes made to the base models regarding core volumes, ECCS model, BB flow resistance, break pressure boundary conditions, break flow multipliers, core inlet blockage, and calculation inputs in Tables 6-1 through 6-4 maintain adequate conservatism.

2.29.2 Response to RAI 4.29

The base plant specific model used for the thermal-hydraulic analyses in WCAP-17788-P and associated Request for Additional Information (RAI) responses have not been submitted to the NRC for review. However, the noding arrangement and modeling approach are consistent with the Cold Leg Pump Discharge (CLDP) Loss of Coolant Accident (LOCA) modeling options described in Sections 4 and 9 of BAW-10192P-A, Volumes I and II (Reference 4.29-1). While the specific models used for existing plant Analysis of Records (AORs) were not submitted to the NRC, the supporting documents with the models have been discussed and made available during NRC audits. For the GSI-191 Hot Leg Break (HLB) analyses, modifications to the Short Term Core Cooling (STCC) models and methods were described in response to RAI 4.22. The changes to the models and methods were discussed and justified for this application in that RAI response.

A range of Emergency Core Cooling System (ECCS) flows were considered for the GSI-191 analyses. The maximum flow was considered for the timing for sump switchover to produce a bounding decay heat to be used for the complete core inlet blockage simulation. The minimum ECCS flow rates are described in the response to RAI 4.5a. The minimum flow was considered for achieving the minimum inventory in the Reactor Vessel (RV) at the time that the core blockage was imposed. The minimum ECCS flow, with the possibility for operator throttling of the Low Pressure Injection (LPI) pumps for Net Positive Suction Head (NPSH) considerations, was used after sump switchover to maximize the likelihood for core uncovering. This combination of the minimum and maximum ECCS flows is conservative for the GSI-191 applications. Further, as described in the response to RAI 4.5a, the minimum ECCS flow rates assumed in the analyses bound all B&W plants.

The barrel/baffle geometry and flow resistance is based on a nominal resistance and is essentially identical for all B&W-designed plants (see response to RAI 4.4). Use of nominal flow resistances for components in the Reactor Coolant System (RCS) or the

core is consistent with the approach used in developing the B&W plant Evaluation Model (EM) plant models. [

]

The containment pressure for STCC LOCA analyses uses a minimum value as this maximizes the steam binding effect that minimizes the core reflooding rate. Since the analyses are designed to cover the Long Term Core Cooling (LTCC) phase of the transient, use of all the containment heat removal systems can suppress the pressure during the later portion of LTCC. Therefore to bound the effects of the pressure suppression systems, a constant containment pressure of 14.7 psia was modeled for the entire event. The lower pressure early in the transient minimizes the mass inventory in the RV due to the increased flashing and boiling that effects the level swell. Starting with a lower inventory at the time of Sump Switch Over (SSO), core inlet blockage is more challenging as it limits the liquid inventory in the vessel that is used to ensure that the core remains covered and cooled. Therefore a low containment pressure bounds the results from a more realistic value expected during the duration of the B&W LOCA analyses.

The B&W analyses model the break as a Double-Ended Guillotine (DEG) with a discharge coefficient of 1.0 for the first part of STCC when the flow is choked. The analysis reported in RAI 4.22, showed that after 57 seconds the differential pressure across the DEG break is low enough that it is no longer choked. Once the break unchokes, the flow is calculated based on the momentum equation. The break junction is modeled with the full hot leg pipe area without any adjustments to the area.

A complete core inlet blockage is simulated at 20 minutes by applying a form loss coefficient of 1.0 E+8 to the core inlet. This form loss was applied to the average core, hot channel, and bypass inlet junctions. When this resistance is applied, the flow across the core inlet is less than 2 gpm. It is clear from the fuel assembly testing documented in WCAP-17788-P, Volume 6 and the chemical effects testing documented in Volume 5, that this type of blockage cannot occur immediately after SSO. Blocking the core at this point in time maximizes the decay heat removal requirements and provides the largest challenge to core decay heat removal.

Each of the operating B&W plants contains the same number of fuel assemblies (177) with effectively the same baffle configuration and resistance. The key input relative to core uncovering is a maximum plant core power level combined with the minimum ECCS flow. As described in the response to RAI 4.5a, these inputs are combined to ensure adequate conservatism is included in the model inputs used.

References - RAI 4.29

4.29-1 AREVA Document BAW-10192PA, Revision 0, *BWNT LOCA - BWNT Loss-of-Coolant Accident Evaluation Model for Once-Through Steam Generator Plants.*

2.30 RAI 4.30

2.30.1 Statement of RAI 4.30

Figure 8-19 shows two time periods after complete core blockage during which the downcomer level remains steady (around 19 and 22 ft) before leveling out for the remainder of the transient. This could be explained by an accumulation of injected liquid in parts of the RCS outside of the RV. In addition, possible transport of liquid into the reactor upper plenum via the SG U-tube bundles can take place after filling the cold leg side of the RCS.

The variable m_{split} is defined as the flow split between the core inlet and AFPs. Figures 8-5, 9-4, 10-5, and 11-4 depict the calculated inputs for m_{split}.

(a) Was passage of ECCS liquid into the upper plenum via the SGs predicted for any of the runs used to produce the results shown in Figures 8-5, 9-4, 10-5, and 11-4? For each case that predicted flow into the upper plenum via the SGs, plot (in units of lbm/s) the rate of liquid flow that enters into the core, the AFPs, the reactor upper plenum through each loop, and the total amount into the upper plenum via all loops as functions of time.

(b) Define how m_{split} is calculated in Case 1B considered in Figure 8-19 and illustrate the m_{split} calculation for this case by plotting the rate (in units of lbm/s) of liquid flow into the core and into the BB AFP, the ECCS recirculation flow, the flow into the upper plenum via the SGs, if predicted, and the calculated m_{split} ratio (in dimensionless units) as functions of time.

(c) Provide details of the calculation of m_{split} for any runs that resulted in liquid transport into the reactor upper plenum via the SGs.

2.30.2 Response to RAI 4.30

2.30.2.1 Part a

A new analysis for the B&W plant category was performed in response to RAI 4.22. The results from this case demonstrate that no liquid flow was predicted through either Steam Generator (SG). This result can be confirmed by examining Figures RAI-4.17-4 and RAI-4.17-9.

2.30.2.2 Part b

This RAI pertains to the Westinghouse Electric Company (WEC) plant category and therefore requires no response for the B&W plant category.

2.30.2.3 Part c

A new analysis for the B&W plant category was performed in response to RAI 4.22. The results from this case demonstrate that no liquid flow was predicted through either SG. This result can be confirmed by examining Figures RAI-4.17-4 and RAI-4.17-9.

Further, as described in RAI 4.20, the use of m_{split} is not needed to determine a fiber limit for the operating B&W plants. That is, within the context of the hot leg break methodology described in WCAP-17788, Volume 1, m_{split} is set to 1.0 for all times after Sump Switch Over (SSO).